Università degli Studi di Milano

PhD Course in

Experimental Medicine

CYCLE XXXIV

PhD thesis

Pattern of innate immunity in patients affected by myelodysplastic syndrome (MDS) either before and after hematopoietic stem cell transplant (HSCT)

Candidate: **Dr. Michela Calvi**

Tutor: **Prof. Domenico Mavilio**

Supervisor: **Dr. Clara Di Vito**

Director: **Prof. Nicoletta Landsberger**

Academic Year 2021-2022

1 Abstract

Myelodysplastic syndromes (MDS) are a heterogenous group of myeloid neoplasms that primarily affect elderly people and, in the context of population aging, MDS incidence is set to increase substantially. MDS patients have a variable risk of progression to acute myeloid leukemia (AML) and are characterized by ineffective hematopoiesis, cytogenetic changes and molecular abnormalities.

In the past decade significant efforts have been made to understand the pathophysiology of MDS. It has become increasingly evident that early driver mutations dictate the clonal proliferation of myelodysplastic cells and the trajectories of evolution of MDS with distinct clinical phenotypes. However, the definite pathogenetic mechanism of MDS is still not fully clarified, hindering the clinical decision-making process. Indeed, frontline pharmacological therapies, mainly based on the use of hypomethylating agents (HMAs), are not curative and the current patient risk stratification, aimed at identifying MDS patients with a higher risk to progress to AML, ineffectively predicts patient prognosis and response to therapies. Moreover, the only curative treatment for high-risk MDS patients is hematopoietic stem cell transplant (HSCT), however, only a small portion of patients is eligible for it.

The dysregulation and dysfunction of the immune system with the acquisition of an immunosuppressive signature are emerging as important characteristics in the prognosis and the clinical outcome of MDS patients. Indeed, although MDS patients are generally lymphopenic, cellular immunity seems to be up-regulated in low-risk MDS patients and impaired in high-risk MDS patients. For this reason, a deeper investigation of the immune populations is essential to identify new clinically relevant MDS prognostic and/or predictive markers. Furthermore, the alteration of the bone marrow niche together with the cytokine unbalance further contributes to increase genomic instability, to repress normal hematopoiesis and to determine an immune tolerant microenvironment in the of MDS patients. Despite this evidence, the primary orchestrators of the dysregulated MDS microenvironment have not yet been identified.

In this context, innate lymphoid cells (ILCs) are emerging as important actors in the pathophysiology of different cancers, by generating a suppressive and tolerant environment. Indeed, we and others demonstrated that ILC subset distribution and functions in AML are altered and contribute to immunotolerance. However, a comprehensive immune-phenotypic characterization of ILCs aiming at investigating their involvement in MDS pathogenesis, progression and in response to the main therapeutic interventions is still lacking.

The solely ILC subpopulation investigated in MDS is represented by NK cells. However, the experimental data available nowadays show contradictions.

In this PhD thesis, we aim at performing a deep characterization of cytotoxic, namely NK cells, and helper ILC frequency, phenotype and function in a large cohort of MDS and AML patients during the natural history of the disease and in the response to HMA treatment and also their immune reconstitution (IR) upon haploidentical-HSCT.

Our data demonstrated that MDS patients, and especially those with high blast counts, have a deficient ILC-poiesis characterized by the accumulation of ETP2s, a preferential differentiation toward dysfunctional ILC1s, accompanied by the reduction of total NK cells, with a skewing toward less differentiated NK cell subsets that are functionally impaired. This pathological ILC differentiation is related to a defect endowed by ILC progenitors, which are able to modify the morphology and functional properties of MSCs in the BM niche.

2 Disclosure for research integrity

The research proposed in this manuscript was conducted following the European Code of Conduct for Research Integrity, which includes the values of reliability, rigor, honesty, respect and transparency.

3 Abbreviations

ACK	Ammonium-Chloride-Potassium
ADCC	Antibody-dependent cellular cytotoxicity
AHR	Aryl hydrocarbon receptor
AML	Acute myeloid leukemia
aNKR	Activating NK cell receptors
AREG	Amphiregulin
BiKE	Bispecific killer cell engagers
BM	Bone marrow
BMMC	Bone marrow mononuclear cells
C	CCUS/ICUS
CCUS	Clonal cytopenia of undetermined significance
CD18	β2-integrin
CD62L	L-selectin
CHIP	Clonal hematopoiesis of indeterminate potential
CLP	Common lymphoid progenitor
CRTH2	Prostaglandin D2 receptor 2
DAMP	Damage-associated molecular pattern
DC	Dendritic cells
DMEM	Dulbecco's Modified Eagle Medium
DMSO	Dimethyl Sulfoxide
DNAM-1	DNAX-accessory molecule-1
Eomes	Eomesodermin
ETP	Early tonsillar progenitor
EV	Evaluation
FBS	Fetal Bovine Serum
GM-CSF	Granulocyte-macrophage colony-stimulating factor
Haplo	Haploidentical
HBSS	Hanks' Balanced Salt Solution
HC	Healthy control

HLA-I	Human leukocyte antigen class 1
HMA	Hypomethylating agent
HSC	Hematopoietic stem cell
HSCT	Hematopoietic stem cell transplantation
ICUS	Idiopathic cytopenia of undetermined significance
IFN-γ	Interferon γ
IL	Interleukin
IL1RL1	IL33 receptor
ILC	Innate lymphoid cells
ILCp	ILC progenitor
IMDM	Iscove's Modified Dulbecco's Media
iNKR	Inhibitory NK cell receptors
iNKs	Immature NK cells
Iono	Ionomycin
IPSS	International Prognostic Scoring System
IPSS-M	International Prognostic Scoring System Molecular
IPSS-R	Revised International Prognostic Scoring System
IR	Immune-reconstitution
k-NNG	k-nearest neighbor graph
KIR	Killer Ig-like receptor
KLRG1	Killer cell lectin-like receptor subfamily G member 1
LN	Lymph nodes
LTi	Lymphoid tissue inducer
mAbs	Monoclonal antibodies
MDS	Myelodysplastic syndromes
MDSC	Myeloid-derived suppressor cell
MSC	Mesenchymal stromal cell
NCR	Natural cytotoxicity receptor
NF-κB	Nuclear factor kappa-light-chain-enhancer of activated B cells
NK	Natural Killer
NKG2	C-type lectin receptor

NLRP3	Pyrin domain-containing protein 3
NMA	Non-myeloablative conditioning
PB	Peripheral blood
PBMC	Peripheral blood mononuclear cells
PBS	Phosphate-buffered saline
PD-L1	Programmed cell death-ligand 1
PGD2	Prostaglandin D2
PMA	Phorbol 12-myristate 13-acetate
RAG	Recombination-activating gene
RIC	Reduced-intensity conditioning
RORγt	Factor retinoic acid orphan receptor isoform γt
ROS	Reactive oxide species
RT	Room temperature
SA-PE	Streptavidin-phycoerythrin
SCF	Stem cell factor
SCGM	Stem Cell Growth Medium
SD	Standard Deviation
SLT	Secondary lymphoid tissues
T-bet	T-box transcription factor expressed in T cells
TF	Transcription factors
TGF-β	Transforming growth factor-β
Th	T helper
TL1A	TNF-like ligand 1 A
TLR	Toll-like receptor
TNF-α	Tumor necrosis factor-alpha
TRAIL	TNF-related apoptosis ligand
TSLP	Thymic stromal lymphopoietin
UMAP	Uniform manifold approximation and projection
UnCD56^{dim}	Unconventional CD56^{dim} NK cells
WHO	World Health Organization

4 Introduction

4.1 Myelodysplastic syndromes

Myelodysplastic syndromes (MDS) are a heterogeneous group of acquired myeloid neoplasm with an increased risk of progression to acute myeloid leukemia (AML). MDS are characterized by clonal disorders of hematopoietic stem and progenitor cells, ineffective hematopoiesis, peripheral cytopenias, genetic instability and chromosomal abnormalities (1, 2) MDS have a higher incidence in male and predominantly occur in elderly people with a median age at diagnosis of 65-70 years. (1, 2) The annual incidence of these neoplasms is about four to five cases per 100 000 people (reaching 75 cases per 100 000 individuals over age 70 years). However, considering the higher prevalence in elderly patients, the population aging in developed countries, as well as higher diagnostic awareness, the incidence of MDS is set to increase substantially in coming decades. (3, 4)

Disorder	Diagnostic Criteria
Myeloid neoplasms with myelodysplasia	
MDS	Persistent cytopenia in one or more peripheral-blood cell lineages and morphologic dysplasia (≥10% dysplastic cells) in one or more bone marrow cell lineages; on the basis of morphologic and cytogenetic abnormalities, MDS are categorized into the following subtypes: MDS with single-lineage dysplasia MDS with multilineage dysplasia MDS with ring sideroblasts and single-lineage dysplasia or multilineage dysplasia MDS with isolated del(5q) MDS with excess blasts type 1 or type 2 MDS, unclassifiable
Myelodysplastic–myeloproliferative neoplasms	Myeloid neoplasms with clinical, laboratory, and morphologic features that overlap those of MDS and myeloproliferative neoplasms; myelodysplastic–myeloproliferative neoplasms are divided into the following subtypes: Chronic myelomonocytic leukemia BCR-ABL1–negative atypical chronic myeloid leukemia Myelodysplastic–myeloproliferative neoplasm with ring sideroblasts and thrombocytosis Juvenile myelomonocytic leukemia
Therapy-related myeloid neoplasms	MDS, myelodysplastic–myeloproliferative neoplasms, and acute myeloid leukemia that occur as late complications of chemotherapy or radiotherapy
MDS precursor conditions	
CHIP	Normal peripheral-blood cell counts with a somatic mutation, at a variant allele frequency of at least 2%, in a gene that is recurrently mutated in myeloid neoplasms
CCUS	Unexplained cytopenia in one or more peripheral-blood cell lineages; a somatic mutation, at a variant allele frequency of at least 20%, in one or more genes that are recurrently mutated in myeloid neoplasms; and insufficient WHO criteria for a diagnosis of MDS, essentially because of lack of overt dysplasia (<10% dysplastic cells in any bone marrow cell lineage), excess blasts, and MDS-defining chromosomal abnormalities

Table 1 - Diagnostic criteria for myeloid neoplasms with myelodysplasia and precursor conditions for MDS.
(4)

Diagnosis of myeloid neoplasm is based on the analysis of: i) peripheral blood (PB), to assess cytopenias; ii) bone marrow (BM) aspirates, to detect morphologic dysplasia and blast number; iii) BM biopsy, to assess marrow cellularity and fibrosis; iv) conventional

cytogenetics to detect chromosomal abnormalities. (3, 4) The diagnostic criteria defined by the 2016 revision of the World Health Organization (WHO) for all myeloid neoplasm are listed in **Table 1**. (5) Among myeloid neoplasm with myelodysplasia, the WHO classification differentiates primary MDS from neoplasms with myelodysplastic-myeloproliferative overlapping features from therapy-related MDS, which occur as a late complication of treatment, such as chemotherapy and radiotherapy. (4, 5) In addition, the WHO classification includes, among the myeloid neoplasm without myelodysplasia, clonal hematopoiesis of indeterminate potential (CHIP) and clonal cytopenia of undetermined significance (CCUS), which are considered MDS precursor conditions. (4)

4.1.1 Pathophysiology of MDS

The pathophysiology of MDS is a multistep process (**Figure 1**) that leads to the growth and spread of a somatically mutated clone. (1, 2)

The first step consists in an initiating driver mutation occurring in a hematopoietic stem cell (HSC) capable of self-renewal, providing a selective advantage to the clone over the wild-type cells and giving rise to clonal hematopoiesis. (4)

The second (CHIP) phase is characterized by the propagation of myelodysplastic clones to other BM districts, forming local clones. When hematopoietic cells carrying the somatic mutation account for at least 4% of all bone marrow cells, the condition is defined as CHIP.

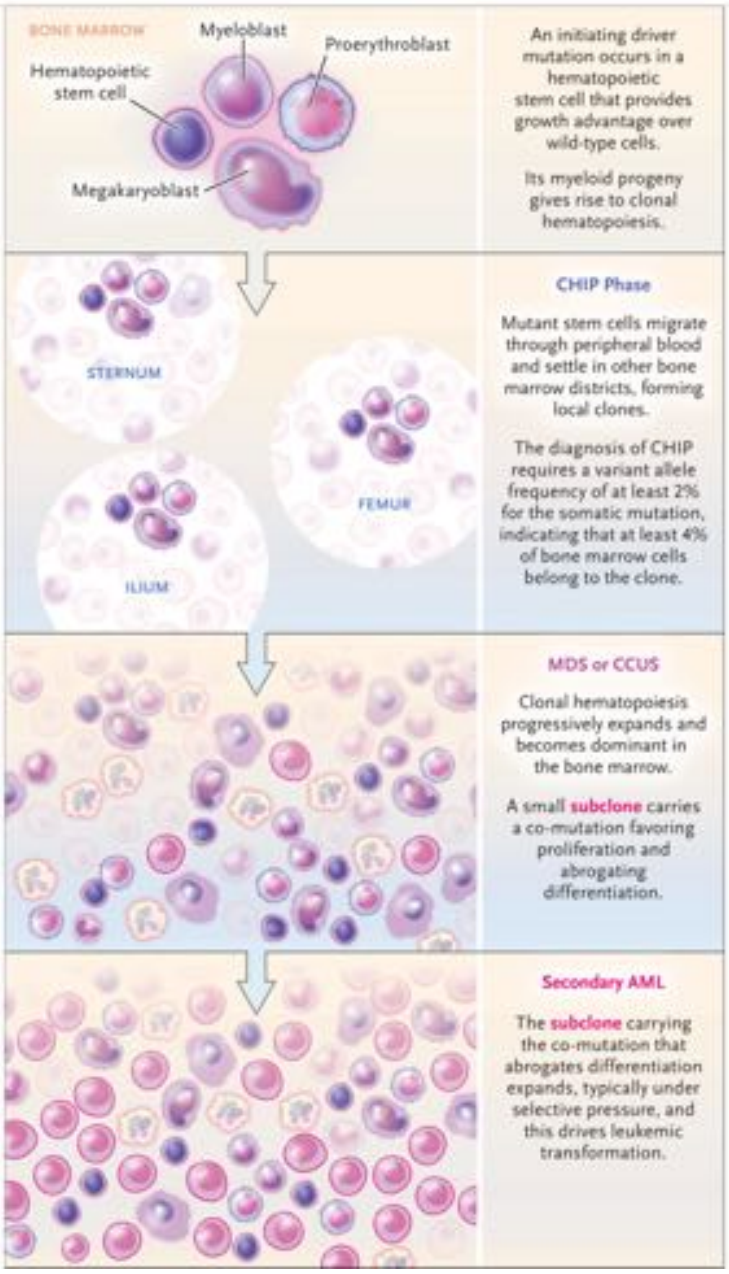

Figure 1 - General model of the growth and propagation of MDS.
(4)

The third (MDS or CCUS) phase is characterized by clonal dominance. Indeed, at this point the clonal hematopoiesis progressively expands and additional mutations associated with clonal progression may occur in progenitor cells, conferring them a self-renewal capability and resulting in the clonal origin of most of bone marrow hematopoietic cells. (4) At this point, the disease is clinically manifested as cytopenia and morphologic dysplasia. Indeed, the paradox of clonal hematopoiesis is that the founding mutation provides an advantage at the level of stem cells and progenitor cells but increases susceptibility of clonal myeloid progenitors to apoptosis, which leads to ineffective hematopoiesis and cytopenia despite a generally hypercellular marrow. (2, 4) This condition can meet the diagnostic criteria for MDS or CCUS. (5)

The progression to the fourth (secondary AML) phase is thought to result from a subsequent shift from apoptosis to proliferation of the clonal progenitors. Indeed, the acquisition of additional driver mutations or the emergence of preexisting ones leads to the selection of subclones of hematopoietic cells with increasingly impaired differentiation capacity. When the proportion of blast cells increases to 20% or more, a diagnosis of secondary AML can be made. (2, 4)

4.1.2 Genetic abnormalities in MDS

Genetic defects play a major role in the pathogenesis of MDS, including cytogenetic abnormalities, gene mutations, and abnormal gene expression. Thanks to the development of advanced high-throughput sequencing technologies, in the past decade, a broad range of recurrently genetic abnormalities in MDS have been identified (**Table 2**). (4, 6, 7)

Chromosomal abnormalities have been detected in approximately 50-60% of MDS patients, and include the deletions of chromosome 5q and 7q, trisomy 8, and complex karyotypes (**Table 2A**). In addition, recurrent somatic mutations in more than 50 genes have been identified in 80-90% of MDS (**Table 2B**). These frequently mutated genes belong to different biologic pathways, including RNA splicing, DNA methylation, histone modification, transcription regulation, DNA-repair control, signaling, and the cohesin complex. (8-11) Most patients have different combinations of pathway mutations, accounting for the heterogeneity of these disorders meaning different clinical phenotypes and outcomes. (12)

4.1.2.1 Recurrently chromosomal abnormalities

Clonal and recurrent cytogenetic abnormalities, including trisomy 8 (+8), monosomy 7 (-7), deletion of the long arm of chromosome 7 (del(7q)), deletion of the long arm of chromosome 5 (del(5q)), are often present at disease presentation and play a crucial role in disease progression. (6)

The del(5q) is the initiating driver mutation that originates in HSCs and leads to haploinsufficiency of multiple genes according to the extent of the deleted region. (2) Patients with the isolated del(5q) exhibit a homogenous clinical phenotype characterized by macrocytic anemia, thrombocytosis and favorable prognosis. (13, 14)

On the other hand, the presence of -7/del(7q) carries a uniformly poor prognosis. (14) Indeed, on the long arm of the chromosome 7 are located genes such as *CUX1*, involved in DNA repair mechanisms, *LUC7L2*, involved in the splicing process, *EZH2*, involved in gene expression regulation through methylation, and *SAMD9L* which negatively regulates cell proliferation. (6)

Trisomy 8 is thought to be a secondary or late event in the MDS transformation process. The presence of isolated +8 is related to an intermediate prognosis according to

A

Chromosomal abnormality	Frequency
Loss of chromosome 7 or del(7q)	>10
del(5q)	>10
Gain of chromosome 8*	>10
del(20q)	5–10
Loss of Y chromosome[a]	5-10
Isochromosome 17q or t(17p)	2-4
Loss of chromosome 13 or del(13q)	2-4
del(11q)	2-4
del(12p) or t(12p)	2-4

B

Mutated gene		Frequency	Mutated gene		Frequency
RNA splicing	SF3B1	>10	*DNA repair control*	TP53	5-10
	SRSF2	>10		PPM1D	<2
	U2AF1	5-10		BRCC3	<2
	ZRSR2	5-10	*Signaling*	CBL	5-10
	PRPF8	<2		NRAS	5-10
	LUC7L2	<2		KRAS	2-4
	U2AF2	<2		NF1	2-4
Epigenetic regulators (DNA methylation and histone modification)	TET2	>10		PTPN11	2-4
	ASXL1	>10		JAK2	2-4
	DNMT3A	>10		MPL	2-4
	EZH2	5-10		SH2B3	<2
	BCOR	5-10		KIT	<2
	IDH2	5-10		GNB1	<2
	IDH1	2-4	*Cohesin complex*	STAG2	5-10
	PHF6	2-4		CTCF	<2
	BCORL1	<2		RAD21	<2
	ATRX	<2		SMC3	<2
	EP300	<2		SM1A	<2
	ZBTB33	<2	*Miscellanea*	DDX41	2-4
Transcription regulation	RUNX1	>10		SETBP1	2-4
	CUX1	2-4		ETNK1	2-4
	ETV6	2-4		NPM1	<2
	CEBPA	2-4		KMT2C	<2
	GATA2	<2		CSNK1A1	<2
	WT1	<2			
	KDM3A	<2			

Table 2 – Recurrent genetic abnormalities in MDS.
(A) Recurrent chromosomal abnormalities.
(B) The fifty recurrently mutated genes subdivided in biological pathways. (7, 8)

clinical outcomes. (14) Although the precise mechanisms of the contribution to tumorigenesis remain unclear, trisomy 8 cells showed resistance to apoptosis by the downstream upregulation of the anti-apoptotic elements, including c-myc. (15)

4.1.2.2 Recurrently mutated genes

Somatic mutations in genes belonging to different biological pathways play an important role in the pathogenesis and prognosis of MDS.

Mutations in genes that are involved in the spliceosome complex (i.e. SF3B1, SRSF2 and U2AF1) are generally early genetic events that drive clonal dominance and shape the future trajectories of clonal evolution. They are heterozygous and mutually exclusive, most likely because of synthetic lethal interactions. (12) The SF3B1 mutation identifies a distinct subtype of MDS that is characterized by ring sideroblasts, ineffective erythropoiesis, macrocytic anemia and a relatively good prognosis. The mutant SF3B1 splicing factor leads to nonsense-mediated decay of multiple transcripts or generation of isoforms that result in the expansion of HSCs. (16) Conversely, mutations in SRSF2 and U2AF1 are generally attributable to a poor clinical outcome. (17) Mutated SRSF2 and U2AF1 cause different splicing aberrations from those caused by SF3B1, which lead to genomic instability and are almost invariably involved in combinatorial mutation patterns. (4)

Aberrant DNA methylation and histone modification are associated with gene silencing, including tumor suppressors, and play a central role in the pathogenesis of MDS. Indeed, mutations in epigenetic modifiers, such as TET2 and DNMT3A, enhances self-renewal and impairs differentiation, leading to clonal outgrowth of mutant stem cells and clonal dominance. (18)

The presence of somatic mutation of genes belonging to the DNA repair machinery, such as p53, is instead correlated with inferior survival, risk factors for leukemic transformation, and early relapse after various treatments, whereas the remaining mutated genes mainly contribute to clonal progression. (19)

Disease progression and evolution into AML may occur with different mutation patterns. Indeed, SF3B1-mutated MDS has a long-lasting chronic phase, and only a minority of cases eventually evolve to AML, typically through the acquisition or expansion of somatic mutations, while cases of MDS with combinations of mutated genes, such as SRSF2, U2AF1, RUNX1, STAG2, or IDH2, are typically characterized by an excess of blasts at the onset of clinical disease and gradually progress to AML, with a clear continuum between the

myelodysplastic and leukemic phases, which are distinguishable only on the basis of the percentage of circulating blasts. (4, 20)

4.1.3 Risk stratification

MDS encompass a wide spectrum of conditions that vary with respect to prognosis and the risk of disease progression. Indeed, clinical outcomes can vary greatly, even between patients considered to have the same MDS subtype. To overcome this heterogeneity, the International Prognostic Scoring System (IPSS), and then later revised (IPSS-R), were introduced with the aim to provide discriminatory prognostic risk assessment regarding overall survival and risk of progression to AML. (21) IPSS-R is now universally used for risk stratification in MDS. This prognostic model defines five major prognostic categories, on the basis of cytogenetic abnormalities (**Table 3A**), the percentage of marrow blasts, the hemoglobin level, the platelet count, and the absolute neutrophil count (**Table 3B**). (21) In clinical practice, the IPSS-R allows

A

Cytogenetic prognostic subgroups	Cytogenetic abnormalities
Very good	-Y, del(11q)
Good	Normal, del(5q), del(12p), del(20q), double including del(5q)
Intermediate	del(7q), +8, +19, i(17q), any other single or double independent clones
Poor	-7, inv(3)/t(3q)/del(3q), double including -7/del(7q), Complex: 3 abnormalities
Very poor	Complex: >3 abnormalities

B

Prognostic variable	0	0.5	1	1.5	2	3	4
Cytogenetics	Very Good		Good		Interm ediate	Poor	Very Poor
BM Blast %	<=2		>2-<5%		5-10%	>10%	
Hemoglobin	=>10		8-<10	<8			
Platelets	=>100	50-<100	<50				
Absolute neutrophil count	=>0.8	<0.8					

C

Risk Category	Risk score	Median OS (yr)	
Very Low	<=1.5	8.8	**Lower-risk** Score <= 4.5 Median OS = 5.9 yr
Low	>1.5 - 3	5.3	
Intermediate	>3 - 4.5	3.0	
High	>4.5 - 6	1.6	**Higher-risk** Score > 4.5 Median OS = 1.5 yr
Very High	>6	0.8	

***Table 3 - The Revised International Prognostic Scoring System (IPSS-R)**. (A) IPSS-R Cytogenetic risk groups, (B) IPSS-R Prognostic Score Values used to calculate the final score-risk of MDS patients, (C) IPSS-R Prognostic Risk Categories defined on the basis of the calculated scores used to estimate the risk of evolution to AML and expected survival. (21)*

clinicians to distinguish between patients with lower-risk MDS (score ≤3.5; median survival, 5.9 years) and those with higher-risk MDS (score >3.5; median survival, 1.5 years) (**Table 3C**). (21) At the clinical onset of the disease, lower-risk MDS account for about two thirds of all cases. (4)

As previously mentioned, the current IPSS-R score risk considers only recurrent chromosomal abnormalities, detected in about 50%, and not gene mutations. However, by combining cytogenetics with gene sequencing, 90% or more of patients with MDS are found to carry a clonal genetic lesion, thus helping in a more accurate patient risk stratification. (11, 17) In addition, a portion of patients with unexplained cytopenia and classified as CCUS, could be diagnosed only by means of molecular profiling, since they do not meet the current diagnostic criteria for MDS but they carry somatic gene mutations. (22)

Since somatic mutations have been shown to be valuable prognostic biomarkers in multiple studies, the assessment of the molecular profile could improve patient risk stratification and the clinical decision making. (12, 23, 24) To this end, the IPSS-Molecular (IPSS-M) prognostic model have been recently developed combining genomic profiling with the

Category and Variable	Adjusted Hazard Ratio (95% CI)†	Model Weight‡
Clinical		
Bone marrow blasts — %	1.07 (1.05–1.09)	0.0704
min(Platelets,250) — $x10^9$/l	0.998 (0.997–0.999)	−0.00222
Hemoglobin — g/dl	0.84 (0.81–0.88)	−0.171
Cytogenetic		
IPSS-R cytogenetic category§	1.33 (1.21–1.47)	0.287
Gene main effects (17 variables, 16 genes)¶		
TP53^{multihit}	3.27 (2.38–4.48)	1.18
MLL^{PTD}	2.22 (1.49–3.32)	0.798
FLT3$^{ITD+TKD}$	2.22 (1.11–4.45)	0.798
SF3B1^{hs}	1.66 (1.03–2.66)	0.504
NPM1	1.54 (0.78–3.02)	0.430
RUNX1	1.53 (1.23–1.89)	0.423
NRAS	1.52 (1.05–2.20)	0.417
ETV6	1.48 (0.98–2.23)	0.391
IDH2	1.46 (1.05–2.02)	0.379
CBL	1.34 (0.99–1.82)	0.295
EZH2	1.31 (0.98–1.75)	0.270
U2AF1	1.28 (1.01–1.61)	0.247
SRSF2	1.27 (1.03–1.56)	0.239
DNMT3A	1.25 (1.02–1.53)	0.221
ASXL1	1.24 (1.02–1.51)	0.213
KRAS	1.22 (0.84–1.77)	0.202
SF3B1^{ns}	0.92 (0.74 1.16)	−0.0794
Gene residuals (1 variable, 15 genes; possible values of 0, 1, or 2)‖		
min(Nres,2)	1.26 (1.12–1.42)	0.231

Table 4 - IPSS-M Risk score construction from a multivariable regression for leukemia-free survival.
(25)

hematologic and cytogenetic parameters already used for the IPSS-R. (25) This led to a model with four categories of features: hemoglobin level, platelet count, and marrow blasts; IPSS-R cytogenetic category; 17 binary features from 16 prognostic genes (ASXL1, CBL, DNMT3A, ETV6, EZH2, FLT3, IDH2, KRAS, MLL^{PTD}, NPM1, NRAS, RUNX1, $SF3B1^{5q}$, $SF3B1^{\alpha}$, SRSF2, $TP53^{multihit}$, and U2AF1); and a feature representing the number of mutated genes (Nres) from a residual group of 15 genes (**Table 4**). The IPSS-M score was built as a weighted sum of prognostic variables observed for each patient. (25)

A six-category risk schema was defined for IPSS-M as follows (**Figure 2A**): very low, low, moderate low, moderate high, high, and very high. The IPSS-M risk categories demonstrated strong prognostic separation across all end points (**Figure 2B**). (25) Compared with the IPSS-R, the IPSS-M resulted in improved prognostic accuracy across all long-term clinical end points (overall survival, leukemia free survival, AML transformation) and restratified nearly half of patients with MDS (34% upstaged and 12% downstaged). (25)

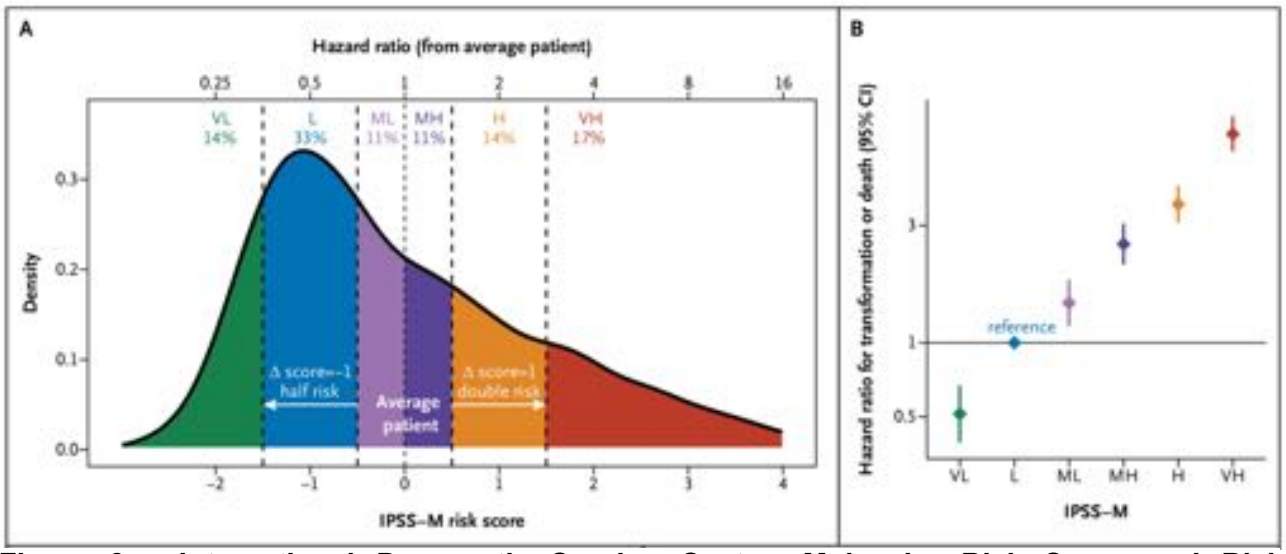

Figure 2 - International Prognostic Scoring System–Molecular Risk Score and Risk Categories.

(A) Density plot showing on the bottom x-axis the IPSS-M score and on the top x-axis the corresponding hazard ratio. Vertical dashed lines represent cutoffs that are applied to the score to define the six IPSS-M risk categories. (B) Hazard ratios are provided for the risk of death or transformation of the IPSS-M risk categories. (25)

4.2 Treatment of myelodysplastic syndromes

Different therapeutic strategies for the treatment of MDS have been developed in years and risk stratification is of utmost importance for the choice of the most suitable treatment for the patient. Indeed, patients with lower-risk MDS are primarily candidates for treatments aimed at ameliorating cytopenias and improving quality of life, while patients with higher-risk MDS are considered for therapies capable of altering the natural disease course, preventing evolution to AML, and thus prolonging survival. (2, 25)

4.2.1 Hematopoietic stem cell transplantation

Hematopoietic stem cell transplantation (HSCT) is the curative strategy to treat a wide range of acquired and inherited, malignant and nonmalignant, hematologic diseases together with genetic disorders. (26) HSCT consists in the intravenous infusion of healthy hematopoietic stem and progenitor cells from a donor. These cells are able to reach and re-populate the bone marrow, in a process called homing, in order to replace the entire hematopoietic and immune system of the recipient (27).

Several protocols for HSCT have been developed over the time characterized by a different combination of donor type, HSC source and conditioning regimen before transplant. (28)

At present, allogenic HSCT is the only potentially curative treatment for MDS, mainly undertaken for high-risk patients. However, this approach is associated with substantial morbidity and mortality, mainly due to the toxicity of myeloablative conditioning regimens. For these reasons, only a small portion of MDS patients is eligible for the transplant. (1) To assess the patient eligibility, different criteria are considered, including the presence of comorbidities and impaired functional status, which can lead to poor outcome, and the timing of the transplantation which must be a balance between a risk of transplant-related mortality in patients who might expect long-term survival without transplantation and transplant-related risks, including relapse, in patients with advanced disease. (2)

Since the median age at diagnosis exceeds 70 years and the use of myeloablative conditioning regimens can be fatal for elderly patients, MDS patients eligible for HSCT are more suitable for a reduced-intensity (RIC) or non-myeloablative (NMA) conditioning regimens before the transplant. Moreover, to reduce transplant-related risks, HLA-identical donors are preferred to autologous HSCT. (29) In the last decade, the use of HLA-haploidentical (haplo) donors paired to RIC regimens is further increasing the possibility to access to HSCT to high-risk MDS patients. (30)

In case of eligibility for the transplant, germline predisposition becomes clinically relevant whenever transplantation with a graft from a family donor is planned, since the donor may carry a predisposing mutation. A gene panel specifically designed for germline mutation analysis may inform decision making in these cases. (31)

4.2.2 Hypomethylating agents

MDS at advanced states are characterized by a widespread gene hypermethylation, leading to the silencing of critical tumor suppressor genes involved in cancer-related pathways, such as invasion, DNA repair, and cell cycle regulation. The possibility to induce re-expression of

the silenced tumor suppressor genes led to the pursuit of drugs with hypomethylating potential. Nowadays, the use of hypomethylating agent (HMA), azacytidine or decitabine, represents the first line treatment in patients with higher-risk MDS who are ineligible for transplantation. (32)

Both azacytidine and decitabine are incorporated into newly synthesized DNA and inhibit DNA methylation. Additionally, azacytidine incorporates into RNA, thereby also inhibiting RNA synthesis and protein metabolism (33). About half of the patients treated with HMA have a hematologic response, including some with a complete response. Treatment is associated with prolonged survival, although the duration of response is often less than 2 years. (30) Responses can also be observed in patients with adverse cytogenetic features or high-risk mutations, while patients with biallelic defects in TP53 invariably have a poor outcome. (34) Unfortunately, HMA are not curative since the treatment does not eliminate founder clones, which continue to drive hematopoiesis. (4)

4.2.3 Chemotherapy

Intensive chemotherapy represents a therapeutic strategy for patients with high-risk MDS or secondary AML and it mainly uses the combinations of chemotherapeutic drugs as for the treatment of *de novo* AML. However, it yields only 40-60% complete remissions and short-term effects (median <12 months) than in *de novo* AML. (2)

With the advent of HMA, chemotherapy is used less frequently in patients with MDS. It may be considered in patients ineligible for transplantation, below the age of 60 years, with 10% or more bone marrow blasts without adverse cytogenetic characteristics. (4)

4.2.4 Treatment of lower-risk myelodysplastic syndromes

Among low-risk patients, some present mild cytopenias and minimal symptoms, hence they do not require to be treated immediately but watchful observation is appropriate. When treatment is required, the main objective is to ameliorate the fatigue caused by cytopenia, primarily anemia, and improve the quality of life. (4, 30) Most of MDS patients become dependent on regular red-cell transfusions during their clinical course. However, this can lead to parenchymal iron overload and its clinical consequences. (4)

For this reason, to ameliorate the anemia, the first line treatment is the administration of erythropoiesis-stimulating agents, recombinant erythropoietin and darbepoetin, which increase red-cell production and have a median duration of response of 1 to 2 years. (30)

Furthermore, several drugs have given good results in the treatment of low-risk MDS patients. Among them, lenalidomide, an immunomodulatory drug, used in the treatment of patients with isolated del(5q). Lenalidomide treatment induces transfusion independence and many patients with a response to the treatment have a cytogenetic remission, clearly indicating that this is a true targeted therapy. Indeed, lenalidomide treatment induces p53-dependent apoptosis of cells harboring del(5q). (30) After 2 to 3 years, however, most patients have a relapse caused by selection of hematopoietic cells that are resistant to lenalidomide and a recurrence of anemia. (4)

Luspatercept, a recombinant protein that binds transforming growth factor β superfamily ligands to enhance late-stage erythropoiesis, is used for the treatment of transfusion-dependent patients with MDS and ring sideroblasts who have not had a response to erythropoiesis-stimulating agents and results in transfusion independence in 38% of cases. (30)

The first-line treatment options for patients with MDS related thrombocytopenia are platelet transfusions and thrombopoietin-receptor agonists, which can ameliorate the quality of life but without reducing the risk of AML progression or death. (30)

Low-risk MDS patients who are failed by all these agents are considered for anti-T cell immunosuppressive therapy, HMA therapy or allogenic HSCT. (30)

4.2.5 Emerging strategies for the management of MDS

Our expanding knowledge about the biology of MDS leads to the identification of those dysfunctional pathways involved in the onset and the progression of the disease and, of consequence, several agents targeting these pathways are in development.

Patients who are failed by the aforementioned first-line agents, as well as those with transfusion dependence and poor-risk genetic features should be referred to tertiary centers for enrollment into clinical trials. (30)

Among the promising emerging agents for the management of low- and high-risk MDS, there are for example roxadustat, an oral hypoxia-inducible factor capable to increase endogenous erythropoietin levels and to regulate iron metabolism; the telomerase inhibitor imetelstat; new hypomethylating agents such as guadecitabine and orally bioavailable formulations; modulators of the spliceosome machinery such as H3B-8800; the TP53 activator drugs APR-246 and ALRN-6924; IDH inhibitors and immune checkpoint inhibitors. (30)

4.3 Microenvironmental niche dysfunction in myelodysplastic syndromes

The BM microenvironment, which comprises interstitial cells, helper cells, and sympathetic nerve cells, plays an essential role in the maintenance and development of HSC. Indeed, it regulates quiescence, self-renewal, proliferation, and differentiation of stem cells. (35)

Whereas the majority of current MDS studies focus on genetic and epigenetic events required for the rising and clonal outgrowth of mutant stem, recent advances highlighted the role of abnormal HSC niche in MDS pathogenesis. (3, 36) Indeed, several driver mutations (i.e. IDH and SRSF2) do not give a proliferative advantage *per se*. Thus, the interaction with the microenvironment and immune cells might be accountable for the clonal expansion of the mutated cells. (37)

Although many microenvironmental alterations might simply be related to aging, mutant hematopoietic cells themselves may alter the stem-cell niche for example through activation of the innate immune system and related inflammatory signaling. (4)

Among the facets of microenvironmental niche dysfunction, abnormal stromal cell, immune cell dysfunction and skewed pro-inflammatory factor production are central to MDS development and progression (**Figure 3**). (37)

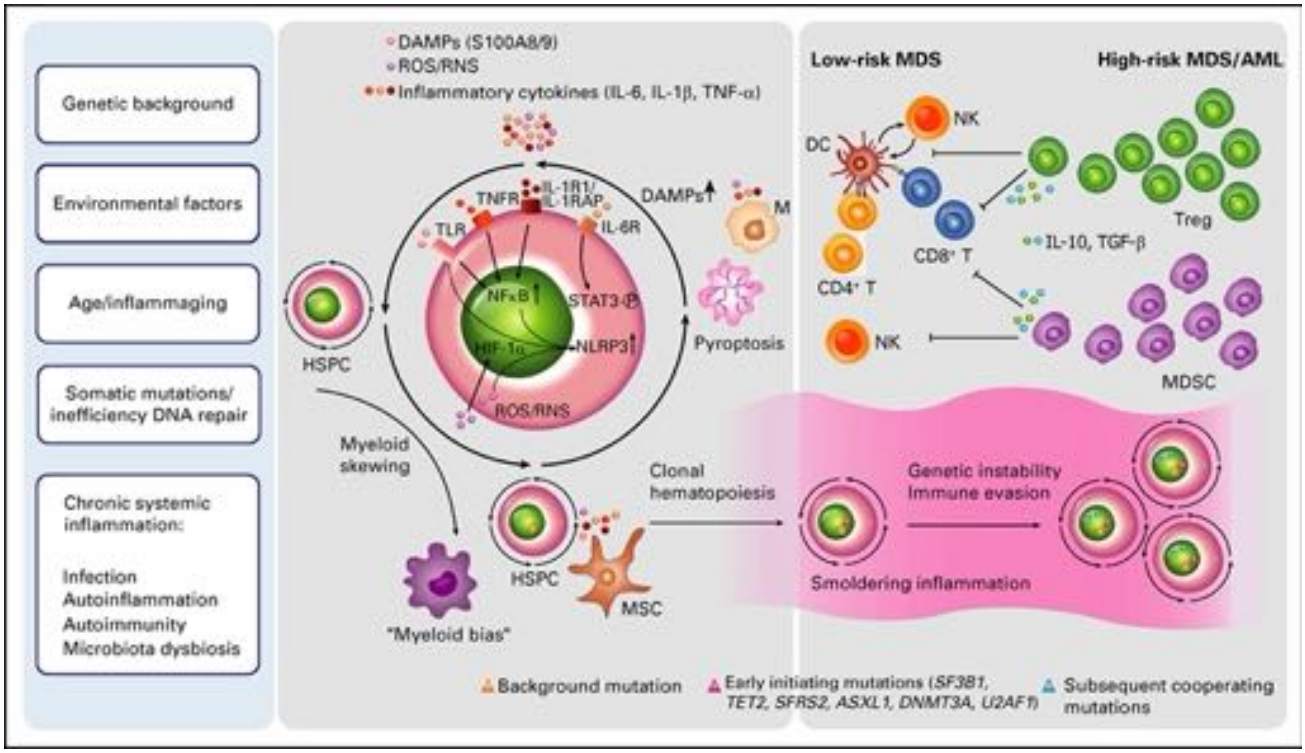

Figure 3 - Microenvironmental alteration contribution in setting the biologic background for MDS development.
(3)

4.3.1 Mesenchymal stromal cells

Mesenchymal stromal cells (MSCs) and their progeny are important components of the bone marrow niche that regulate HSC self-renewal and differentiation by cell-to-cell contact or through paracrine signals. (36) Moreover, MSCs can differentiate into osteoblast, osteoclast, adipocyte, chondrocyte and epithelial cells which provide stromal support to bone marrow hematopoietic niche. (36) MSCs also participate in immunomodulation and immune dysregulation in the tumor microenvironment, interacting with various immune cell types, including T cells, Natural Killer (NK) cells, and myeloid cells. (38)

MSCs undergo functional decline with systemic aging resulting in the decrease of bone-forming osteoblasts and increasing the generation of bone-resorbing osteoclasts. (39)

This is further worsened in MDS where MSCs have accumulated genetic mutations and chromosomal aberrations different from those found in HSC, and display activation of key inflammatory pathways together with a greater reduction of osteoblast and increase of osteoclast that lead to the disruption of the bone marrow architecture. (36) In this context, it has been shown that treatment with hypomethylating therapy significantly ameliorates these abnormalities in MDS-MSC properties, including osteogenic differentiation, proliferation and gene expression, and also leads to significant improvements in their ability to support hematopoietic cells (40).

MDS-MSCs produce several cytokines and other factors that exert immunomodulatory functions that could further promote propagation of malignant HSCs. (40) For example, MSC from MDS patients are characterized by a higher reactive oxide species (ROS) production that can drive the overexpression of membrane bound transforming growth factor-β (TGF-β) on monocytes, which in turn exert strong inhibition of NK and T cell function. (41)

Some of these MDS-MSC alteration can be attributed to the capability of MDS hematopoietic cells of shaping and instructing MSC to sustain clonal hematopoiesis. (40) However, the fact that MDS-MSCs often harbor different genomic mutations than HSC begs the question whether MDS-MSC defects or HSC defects came first. In this context, there are plenty of data showing that a perturbed stroma can induce BM failure and dysplastic hematopoiesis, suggesting that stromal defects may come first, possibly due to cellular senescence. (36, 42) The functional relevance of this altered MSCs for the development and progression of MDS in patients is demonstrated by their capacity to propagate MDS after orthotopic intra-femoral transplantation coupled with the infusion of MDS HSC into NSG mice. In contrast, the sole transplantation of MDS HSC only gave rise to inefficient and often transient engraftment. (40)

4.3.2 Increase of pro-inflammatory factors in MDS

Normal human aging represents a state of chronic low-grade sterile inflammation, commonly referred to as “inflammaging”, caused by the accumulation of endogenous inducers of sterile inflammation, including damage-associated molecular patterns (DAMPs) released by stressed, damaged, malfunctioning or dead cells. (43) Ligation of DAMPs to Toll-like receptors (TLRs) induces nuclear factor kappa-light-chain-enhancer of activated B cells (NF-κB)-mediated transcription of proinflammatory cytokines, including tumor necrosis factor-alpha (TNF-α), interleukin (IL)1β, IL6, and transcriptional priming of pyrin domain-containing protein 3 (NLRP3) inflammasome components. The activation of the NLRP3 inflammasome drives pyroptosis of HSC, consequent cytopenias, and an inflammatory circuit, with the production of IL1β, TNF-α and interferon γ (IFN-γ), that may support the propagation of the MDS clone through various pathways. (3)

Besides age-related inflammation MDS niche is further characterized by an altered concentration of numerous inflammatory cytokines, originating from the interaction of the MDS clone with bone marrow MSCs and infiltrating immune effector cells. (44) Several of these cytokines have been related to apoptosis of hematopoietic cells in MDS, a mechanism suggested to account for the ineffective hematopoiesis. (45) Among them, TNF-α is well recognized as a cytokine promoter of apoptosis in erythroid cells in early stages of MDS and was also recently shown to modulate gene expression in MSCs inducing production of proinflammatory cytokines, such as IL6, IL8, and IL32. (46)

The increased concentration of pro-inflammatory cytokines may also provide the selective immune pressure of neoplastic clones by simultaneously enhancing their growth and exhausting non-neoplastic clones. (3) On the other hand, cytokine-mediated induction of immune-inhibitory molecules like programmed cell death-ligand 1 (PD-L1) may contribute to immune cell suppression and reduced immune surveillance. Furthermore, excess DAMPs may expand myeloid-derived suppressor cells (MDSCs), which overproduce suppressive cytokines, such as IL10 and TGF-β, contributing to the subsequent immunosuppression and ineffective hematopoiesis. (3)

4.3.3 Altered immune signature in MDS

The combination of the microenvironmental changes described above compromise the immune response of MDS patients. The immune contexture dynamically changes with disease progression. Indeed, low risk patients are more characterized by a pro-inflammatory immune signature and higher numbers of effector-type cells, while high-risk patients are

more related to an immune suppressive milieu and the expansion of immunosuppressive cells (**Figure 3**). (3)

Among the effector cells that are expanded in BM niche of low-risk patients IL17-producing T helper (Th) cells are important inducer of inflammatory cytokine environment and may play a role in the conversion of regulatory T cells towards effector T cells; dendritic cells (DC) uptake apoptotic cells and mature in presence of the pro-inflammatory cytokines IL6 and TNF-α, which are present at high levels in low-risk MDS, and activate specific T-cells; cytotoxic T cells play a major role in immune cytotoxicity of BM clones. (47-49)

On the other hand, in high-risk MDS patients it has been described an expansion of the immune suppressive T regulatory cells and MDSCs, paralleled by a reduction in the number and function of bone marrow dendritic cells, peripheral cytotoxic T cells, and NK cells likely supporting immune evasion and disease progression. (50-53)

Many other attempts have been done trying to characterize different immune compartment in MDS patients, however the lack of a correct stratification of results according to patient risk often leads to controversial results due to the high heterogeneity of the disease.

Overall, the cellular immune response in established MDS is multifactorial and follows a stepwise transformation from an activated protective to a more immunosuppressive response as the disease progresses underlying the role of the immunome as an important and independent factor in the stratification of MDS patients. Moreover, the characterization of the immune profile at the time of diagnosis could be useful also in identifying patients who may benefit to novel immunotherapies. (3)

4.4 Innate lymphoid cells

Innate lymphoid cells (ILCs) are the most recently identified constituents of the innate immune system and have been the focus of intense investigation over the past decade. Indeed, starting from 2008, several independent laboratories around the world identified, in both humans and mice, these lymphocytes lacking recombination-activating gene (RAG)-dependent rearranged antigen-specific receptors and playing key roles in controlling tissue homeostasis in the context of infectious diseases, chronic inflammation, metabolic homeostasis and cancer. (54, 55)

Nowadays, ILCs are defined as a heterogenous group of innate cells which are considered the innate counterpart of adaptive T lymphocytes. Indeed, ILCs share with T cells the transcription factors (TFs) governing their differentiation and the same cytokines in response to inflammatory insults which allow the classification of ILCs into different subsets: ILC1,

ILC2 and ILC3 which produce Th1-, Th2- and Th17/22-cytokines, respectively (**Figure 4**). (56, 57)

Given their phenotypic, developmental and functional similarities, the previously discovered and better characterized innate lymphocytes are now included in the ILC family:

NK cells, which constitute the innate counterpart of cytotoxic T lymphocytes, are grouped with ILC1;

lymphoid tissue inducer (LTi) cells, involved in the formation of lymph nodes (LNs) during embryogenesis, are grouped with ILC3. (56, 58, 59)

Differently from NK cells, that are mainly circulating lymphocytes, ILC1, ILC2 and ILC3, namely helper ILCs, are primarily tissue resident cells and have been found in both lymphoid and non-lymphoid tissues. They are particularly enriched at the mucosal surfaces of several organs, such as gut, lungs and skin, where, given their innate nature, ILCs represent one of the primary sources of pro- and anti-inflammatory cytokines and play fundamental roles in tissue homeostasis and disease, by promoting immune responses, inflammation, tissue repair and tolerance to commensal microbiota. (60-63) Despite being a rare population in PB, several lines of evidence indicate that circulating helper ILCs are characterized by a unique pattern of cytokine receptors, thus suggesting that they are not exclusively tissue resident. (64)

A peculiarity of ILCs is the so-called plasticity phenomenon which consists in their ability, in both humans and mice, to switch from a subset into another depending on the presence of cytokines and NOTCH ligands in their environment. This process is regulated by a complex network of TFs. Briefly, ILC2s and ILC3s transdifferentiate into ILC1s in response to IL1β and IL12, whereas IL1β and IL23 can drive the plasticity of ILC1s and ILC2s towards ILC3s. The transdifferentiation of ILC2s into ILC1s or ILC3s can be reversed by IL4. ILC2s requires TGF-β in addition to IL1β and IL23 to differentiate into ILC3s. (65) Moreover, NK cells, in a TGF-β-rich tumor environment, transdifferentiate into ILC1-like cells devoid of cytotoxic activity. (66, 67) Likely, plasticity of ILCs is the mechanism of tissue-resident ILCs to dynamically adapt to a given stimulus, such as an inflamed state. (68)

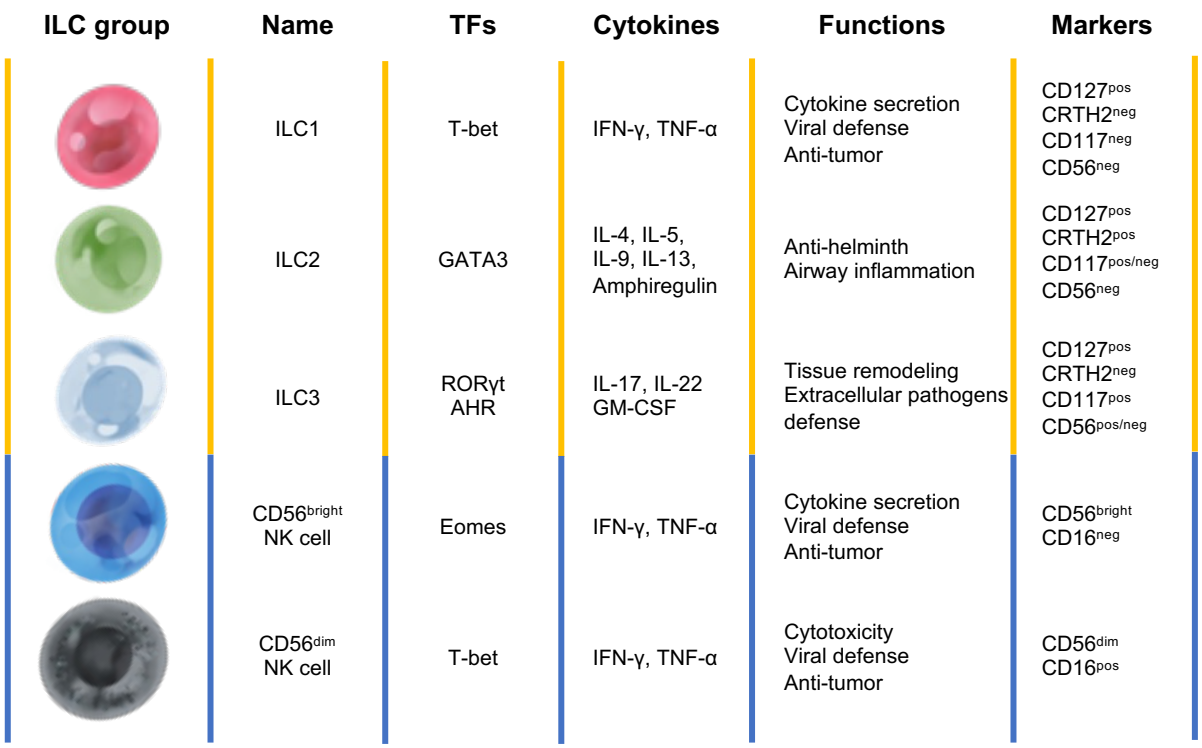

Figure 4 - General features of ILC subsets.
Summary table showing the main transcription factors (TFs) governing the development, the cytokine production, the functions and marker expression in the different ILC subsets. Figure from (54)

Focusing on circulating ILCs, which comprises helper ILCs and NK cells, they are identified as lineage (CD3, CD14, CD15, CD19, CD20, CD33, CD34, CD203c and FcεRI) negative lymphocytes. (69) Total helper ILCs are defined as $CD16^{neg}$ cells that constitutively express the IL7 receptor-α chain (CD127) and the different subsets are identified according to the expression of CRTH2, cKit (CD117) and CD56: ILC1s are $CRTH2^{neg}CD117^{neg}CD94^{neg}$, ILC2s are $CRTH2^{pos}CD117^{pos/neg}CD94^{neg}$ and ILC3s $CRTH2^{neg}CD117^{pos}CD94^{pos/neg}$ (**Figure 4**). (56, 69, 70) In addition, among lineage negative cells, different NK cell subsets can be identified according to the differential expression of CD56 and CD16. (71) The most frequent subsets in peripheral blood are $CD56^{bright}CD16^{neg}$ ($CD56^{bright}$) and $CD56^{dim}CD16^{pos}$ ($CD56^{dim}$) (**Figure 4**). (71-73)

4.4.1 Group 1 ILC

Group 1 ILCs, which comprises NK cells and ILC1s, require IL15 for their differentiation, homeostasis, and function and they are characterized by the production of IFN-γ and TNF-α in response to IL12 and IL18. (56, 58, 74, 75) Similarly to NK cells, ILC1s express natural cytotoxicity receptors (NCRs) and the T-box transcription factor expressed in T cells (T-bet).

(75-77) In addition, both ILC1s and NK cells require the expression of HOBIT TFs, encoded by *Zfp683*, for their differentiation and functional programs. (78, 79)

Despite these overlapping features, NK cells and ILC1s are two phenotypically and functionally distinct immune cell subsets. Indeed, while ILC1s require T-bet for their development, NK cells need T-bet expression only for maturation and require the expression of the transcription factor Eomesodermin (Eomes) for differentiation. (75, 77) Moreover, ILC1s are fundamentally tissue-resident lymphocytes, whereas NK cells can circulate across lymphoid organs via the bloodstream and lymphatic system to act as immune sentinels. (80, 81) Also the regulation of these two subsets is different, indeed ILC1s activation mainly relies on soluble factors and, to a lesser extent on the engagement of NCRs, especially NKp46, but also on TNF-related apoptosis ligand (TRAIL). (82)

Although phenotype and regulation of NK cells and ILC1s are distinct, the overlap in effector functions, such as IFN-γ production and promotion of type 1 immunity together with the limitations in specifically targeting these subsets, has thus far hindered dissection of the unique functions of ILC1s, and further research will be required to address this question. (82)

4.4.1.1 NK cells

NK cells represent approximately 5-15% of circulating lymphocytes in PB and are involved in both cytokine production and cytotoxic responses.

NK cell effector-functions are tightly regulated by the balance between both activating and inhibitory NK cell receptor (aNKR and iNKR) signaling, which is strongly related to the “education” processes occurring during NK cell development, together with environmental cues. (83) NK cell education is defined as the mechanism ensuring NK cell responsiveness against non-self targets while retaining tolerance versus autologous cells. This occurs during NK cell development through the sequential acquisition of iNKR and their binding to self human leukocyte antigen class 1 (HLA-I) molecules. (84, 85) However, the downregulation of HLA-I and/or the upregulation of ligands for aNKRs on target cells drives NK cell activation which manifests with the release of cytotoxic granules and/or through the production of inflammatory cytokines. (85)

The main classes of receptors specific for HLA-I molecules, hence mediating self-recognition or NK cell activation, include killer Ig-like receptors (KIRs, also known as CD158), which are able to recognize different HLA-A, -B, and -C allotypes and C-type lectin receptors (CD94/NKG2) binding the non-classical HLA-E molecules. (86-88)

The two main circulating subsets are $CD56^{bright}$ and $CD56^{dim}$, which play different roles within the innate immune system. (89)

$CD56^{bright}$ represents about 10% of total peripheral blood circulating NK cells, while these cells are mainly enriched in secondary lymphoid tissues (SLTs). (73) This NK cell subset is characterized by the highest expression of the inhibitory receptor CD94/NKG2A, the hematopoietic stem cell marker CD117 and of the activating receptor NKp46 compared to other NK cell subsets. (73, 90)

Moreover, $CD56^{bright}$ NK cell subset appears to be the only lymphocyte population with constitutive expression of the high-affinity heterotrimeric IL2R (IL2Rαβγ), showing a high proliferative response to picomolar concentrations of IL2. (90) However, $CD56^{bright}$ NK cells are poorly cytotoxic and are the primary source of immunoregulatory cytokines, including IFN-γ, TNF-α, TNF-β, and GM-CSF, in response to monocyte-derived cytokine stimulation. (73)

On the other hand, $CD56^{dim}$ NK cells constitute the majority of circulating NK cells and are characterized by high expression levels of CD16, which make them efficient mediators of antibody-dependent cellular cytotoxicity (ADCC) binding to opsonized targets. (73, 91) Moreover, $CD56^{dim}$ NK cells have a high content of cytolytic granules, composed by perforin and granzymes, resulting in higher cytotoxic capabilities compared to $CD56^{bright}$ NK cells. (73) $CD56^{dim}$ NK cell subset also displays a stronger expression of C-X-C motif chemokine receptor 1 (CXCR1), CX3CR1 and CD11a compared to $CD56^{bright}$ NK cells, that is reflected on migratory ability towards acute inflammatory sites. (73, 90)

$CD56^{bright}$ and $CD56^{dim}$ are considered two sequential stages of terminal NK cell maturation. Indeed, $CD56^{bright}$ NK cells, together with a higher proliferative rate, show significantly longer telomeres compared to $CD56^{dim}$, which are also devoid of proliferative response. (73, 92) In addition, following hematopoietic stem cell transplantation *in vivo*, the immune reconstitution of donor-derived $CD56^{bright}$ NK cell subset precedes the appearance of the more differentiated $CD56^{dim}$ NK cells. (73, 93)

The transition from $CD56^{bright}$ to $CD56^{dim}$ NK cells involves the progressive loss of CD94/NKG2A, the downregulation of CD56, NKp46 and CD117, the expression of CD16 and the acquisition of combination of KIR molecules, in order to form a relatively stable repertoire of receptors which is mainly genetically determined. (73, 90)

4.4.2 Group 2 ILC

ILC2s are involved in several processes, including lipid metabolism, expulsion of helminth parasites as well as tissue repair. (55, 94) ILC2s are considered the innate counterpart of Th2 cells since they express the highest level of the transcription factor GATA3 and are characterized by the production of Th2-associated cytokines, such as IL4, IL5, IL9, IL13 and amphiregulin (AREG) in response to IL25, IL33 and thymic stromal lymphopoietin (TSLP). (95-97) ILC2 have been described in a variety of human tissues, including tonsils, BM, spleen, skin, adenoids, adipose tissue, lung LNs, where they play a primary role in the innate local immunity against infections in different organs due to their higher production of cytokines compare to Th2 cells. (98, 99)

ILC2s are further characterized by the expression of the transcription factor BCL11B which controls their identity, the prostaglandin D2 receptor 2 (CRTH2), the IL33 receptor (IL1RL1) and by variable levels of CD117, all involved in ILC2 localization and function. (100-103) More recently, it has been shown that ILC2s express the killer cell lectin-like receptor subfamily G member 1 (KLRG1), a co-inhibitory receptor previously reported in T and NK cells that binds to the members of the cadherin family and is upregulated during infection in response to IL25. (104, 105)

ILC2 effector-functions are mainly regulated by soluble factors including cytokines, neuronal factors, inflammatory mediators, and hormones. In addition to IL2 and IL7, which are broadly sensed by ILCs and adaptive lymphocytes, the cytokines IL4, TNF-like ligand 1 A (TL1A), TGF-β, stem cell factor (SCF) stimulate ILC2 activation, however the alarmins IL25, IL33, TSLP, and prostaglandin D2 (PGD2) are the major activators of ILC2s. (82)

4.4.3 Group 3 ILC

Group 3 ILCs, consisting of ILC3s as well as LTis, share features with Th17/22 cells, including the expression of the transcription factor retinoic acid orphan receptor isoform γt (RORγt), required for their development and function, and the aryl hydrocarbon receptor (AHR). (106) Group 3 ILCs can produce IL17, IL22 and granulocyte-macrophage colony-stimulating factor (GM-CSF) in response to IL23, IL1β, or NCR ligands, mirroring Th17/22 response. (56, 107) Regardless of the functional association with ILC3s, LTis are considered a separate ILC lineage. Indeed, LTis are involved in the secondary lymphoid organ formation during embryogenesis and adulthood and in their restoration following infection, whereas ILC3s mainly contribute to the immune responses against specific extracellular pathogens

and in the maintenance of tissue homeostasis at mucosal sites, where they are mainly localized. (106, 108, 109)

ILC3s can be further subdivided according to the expression of the NCR NKp44: human NKp44^{pos} ILC3s, largely co-expressing NKp46, are the majority in adult tonsil and intestine and represent an exclusive source of IL22, while NKp44^{neg} ILC3s are the major population in fetal LNs and preferentially express IL17 transcripts. (106)

ILC3 activation is mainly regulated by soluble factors, such as cytokines, neuronal factors, metabolites, and inflammatory mediators. Important regulatory cytokines include IL1α, IL1β, IL2, IL7, IL23, TL1A, SCF, and TSLP, which are secreted by a variety of cells including myeloid cells, T cells, epithelial cells, and stromal cells. (82, 110)

Differently from tissues, ILC3s are under-represented in the circulating lymphocyte pool. However, a subpopulation of cells phenotypically resembling to NKp44^{neg} ILC3s has been recently described in cord blood and adult PB. However, most PB CD127^{pos}CD117^{pos} ILCs express low levels of RORγt, do not produce any of the ILC cytokine signatures following stimulation with IL1β and IL23 and their transcriptome is different from that of mature ILC3s present in secondary lymphoid organs. (111, 112) Circulating CD127^{pos}CD117^{pos} ILCs are instead multi-potent ILC precursors (ILCp) that retain the ability to give rise to functionally mature helper ILC subsets, as well as to Eomes^{pos} NK cells, after in vitro culture with appropriate cytokine mix or after transfer *in vivo* into immunodeficient mice. (107, 112)

4.4.4 ILC development

ILCs originate from the BM common lymphoid progenitor (CLP) and require the common γ chain of the IL2 receptor and the transcriptional repressor ID2 for their development. (113, 114) As we reviewed in (54) ILCs, despite their similarities with T cells, arise from distinct developmental pathways and display unique epigenetic and transcriptional programs. (64) However, the study of the human ILC differentiation is still in its infancy because of the lack of comparable genetic and tracing tools of lymphoid development that are available in animal models and the heterogeneity of definition of progenitor and identification of lineages based solely on cytokine secretion or on few surrogate markers. (54) Despite these limitations, over the past years a map of human ILC development (**Figure 5**) has been under construction by taking advantage of both murine ILC-developmental model and the pre-existing model of human NK cell development that dates back before the discovery of helper ILCs. (115)

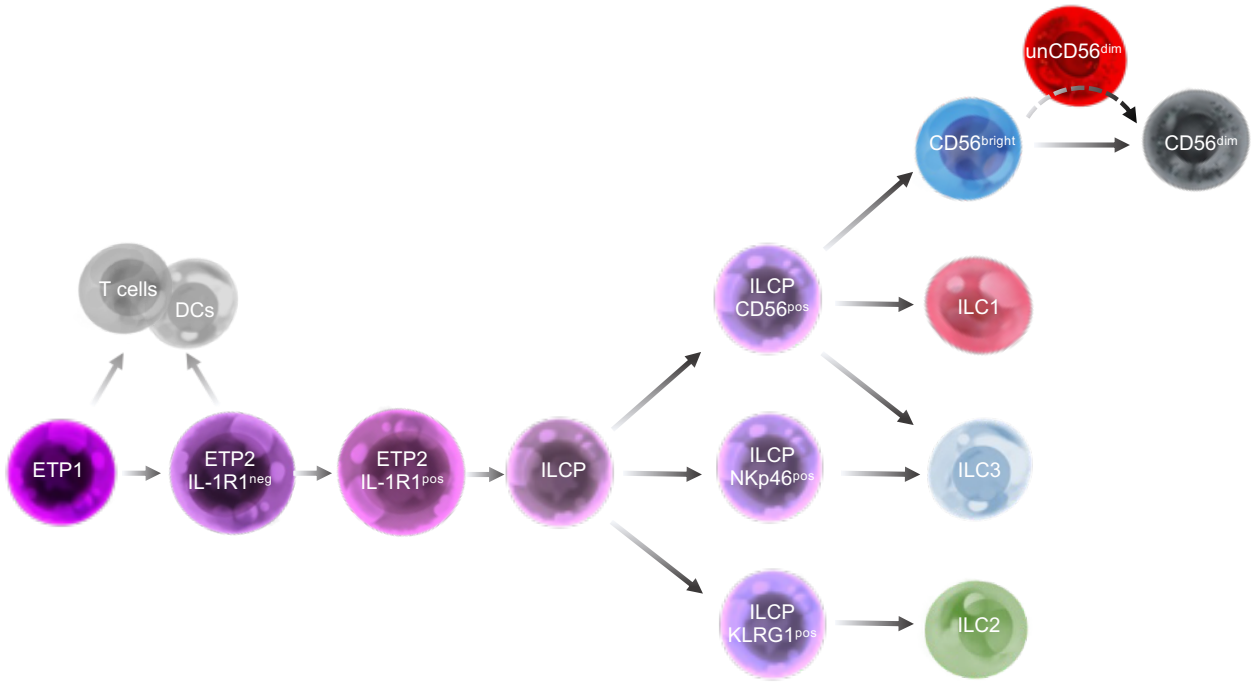

Figure 5 - Schematic representation of different stages of human ILC-poiesis.
Differentiation of ILC starts with the early tonsillar progenitors (ETPs) that still retain the ability to give rise to T cells and dendritic cells (DCs) and differentiate into ILC precursor (ILCps) that branches into progenitors with restricted differentiation potential and give rise to different mature ILC subsets. (54)

The early tonsillar progenitors (ETPs), mainly localized in SLTs, are the most immature ILC progenitors identified in humans. ETPs are subdivided into $Lin^{neg}CD34^{pos}CD10^{pos}CD117^{neg}$ ETP1 and $Lin^{neg}CD34^{pos}CD10^{neg}CD117^{pos}$ ETP2. (115, 116) Both ETP1s and ETP2s are multipotent and could also give rise to T cells and DCs in vitro. (115, 116) In addition, ETP2s can be subdivided into two subsets based on IL1R1 expression. $IL1R1^{neg}$ ETP2s have a residual T-cell and DC potential, whereas $IL1R1^{pos}$ ETP2s are ILC restricted. These population are also characterized by a unique transcription factor signature: ETP1 are $RAG1^{pos}$ and express low levels of ID2 and RORγt, $IL1R1^{neg}$ ETP2s are $ID2^{pos}RORγt^{pos}$ and retain a low expression of RAG1, whereas $IL1R1^{pos}$ ETP2s are $ID2^{pos}RORγt^{pos}RAG1^{neg}$. (117)

The following step of differentiation is $lin^{neg}CD34^{neg}CD7^{pos}CD127^{pos}CD117^{pos}CRTH2^{neg}$ ILCp, characterized by phenotype similarities with ILC3 subset but with the potential for generating all mature helper- and cytotoxic-ILCs, which has been identified in human cord and adult PB as well as fetal liver and several adult tissues. (112)

Consistent with their differentiation potential, ILCps express high levels of TFs such as ID2, GATA3, TCF-7 and ZBTB16. In contrast, moderate to low levels of the lineage-determining TFs RORγt, T-bet, Eomes, cytokine receptors and signature cytokines have been found.

(112) ILCps show a migratory profile including the expression of L-selectin (CD62L) and β2-integrin (CD18). (112) This, together with the presence of ILCps at mucosal sites, is in line with the hypothesis that these cells can populate mucosal tissues where they terminally differentiate into mature ILCs in response to local and environmental triggers, during both homeostatic and inflammatory conditions. (115, 118, 119)

Different ILCp populations with a restricted differentiation potential have been recently described and can be identified based on the expression of CD56, NKp46 and KLRG1. $CD56^{pos}$ ILCps show a restricted potential for NK cells, ILC1s and ILC3s, $NKp46^{pos}$ ILCp predominantly differentiate into ILC3s, whereas $KLRG1^{pos}$ ILC precursors mostly develop into ILC2s. (119, 120)

In NK cell development, which was characterized prior to the discovery of helper ILCs, immature NK cells (iNKs) are the last stage of NK cell differentiation before becoming mature $CD56^{bright}$ NK cells and show phenotypic features that overlap those of ILCp. The transition from iNKs to mature $CD56^{bright}$ NK cells is marked by the acquisition of CD94-NKG2A expression, responsible for the MHC-I-dependent inhibition, and other NK cell receptors, including NKG2D and NKp46, but also by the strong induction of the transcription factor T-bet. (121, 122) This transition from ILCps to mature NK cells is further marked by the downregulation of CD117, CD33, and CD127, by the acquisition of the ability to mediate killing perforin-release- or Fas-ligand-mediated, and by the capacity to produce IFN-γ. (72, 89, 116, 123) The expression of CD56 antigen increases gradually during NK cell development from ETP2s to $CD56^{bright}$ and then decrease from $CD56^{bright}$ to $CD56^{dim}$. (89, 116) The biological meaning of high- or low-expression of this molecule on NK cell surface has not been elucidated so far, however it has been proposed that CD56 antigen may play a role during the developmental process of NK cell, mediating a synapse between precursors and stromal cells. (124)

Moreover, an additional NK cell subset characterized by a $CD56^{dim}CD16^{neg}$/$CD56^{low}CD16^{low}$ phenotype and the expression of surface markers of mature NK cells, such as NKG2D and NKp30, has been identified. (125) This subset, named unconventional $CD56^{dim}$ NK cells ($unCD56^{dim}$), possesses multifunctional ability and superior effector-functions. Indeed, $unCD56^{dim}$ NK cells are endowed with potent cytotoxicity, significantly higher than that of $CD56^{dim}$, and an IFN-γ producing capability comparable to that of $CD56^{bright}$ in response to cytokine stimulation. (125-127) $UnCD56^{dim}$ NK cells are barely detectable in the PB and is mainly enriched in the BM, while their presence in extramedullary tissues has not been investigated so far. (125, 126) In the context of the lymphopenic environment of patients

affected by hematologic malignancies and which underwent haplo-HSCT, others and we reported that unCD56^{dim} NK cells are by far the largest subset of NK cells immune-reconstituting in the first 2-4 weeks after the transplant, compensating the low frequency of the conventional cytotoxic CD56^{dim} NK cells. (125, 128) These data, together with the transcriptional and phenotypic characteristics of unCD56^{dim} NK cells, intermediate between that of CD56^{bright} and CD56^{dim} NK cells, suggest that this subset could represent an additional or alternative stage of NK cell differentiation that drives the NK cell maturation process (**Figure 5**). (125, 126)

4.5 Innate lymphoid cells in myelodysplastic syndromes

4.5.1 NK cells

NK cells are the only ILC subset that have been investigated in MDS patients so far. Indeed, past studies described abnormal NK function, including diminished ADCC and NK cytotoxicity, have been described in a condition named “preleukemia”, a definition that was used to describe the MDS patients with a propensity to progress to AML. (129, 130)

These observations were subsequently confirmed by more recent studies. Indeed, a deficiency in NK cell compartment was observed in the PB of high-risk MDS patients and was associated to a defective differentiation due to an increased percentage of CD56^{bright} and a diminished fraction of CD56^{dim} NK cells. (131) Moreover, NK cells in MDS patients are characterized by an impairment in NK cell cytotoxicity, especially in high-risk patients, correlated with a reduced expression of the activating DNAX-accessory molecule-1 (DNAM-1) and NKG2D receptors on NK cell surface. (52, 131-133)

These observations, together with the implication of NK cells in relapse control following allogeneic HSCT for myeloid leukemia, suggest that NK cells are an extremely important component of immunological tumor surveillance and their decrease in number and/or function in MDS patients supports MDS clone immune evasion and disease progression to AML. (134)

Moreover, it has been shown that *GATA2* deficiency, a transcriptional regulator of hematopoiesis involved in the development of NK cells, monocytes, dendritic cells and B cells, strongly predisposes pediatric patients to the onset of hematological malignancies, especially MDS with the possibility to evolve into AML. (135)

Hence, novel strategies to restore NK cell function and overcome immune suppression in patients with MDS has been proposed. For example, the use of a bispecific killer cell engagers (BiKE) that targets CD16 on cytotoxic CD56^{dim} NK cells along with the myeloid

differentiation antigen CD33 (CD16xCD33) can induce killing of both $CD33^+$ MDS targets and $CD33^+$ immunosuppressive MDSC targets. (136) In addition, several clinical trials are testing the benefits of NK cell infusion for the treatment of MDS with or without HSCT (NCT01593670, NCT00526292, NCT03300492, NCT01904136, NCT00402558, NCT02727803, NCT00392782, NCT01386619, NCT01621477).

4.5.2 Helper ILC

Despite growing evidence highlights an important role of helper ILCs in generating a suppressive and tolerant environment, essential for tumor progression and aggressiveness, their involvement in MDS onset and outcome has not been investigated so far.

In the context of hematologic malignancies, others and we demonstrated that ILC subset distribution and function is affected in AML patients.

ILC1s are enriched and hypofunctional in the peripheral blood and marrow of AML patients compared to healthy donors while a $CD56^{pos}$ ILC1-like population ($Lin^{neg}CD56^{pos}CD94^{pos}CD16^{neg}CD127^{pos}$) shows impaired cytotoxicity in AML patients at diagnosis that is restored in patients who achieve remission. (137, 138) In BM niche of AML patients, mesenchymal stem cell-derived PGD2 activates ILC2s via the CRTH2 receptor to secrete IL5, which in turn drive the expansion of Treg populations and promote AML clone proliferation. (139) A similar observation has been made in acute promyelocytic leukemia, a subset of AML in which tumor-derived PGD2 and NKp30-BH76 engagement activates circulating ILC2s to secrete IL13 that stimulates MDSCs. (140) Finally, also significant decrease in NCR^+ ILC3s but not NCR^- ILC3s were detected in the peripheral blood of AML patients, even if no detectable differences in IL17A or IL22, key ILC3-related cytokines, were observed. (138)

5 Aim of the thesis

MDS are a heterogenous group of myeloid neoplasms that primarily affect elderly people and, in the context of population aging, MDS incidence is set to increase substantially. MDS patients have a variable risk of progression to AML and are characterized by ineffective hematopoiesis, cytogenetic changes and molecular abnormalities.

In the past decade significant efforts have been made to understand the pathophysiology of MDS. It has become increasingly evident that early driver mutations dictate the clonal proliferation of myelodysplastic cells and the trajectories of evolution of MDS with distinct clinical phenotypes. However, the definite pathogenetic mechanism of MDS is still not fully clarified, hindering the clinical decision-making process. Indeed, frontline pharmacological therapies, mainly based on the use of HMAs, are not curative and the current patient risk stratification ineffectively predicts patient prognosis and response to therapies.

The dysregulation and dysfunction of the immune system with the acquisition of an immunosuppressive signature are emerging as important characteristics in the prognosis and the clinical outcome of MDS patients. Indeed, although MDS patients are generally lymphopenic, cellular immunity seems to be up-regulated in low-risk MDS patients and impaired in high-risk MDS patients. For this reason, a deeper investigation of the immune populations is essential to identify new clinically relevant MDS predictive markers. Furthermore, the alteration of the bone marrow niche together with the cytokine unbalance further contributes to increase genomic instability, to repress normal hematopoiesis and to determine an immune tolerant microenvironment in the of MDS patients. Despite this evidence, the primary orchestrators of the dysregulated MDS microenvironment have not yet been identified.

In this context, ILCs are emerging as important actors in the pathophysiology of different cancers, by generating a suppressive and tolerant environment. Others and we demonstrated that ILC subset distribution and functions in AML contribute to immunotolerance. However, a comprehensive immune-phenotypic characterization of ILCs aiming at investigating their involvement in MDS pathogenesis and progression is still lacking.

The solely ILC subpopulation investigated in MDS is represented by NK cells. However, the experimental data available nowadays are contradictory. For example, reduced expression of NKG2D on NK cells has been showed in (52), while (141) and (131) demonstrated an increase and no changes, respectively, in NKG2D expression in MDS patients; (52) reported a reduction in NKp30 expression on NK cells of MDS patients while no reduction was shown

in (131). these contradictory data could be attributable to various causes, such as the restricted cohort of patients, which does not suit with the heterogeneity of the disease, the lack of a precise and univocal patient risk-stratification, and the use of only BM or PB samples.

Our working hypothesis is that ILCs could have important roles in MDS pathogenesis, severity and in the response to HMA treatment by inducing a de-regulation of other immune cells and by creating a tolerant microenvironment that, in turn, increases genomic instability and facilitates disease progression.

In this PhD thesis, we aim at performing a deep characterization of cytotoxic and helper ILC frequency, phenotype and function in a large cohort of MDS and AML patients during the natural history of the disease and in the response to HMA treatment.

Indeed, we believe that the clarification of the immunologic profiles across MDS subtypes and the creation of a new prognostic/diagnostic scoring system comprehensive of immunologic data, could further help to better stratify MDS patients, rapidly identify patients who really benefit from HMA therapies as well as to develop novel effective immunotherapies.

6 Materials and methods

6.1 Patient and healthy control enrollment

In collaboration with the Unit of Leukemia and Myelodysplasia of the Humanitas Cancer Center (Rozzano, Milan, Italy), we prospectively recruited a total of 195 patients with a suspect of MDS.

BM and PB samples were collected at the time of diagnosis, and during the follow-up (every 4 months for patients receiving HMA treatment and every year for the others), for a total of 681 samples (adding up to a mean of 1.6 time point per patient).

Moreover, in collaboration with the Unit of Bone Marrow Transplant of the Humanitas Cancer Center, we enrolled 22 patients affected by hematologic malignancies (4 MDS and 18 lymphoma) who were treated by our published haplo-HSCT protocol. (142). Briefly, recipients received RIC starting from the 6th day before HSC infusion to suppress their immune system and to allow an adequate engraftment (143). To prevent graft versus host disease, cyclophosphamide was administered by intravenous infusion at days +3 and +4 to selectively deplete alloreactive T cells and tacrolimus and mycophenolate mofetil were administered starting from the day +5 (**Figure 6**). (143)

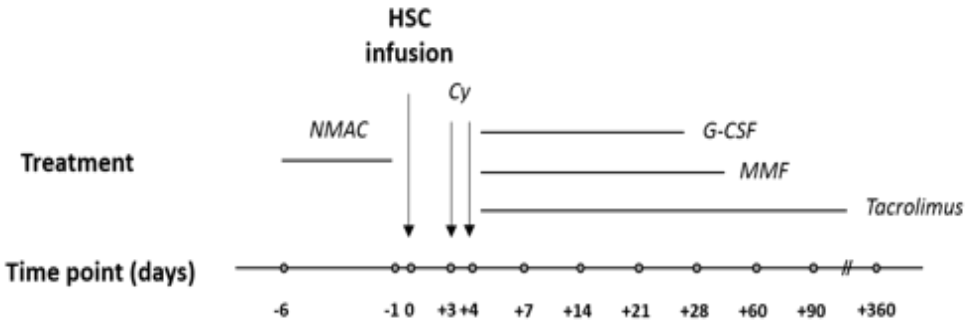

Figure 6 - Baltimore protocol used to treat patients affected by hematologic malignancies and receiving a haplo-HSCT.
Cy: Cyclophosphamide; GCSF: Granulocyte Colony Stimulating Factor; HSC: Hematopoietic stem cells; MMF: Mycophenolate Mofetil; NMA: non myeloablative.

We collected PB samples from both donors and recipients before the transplantation and from the recipients every week for the first month post-h-HSCT and then every month till one year after the transplant, ranging from day +14 to day +386, adding up to a median of 6 samples per patient.

In addition, in collaboration with the Unit of Orthopedics Hip and Prosthesis at Humanitas, we also enrolled 15 age and sex matched healthy controls (HCs) undergoing total hip replacement interventions.

The Institutional Review Board of Humanitas Clinical and Research Institute approved all clinical and experimental procedures. All patients signed an informed consent form in accordance with the Declaration of Helsinki.

6.2 Mononuclear cell isolation from peripheral blood and bone marrow samples

BM and PB samples were withdrawn from both patients and healthy controls in lithium heparin as anticoagulant. PB and BM samples were diluted with sodium chloride physiological solution and Phosphate-buffered saline, pH 7.4 without Calcium and Magnesium (PBS-/-) with 2mM of EDTA, respectively in a 1:1 ratio (volume-to-volume) and mixed gently.

PB mononuclear cells (PBMCs) and BM mononuclear cells (BMMCs) were isolated by density-gradient centrifugation using Lympholyte®-H Cell Separation Media (Cedarlane, Burlington, North Carolina, USA) according to manufacturer's instructions. Briefly, 30 mL of diluted PB or BM were stratified on 17,5 mL of Lympholyte®-H Media in a 50 mL conical tube (Corning, Reynosa, Tamaulipas, México) and centrifuged for 30 minutes (min) at 400 relative centrifugal force (rcf) at room temperature (RT) without brake.

The interphase ring, containing PBMCs or BMMCs between Lympholyte®-H and plasma, was collected and washed with physiological solution or PBS-/- with 2mM of EDTA, respectively. When necessary, cells were resuspended in Ammonium-Chloride-Potassium (ACK) lysis buffer for 5 min at 4°C to remove red blood cells. PBMCs or BMMCs were then counted and frozen in cryovials (Globe Scientific INC., Paramus New Jersey, USA) in a final volume of 1 mL of Fetal Bovine Serum (FBS) (Lonza, Basel, Switzerland) containing 10% Dimethyl Sulfoxide (DMSO) (Sigma Aldrich, St. Louis, Missouri, USA), as cryoprotectant.

6.3 Cell lines

6.3.1 K562

The human leukemic cell line K562 (ATCC® CCL-243™) is a lymphoblastoid immortalized cell line derived from a patient affected by CML in blast crisis. The lack of expression of any MHC-I molecule makes this cell line a highly sensitive *in vitro* target for NK cell cytotoxicity assays. K562 cells were obtained from Clinical and Research Institute Humanitas Cells Bank and tested for the absence of mycoplasma infection before the usage. Cells were cultured in Iscove's Modified Dulbecco's Media (IMDM) (Lonza) supplemented with 10% FBS (Lonza); 1% Penicillin-Streptomycin (Invitrogen, Paisley, UK); 1% Ultra Glutamine (Lonza) and seeded in cell flasks with filter cups (Corning Inc., New-York, USA) at a density

of 10^5-10^6 cells/mL in a humidified atmosphere at 37°C with 5% CO2. Cells were split every 2/3 days to allow cell expansion, using fresh medium.

6.3.2 721.221.G

Mycoplasma free B-lymphoblastoid 721.221-G cell line was obtained from Clinical and Research Institute Humanitas Cells Bank. These cells derive from the LCL 721.221 (ATCC® CRL-1855™) cell line transfected with the complementary (cDNA) encoding for HLA-G1, which allows the surface exposure of the HLA-E molecule, a major ligand for the CD94/NKG2 receptors. (144) 721.221-G cells were cultured in Roswell Park Memorial Institute (RPMI) 1640 Complete Medium (Lonza) consisting of RPMI supplemented with 10% FBS (Lonza); 1% Penicillin-Streptomycin (Invitrogen, Carlsbad, California, USA); 1% Ultra Glutamine (Lonza), and were maintained in the same condition culture as K562 cell line.

6.3.3 OP9

Mycoplasma free murine OP9 (ATCC® CCL-2749™) cell line is an immortalized MSCs cell line established from newborn op/op mouse calvaria. These cells are commonly used as feeder layer to induce the *in-vitro* differentiation of HSCs into lymphoid, myeloid or erythroid lineages. OP9 cells were cultured in Dulbecco's Modified Eagle Medium (DMEM) with 1 g/L glucose (Lonza) supplemented with 20% FBS (Lonza); 1% Penicillin-Streptomycin (Invitrogen); 2.2 g/L sodium bicarbonate (Sigma Aldrich). This adherent cell line was cultured in cell flasks with filter cups (Corning Inc.) at a density of between $4*10^3$ and $1*10^4$ cells/cm^2 in a humidified atmosphere at 37°C with 5% CO2. Medium was changed every 2 to 3 days and subculture was done once a week to allow cell expansion avoiding confluence which may result in osteoblast/adipocyte differentiation.

6.4 Extensive multi color flow cytometry

All the flow cytometry experiments were performed in batch on frozen cells to minimize variability and were acquired at BD FACSymphony™ A5 flow cytometer (San Jose, California, USA).

The anti-human monoclonal antibodies (mAbs) listed in **Table 5** were used for the analysis of the phenotype and function of ILCs in HCs and patients.

Fluorochrome	Antibody	Company	Clone	Superficial/ Intra-cellular (IC) staining	Experiment
PE-Cy5	**CD107a**	BD	H4A3	SUP	Functional assay
BV786	**CD117**	Biolegend	104D2	SUP	ILC panel, Precursor panel, Functional assay, Differentiation assay
BV480	**CD11b**	BD	D12	SUP	Precursor panel, Differentiation assay
APC-H7	**CD127**	eBioscience	eBioRDR5	SUP	ILC panel, Precursor panel, Functional assay, Differentiation assay
BV510	**CD14**	Biolegend	M5E2	SUP	ILC panel, Functional aasay
BUV805	**CD14**	BD	M5E2	SUP	Precursor panel
FITC	**CD14**	BD	M5E2	SUP	Differentiation assay, Sort
FITC	**CD15**	Beckman Coulter	80H5	SUP	ILC panel, Functional assay, Differentiation assay
BUV395	**CD15**	BD	W6D3	SUP	Precursor panel
BUV395	**CD158b1b2j**	BD	CH-L	SUP	ILC panel, Differentiation assay
BUV737	**CD16**	BD	3G8	SUP	ILC panel, Precursor panel, Functional assay, Differentiation assay
PE	**CD16**	BD	3G8	SUP	Sort
BV421	**CD161**	Biolegend	HP-3G10	SUP	Precursor panel, Differentiation assay
FITC	**CD19**	BD	4G7	SUP	ILC panel, Precursor panel, Functional assay, Sort, Differentiation assay
FITC	**CD20**	Biolegend	2H7	SUP	ILC panel, Precursor panel, Functional assay, Differentiation assay
FITC	**CD203c**	Biolegend	NP4D6	SUP	ILC panel, Precursor panel, Functional assay, Differentiation assay
BUV661	**CD3**	BD	UCHT1	SUP	ILC panel, Precursor panel
FITC	**CD3**	Biolegend	HIT3a	SUP	Functional assay, Sort, Differentiation assay
FITC	**CD33**	Biolegend	HIM3-4	SUP	ILC panel, Sort, Functional assay
BV711	**CD33**	Biolegend	WM53	SUP	Precursor panel
FITC	**CD34**	Biolegend	561	SUP	ILC panel, Functional assay
APC	**CD34**	Biolegend	581	SUP	Precursor panel, Differentiation assay
BUV496	**CD38**	BD	HIT2	SUP	Precursor panel, Differentiation assay
BV605	**CD45RA**	Biolegend	HI100	SUP	Precursor panel, Differentiation assay
BUV563	**CD56**	BD	NCAM16.2	SUP	ILC panel, Precursor panel, Functional assay, Differentiation assay
BV605	**CD57**	Biolegend	QA17A04	SUP	ILC panel, Functional assay
Pe-CF594	**CD57**	Miltenyi	REA769	SUP	Differentiation assay
PE-CF594	**CD69**	BD	FN50	SUP	ILC panel, Functional assay
BUV805	**CD8**	BD	SK1	SUP	Functional assay, Differentiation assay
BV570	**CD8a**	Biolegend	RPA-T8	SUP	ILC panel, Precursor panel
PE	**CD94**	BD	HP-3D9	SUP	ILC panel, Precursor panel
BUV661	**CD94**	BD	HP-3D9	SUP	Functional assay, Differentiation assay
PerCP-Cy5,5	**CRTh2**	Biolegend	BM16	SUP	ILC panel, Precursor panel, Functional assay
BV711	**CRTh2**	BD	BM16	SUP	Differentiation assay
FITC	**FcERI**	Biolegend	CRA-1	SUP	ILC panel, Precursor panel, Functional assay, Differentiation assay
PE	**GrzB**	BD	GB11	IC	Functional assay
BUV615	**HLA-DR**	BD	G46-6	SUP	Precursor panel
BUV395	**IFNγ**	BD	B27	IC	Functional assay
APC-R700	**IL1R1**	R&D	Polyclonal	SUP	Precursor panel, Differentiation assay
PE-Cy7	**Ki67**	Biolegend	Ki-67	IC	Functional assay
PE-Cy7	**NKG2A**	Miltenyi	REA110	SUP	ILC panel, Differentiation assay
APC-R700	**NKG2C**	R&D	134591	SUP	ILC panel
BV650	**NKG2C**	BD	134591	SUP	Functional assay, Differentiation assay
PE-Cy5	**NKp30**	Beckman Coulter	Z25	SUP	ILC panel
PE-Cy5	**NKp44**	BC	Z231	SUP	Precursor panel, Differentiation assay
APC	**NKp46**	BD	9E2/NKp46	SUP	ILC panel, Functional assay
BV711	**PD-1**	BD	EH12.1	SUP	ILC panel
BV711	**Perforin**	Biolegend	dG9	IC	Functional assay
AF700	**TNFα**	Biolegend	MAb11	IC	Functional assay
BV421	**Vδ1**	Miltenyi	REA173	SUP	ILC panel
BV650	**Vδ2**	BD	B6	SUP	ILC panel

Table 5 - List of antibodies used in flow cytometry panels.
The list reports all the antibodies used in our panels acquired at BD FACSymphony. Conjugated-fluorochrome, company, clone, type of staining and the experiment in which each antibody has been used are indicated.

All antibodies were titrated on human PBMCs and used at the concentration giving the highest signal-to-noise ratio over background, as described in (145-147).
In all experiments, cells were stained for 15 min at RT with Zombie Aqua™ Fixable Viability Kit (Biolegend) to identify dead cells. Zombie Aqua™ is an amine reactive fluorescent dye that is non-permeant to live cells, but permeant to the cells with compromised membranes. Hence, dead cells will be identified for the positive signal derived from the fluorescent dye (read by BV510 channel) bound to their amine and can be excluded from the analysis to avoid false positive signals.
At the end of the incubation, cells were washed with Hanks' Balanced Salt Solution without Calcium and Magnesium (HBSS -/-) (Euroclone, Milan, Italy) with 2% FBS and EDTA 2 mM and centrifuged for 5 min, at 400 rcf. Cell pellets were then stained for 20 min at RT with the correct mix of mAbs prepared in HBSS -/- with 2% FBS and EDTA 2 mM, in a final volume of 100 ul (up to 10 x 10^6 cells).
In case of intracellular staining, the Cytofix/Cytoperm™ kit (BD Biosciences) was used according to the manufacturer's protocol.

6.5 Functional assay

To assess ILC function, BMMCs were thawed and left overnight in Roswell Park Memorial Institute medium (RPMI-1640, Lonza) with 10% FBS (Lonza) and 1% Penicillin-Streptomycin (Invitrogen) (RPMI complete) supplemented with 100 IU/mL of IL2 (Peprotech, Rocky Hill, New York, USA) at 37°C in 5% CO_2, then re-suspended at 1 x 10^6 cells/mL and cultured with K562 (1:1 BMMCs/target ratio), 771.221.G (5:1 BMMCs/target ratio) or stimulated with 10 ng/mL Phorbol 12-myristate 13-acetate (PMA) plus 0,5 µg/ml ionomycin for 4 hours in the presence of anti-CD107a antibody and Golgi Plug (BD Bioscience). After the incubation, NK cell degranulation capability was assessed evaluating the CD107a expression and Granzyme-B, perforin, TNF-α, IFN-γ ILC production was measured by intra-cellular staining (**Table 5**).

6.6 *In vitro* ILC differentiation

Cells that do not express maturity markers ($CD3^-$/$CD19^-$/$CD14^-$/$CD16^-$) were FACS-sorted from BMMCs of patients through BD FACSAria™ III (**Table 5**). Sorted cells were cultured in

serum-free Stem Cell Growth Medium (SCGM) (Cell Genix, Freiburg, Germany) supplemented with 10% FBS (Lonza); 1% Penicillin-Streptomycin (Invitrogen); 1% Ultra Glutamine (Lonza); 20 ng/ml IL7 (Peprotech); 20 ng/ml IL23 (Peprotech); 20 ng/ml IL1β (Miltenyi); 20 ng/ml IL2 (Miltenyi). Purified cells were maintained for 30 days in presence or not of OP9 and/or the hypomethylating agent 5-Azacytidine (AZA, 1μM) (Sigma Aldrich). Medium was changed every 3 to 4 days, after 7 days 20 ng/ml IL15 (Miltenyi) was added to the medium. ILC generation was assessed by flow cytometry staining (BD FACSymphony™ A5) after 10, 15, 21 and 30 days (**Table 5**).

6.7 Flow cytometry data analysis

6.7.1 Flowjo

Flow Cytometry Standard (FCS) 3.0 files, acquired through BD FACSymphony™ A5 flow cytometer, were analyzed using the FlowJo software (v 10.8.2, TreeStar Inc, Ashland, Oregon, USA).

6.7.2 Unsupervised high-dimensional cytometry data analysis

Conventionally, flow cytometry data are analyzed plotting cells in two-dimensional plots and gating them manually to identify cell population and their phenotype. (148) This manual strategy is still adequate to investigate few parameters on a single sample; however, several weaknesses arise when a more complex flow cytometry panel is applied. (149) Indeed, as the number of measured parameters increases, the number of two-dimensional plots increases exponentially, and the manual analysis become inefficient and often hard to reproduce. (148, 149)

To avoid these problems, in recent years novel computational methods that automatically identify cell population in multi-dimensional flow cytometry data have been developed. These bioinformatic tools, similar to that used in single cells RNA sequencing analyses, combine all marker information at the same time and assessing similarities among cells through a more unbiased and unsupervised approach. (148, 149)

For the analysis of high-dimensional flow cytometry data generated for this study we take advantage of PhenoGraph, one of these computational methods. (150) Before applying it, flow cytometry raw data were pre-processed with FlowJo software version 10.8.2 by using standard manual gating strategy to remove debris and doubles, dead cells and to identify ILCs. CSV files of ILCs only were then exported and submitted to PhenoGraph. (151)

6.7.3 Cluster identification and analysis with PhenoGraph

PhenoGraph is a recently developed clustering algorithm able to robustly discover subpopulations in high-dimensional single-cell data.

The input of this algorithm is a matrix of N single-cell measurements that converts into a k-nearest neighbor graph (k-NNG) in which each cell is depicted as a node that is connected to similar cells, defined as neighbor, by edges. (149, 152)

To obtain this automated partitioning of clusters, PhenoGraph requires a single user-defined constant that is the K parameter, corresponding to the number of nearest neighbors identified in the first iteration of the algorithm. (153) The best choice of k depends upon the data, generally, larger values of k reduce effect of the noise and redudancy on the classification but make boundaries between less distinct subpopulations.

Data obtained using PhenoGraph were reorganized and saved as new FCS files, one for each sample, containing information about cell clustering. These new FCS files were further analyzed using FlowJo version 10.8.2. Clusters representing <0.5% were excluded from the analysis.

Finally, PhenoGraph clusters were visualized using the Uniform manifold approximation and projection (UMAP) algorithm, which is a dimension reduction technique that can be used for visualization of high-dimensional data for their visualization in a two-dimensional scatter plot, named UMAP1 and UMAP2.

6.8 Bead based measurement of cytokines

Bead-based immunofluorescent assay (LEGENDplex™, Biolegend) was used, according to manufacturer instructions, to quantify multiple soluble analytes simultaneously in the plasma of MDS patients and HCs using a flow cytometer. In particular, the concentration of FLT3L, IL10, IL15, IL1α, IL1β, IL2, IL3, IL7, SCF and TGF-β was measured in plasma isolated from both BM and PB samples. LEGENDplex™ utilizes the same principles of sandwich immunoassays: beads of two sizes and differing levels of APC fluorescence, allowing them to be clearly distinguished from each other, and each bead set is conjugated with a specific antibody on the surface for the capture of different analyte.

Plasma samples were incubated with the bead mix for 2 hours at RT. After washing, biotinylated detection antibodies were added and incubated 2 hours at RT. Each detection antibody binds to its specific analyte bound on the capture beads. Streptavidin-phycoerythrin (SA-PE), which binds to the biotinylated detection antibodies, was subsequently added and incubated 30 minutes at RT in order to provide fluorescent signal with intensities in

proportion to the amount of bound analyte. For each bead population, the PE signal fluorescence intensity was quantified using LSRFortessa™ (BD).
The concentration of every single analyte was determined based on a known standard curve using the LEGENDplex™ data analysis software.

6.9 Statistical analysis

Statistical analysis was performed using GraphPad PRISM (version 9.0, La Jolla California, USA). Kruskall-Wallis test (non-parametric anova), two-way anova, unpaired Mann-Whitney test (non-parametric t-test), paired t-test and simple linear regression were used to compare the different variables. Results are represented as a mean ± Standard Deviation (SD). P values are two-sided and were considered significant when $p \leq 0.05$.

7 Results

7.1 Patient stratification

In order to characterize ILCs and understand their role in the pathogenesis of MDS, we enrolled a total of 194 patients subdivided in:

106 MDS patients;

52 MDS patients that progress towards AML;

36 patients having CCUS or ICUS (C), pre-malignant conditions with an increased risk of the occurrence of MDS or another myeloid neoplasm. (4)

Patient's characteristics are reported in **Table 6**.

Patient group		Classification	N	Age (median; range)	Male	Female
All patients			194	70; 21-92	119	75
C			36	62; 31-90	15	21
		CCUS	9	59; 49-90	4	5
		ICUS	27	64; 31-85	11	16
MDS			106	70; 31-92	79	27
	IPSS-R	Very low	21	73; 48-87	17	4
		Low	42	76; 31-92	30	12
		Intermediate	18	67; 48-79	12	6
		High	7	69; 62-91	4	3
		Very high	9	71; 51-82	8	1
	Blast count	Low blasts	73	74; 31-92	55	18
		High blasts	33	68; 53-91	24	9
AML post MDS			52	73; 21-86	25	27

Table 6 - Patients clinical features.
Summary table showing the characteristics of patients included in the experiments. MDS patients are subdivided both according to IPSS-R score and blast count.

Since the analysis of the immunological results according to the IPSS-R patient stratification was ineffective, due to the high variability and the inability to confirm results about NK cells reported in literature, we decided to simplify patient risk stratification and to subdivided

patients only based on blast count, that represents the main clinical parameter in the risk assessment. In particular, we identified:

low-risk patients those having blast percentage ≤4 (low blasts);

high-risk patients those with blast percentage ≥5 (high blasts);

AML post MDS patients those having a blast percentage ≥20.

In addition, samples from patients receiving HMA were divided in pre-HMA and post-HMA.

7.2 High-risk MDS patients show an altered NK cell subset distribution

BMMNCs and PBMNCs were stained with an extensive multi-color flow cytometry panel in order to investigate ILC subset distribution and phenotype. Samples were acquired to a BD FACSymphony A5 and analyzed by FlowJo. In all the experiments, after the exclusion of doublets and death cells, ILCs were identified among lineage^{neg} (CD3/CD19/CD20/CD15/CD33/CD34/CD203c/FcεRI) lymphocytes.

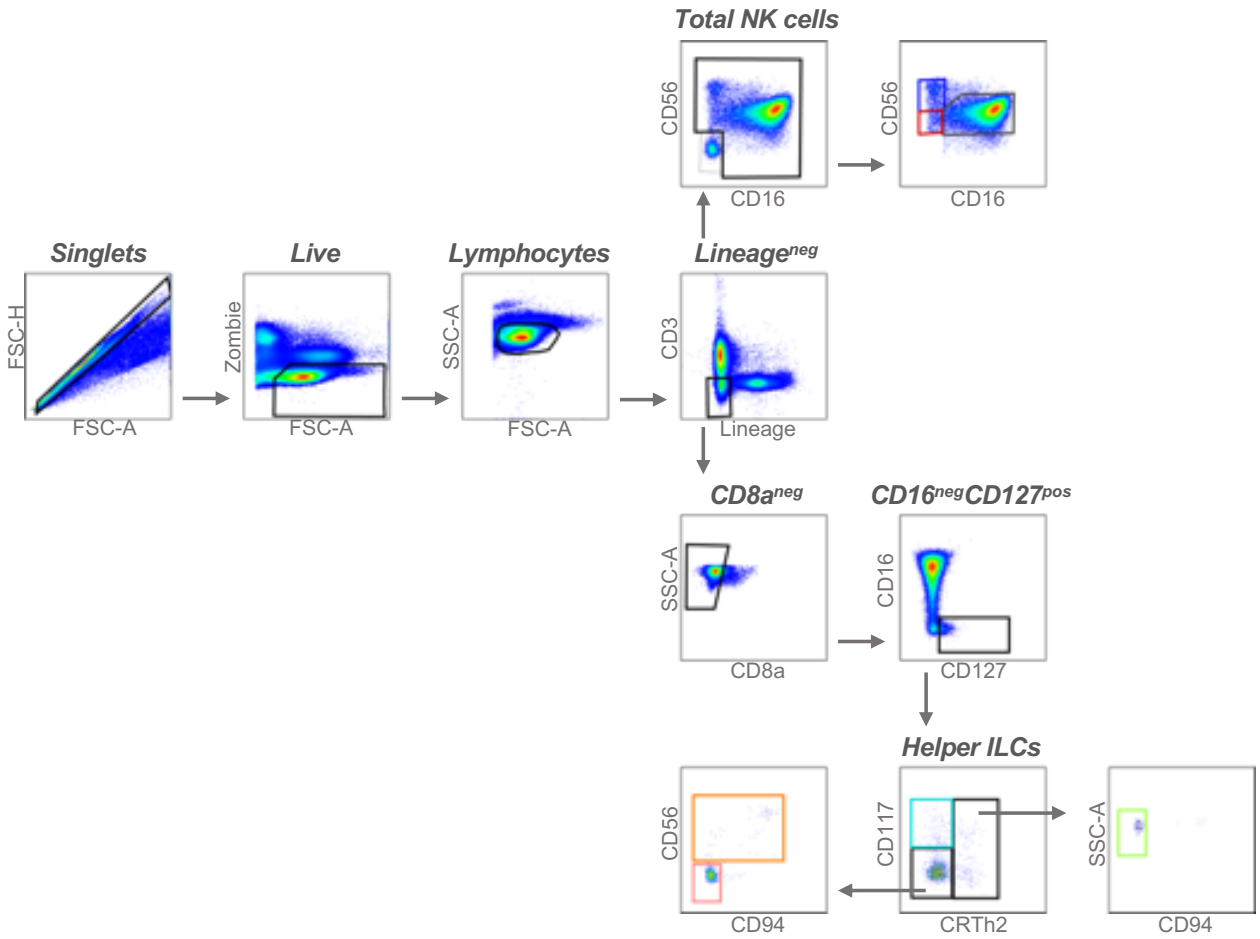

Figure 7 – ILC identification in flow cytometry data.
Representative flow cytometry dot plots from a HC showing the gating strategy used to investigate ILC subset distribution. In the last plots unCD56^{dim} (red), CD56^{bright} (blue), CD56^{dim} (grey), ILC1s (light red), CD56^{pos} ILC1-like cells (orange), ILC2s (green) and ILCp (light blue) are depicted.

Helper ILCs were identified on $CD8^{neg}/CD16^{neg}/CD127^{pos}$ cells and different subsets were distinguished based on the expression of CD117, CRTh2 and CD56. NK cell subsets were identified according to the differential expression of CD56 and CD16 surface marker expression (**Figure 7**). Notably, CD127 expression was not detected on total NK cells, confirming that no helper ILCs were included in this gate (not shown).

Since NK cells are the only ILC population that has been studied in MDS patients, we started our analysis looking at total NK cell frequencies and subset distribution in BM and PB of MDS patients. (52, 131-133) We observed that, while the frequency of total NK cells tend to increase in the BM of C and low-risk MDS patients (**Figure 8A**), their frequency in the PB of high-risk and AML patients was reduced compared to HC, C and low-risk MDS patients (**Figure 8B**). This is partially in line with previous studies reported in literature, in which a reduction of NK cell frequency was described in both BM and PB of MDS patients.

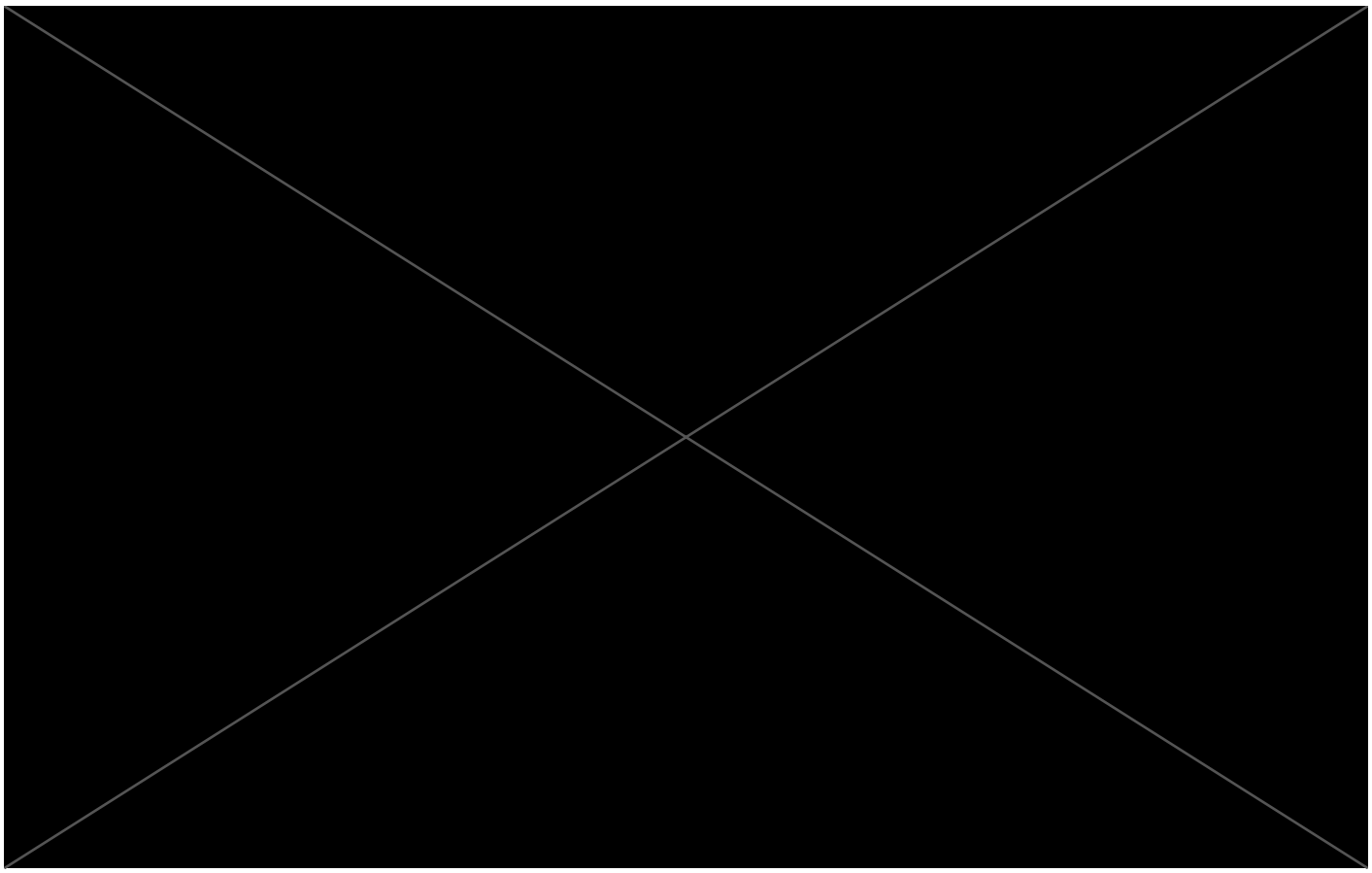

Figure 8 - NK cell and NK cell subsets distribution in MDS patients.
(A-B) Statistical graphs showing the percentage (mean + SD) of total NK cells in BM (A) and in PB (B) of MDS patients (low blasts n=73, high blasts n=33) compared to HC (n=20), C (n=36) and AML patients (n=52), all at time of diagnosis. (C-D) Statistical graphs showing the percentage (mean + SD) of $CD56^{bright}$, $CD56^{dim}$ and $unCD56^{dim}$ NK cell subsets in BM (C) and PB (D) of MDS patients compared to HC, C and AML patients, all at time of diagnosis.
*Kruskall-Wallis test; *p<0.05, **p<0.01, ***p<0.001.*

Looking at NK cell subset distribution, in the BM of high-risk MDS patients and, to a lesser extent, in low-risk MDS and AML patients we observed a reduction of the more terminally differentiated and cytotoxic $CD56^{dim}$ NK cell subset, counterbalanced by the increase of the less differentiated and cytokine producer $CD56^{bright}$ NK cell subset (**Figure 8C**). Moreover, only in the BM of high-risk patients, the low frequency of the $CD56^{dim}$ NK cells was balanced by the increased frequency of the un$CD56^{dim}$ NK cell subset (**Figure 8C**). Similar results were observed also in PB with the exception of AML patients in which we observed less striking differences (**Figure 8D**).

7.3 High-risk MDS patients show the expansion of total ILCs and altered ILC subset distribution

To understand if helper ILC subsets could be involved in the pathogenesis of MDS, we firstly assessed their frequency in different groups of patients. We observed that high-risk patients show an expansion of total helper ILCs in the BM (**Figure 9A**) and in PB (**Figure 9B**) compared to C, low-risk and AML patients. We next wonder if this expansion could be attributable to a particular ILC subset. We thus investigated the distribution of ILC subsets in BM (**Figure 9C**) and PB (**Figure 9D**) of patients. The data obtained demonstrated that high-risk MDS patients show an altered ILC subset distribution, particularly marked in PB district, with the expansion of ILC1s at the expense of ILC2 and ILCp subsets (**Figure 9E**).

Figure 9 - ILC and ILC subsets distribution in MDS patients.
(A-B) Statistical graphs showing the percentage (mean + SD) of total helper ILCs in BM (A) and PB (B) of MDS patients (low blasts n=73, high blasts n=33) compared to HC (n=20), C (n=36) and AML patients (n=52), all at time of diagnosis. (C-D) Summary graphs showing the percentage (mean + SD) of ILC1, ILC1 $CD56^{pos}$, ILC2 and ILCp in BM (C) and PB (D) of MDS patients compared to HC, C and AML patients, all at time of diagnosis. (E) Statistical graphs showing the percentage (mean + SD) of ILC1, ILC1-like $CD56^{pos}$, ILC2 and ILCp in PB of MDS patients compared to HC, C and AML patients, all at time of diagnosis.
*Kruskall-Wallis test; *p<0.05, **p<0.01, ***p<0.001*

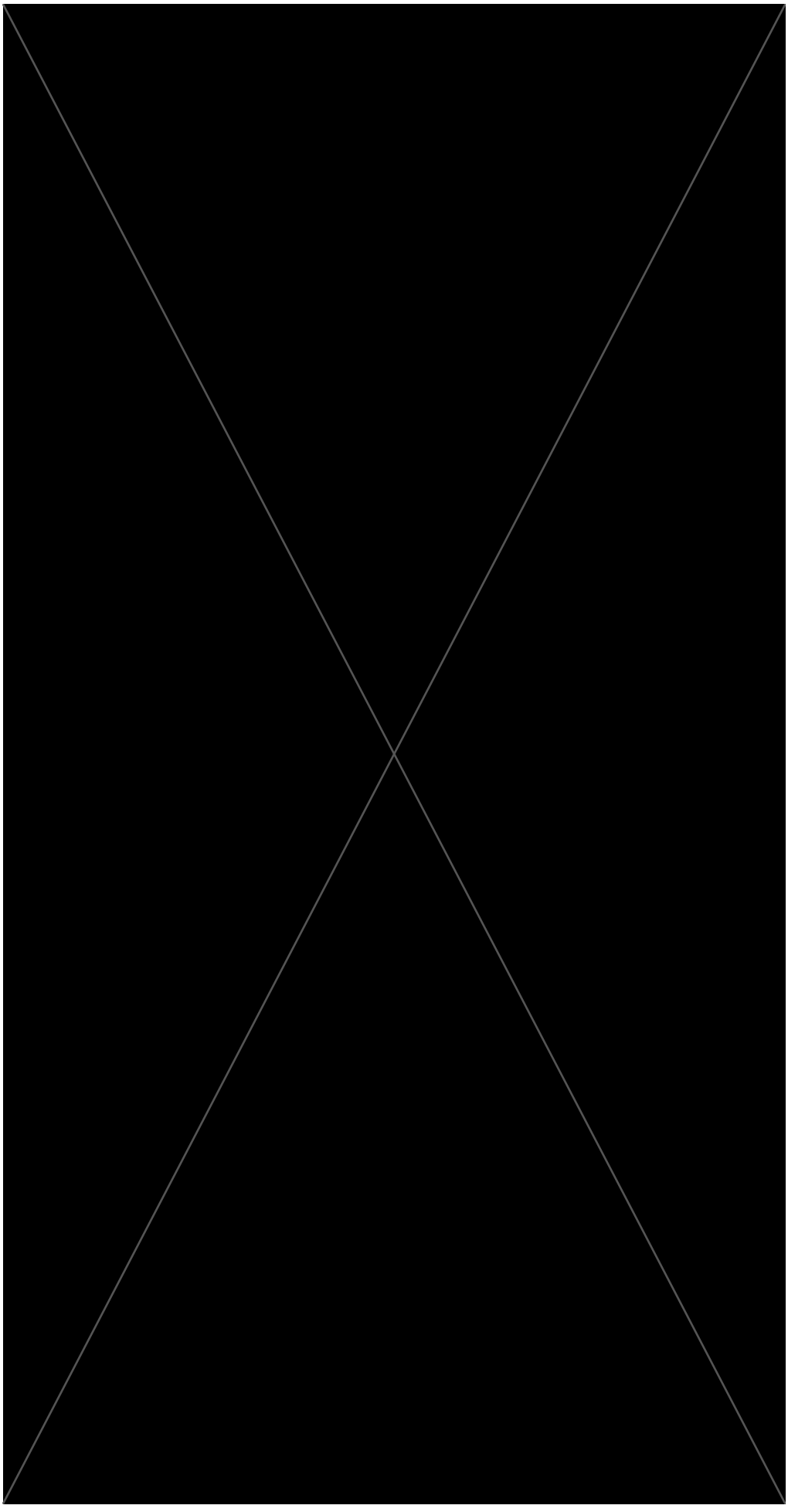

os

7.4 High dimensional single-cell analysis of flow cytometry data

Low-risk and high-risk MDS patients are characterized by differential ILC frequencies and subset distribution. We, thus, wonder if disease status could be related also to a peculiar phenotype of these cells. To gain more insight into ILC diversity, high-dimensional flow cytometry data on total ILCs from the BM of 60 patients (15 C, 15 low-risk, 15, high-risk and 15 AML) were concatenated and analyzed with Phenograph algorithm (k=30). This unsupervised computational method evaluates, at single cell level, differences/similarities of marker expression automatically defining clusters of phenotypically identical cells. (150) We also ran UMAP algorithm, to deconvolute high-dimensional flow cytometry data in a two-dimensional plot and visualize the results generated by Phenograph. (154)

Phenograph algorithm generated 22 clusters of phenotypical identical ILCs, which localize in different area of the UMAP plot (**Figure 10A**). Looking at ILCs from different group of patients, we observed that they differentially distribute on the UMAP plot, suggesting that they might be endowed with distinct phenotypes (**Figure 10B**).

To explore cluster identity we assessed marker expression. (**Figure 10C**). Clusters with a frequency lower than the 1.5% (cluster 3, 4, 9, 17 and 20) were excluded from the analysis. Clusters 10 and 12 are mainly composed by $CD56^{bright}$ and $unCD56^{dim}$ NK cells, expressing CD94/NKG2A and NCRs and differentiate for the expression of CD69 and CD8. Clusters 5 and 7 are mainly enriched by $CD56^{dim}$ NK cells expressing CD94/NKG2A, NCRs CD69 and CD8. Moreover, cells belonging to cluster 7 appear to be licensed NK cells based on the higher expression of the KIR molecule CD158b1b2j. Clusters 15, 19, 16 and 11 identify terminally differentiated $CD57^{pos}$ $CD56^{dim}$ NK cell, with a differential expression of CD158b1b2j, CD94/NKG2A and CD94/NKG2C. Cluster 14 is mainly composed by $unCD56^{dim}$ NK cells expressing CD158b1b2j and CD69, while cluster 6 comprises $CD158b1b2j^{pos}$ $CD56^{dim}$ NK cells. Cluster 13 is composed by unlicensed $CD158b1b2j^{neg}$ $CD94/NKG2A^{neg}$ $unCD56^{dim}$ and $CD56^{dim}$ NK cells. Cluster 1 is mainly composed by $CD56^{bright}CD16^{pos}$ and $CD56^{dim}$ NK cells expressing low levels of NCRs and CD94/NKG2A. Cluster 21 is enriched in $unCD56^{dim}$ and ILCps. Cluster 2 is composed by $CD69^{pos}$ $CD94/NKG2A^{pos}$ $unCD56^{dim}$ and $CD56^{dim}$ NK cells. Cluster 22 represent a contamination of progenitor cells that do not express any of the marker included in the panel. Finally, cluster 8 and 18 are mainly composed by NCR^{neg} ILC1s and are distinguished by the expression of PD-1.

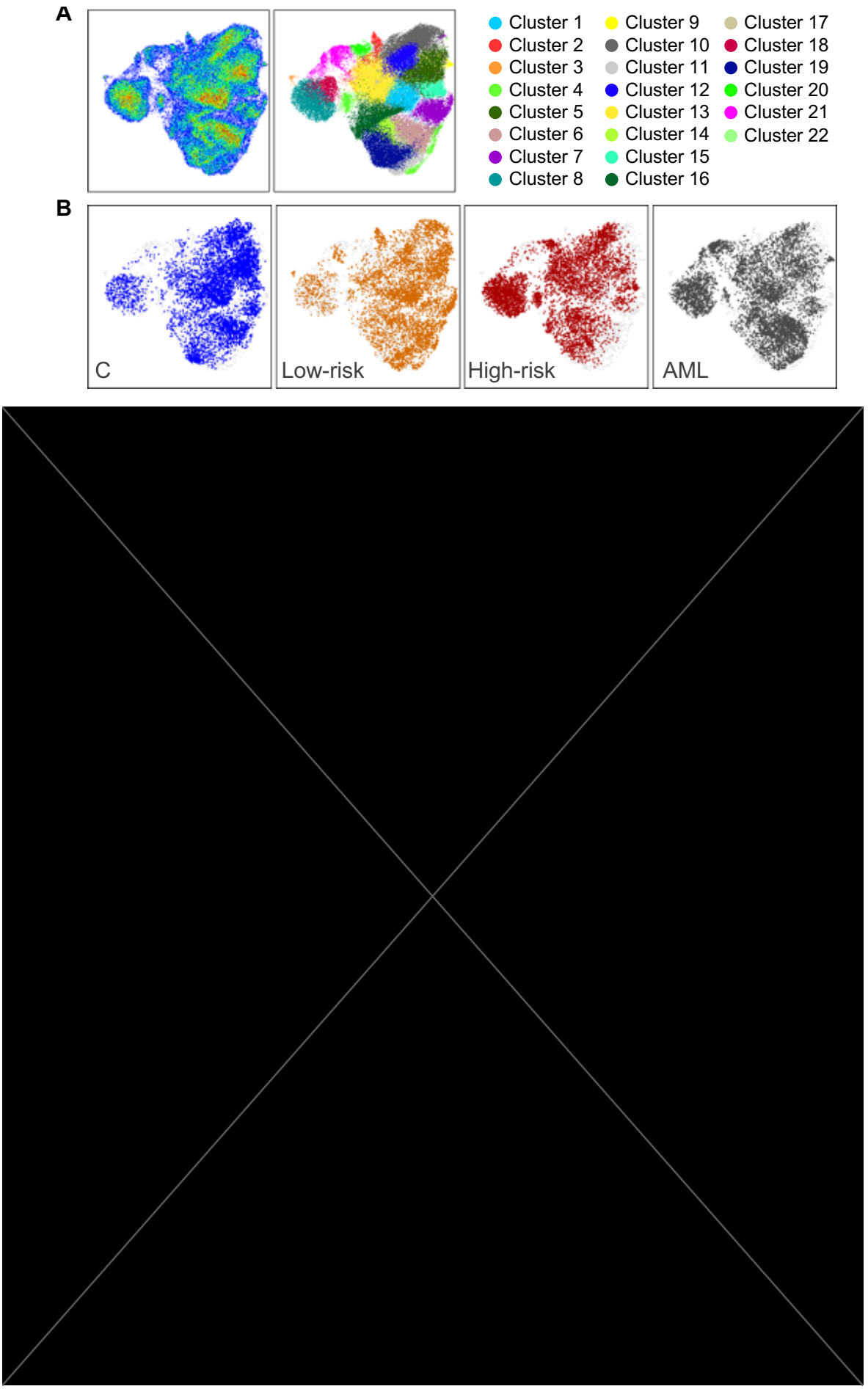
A
Cluster 1
Cluster 2
Cluster 3
Cluster 4
Cluster 5
Cluster 6
Cluster 7
Cluster 8
Cluster 9
Cluster 10
Cluster 11
Cluster 12
Cluster 13
Cluster 14
Cluster 15
Cluster 16
Cluster 17
Cluster 18
Cluster 19
Cluster 20
Cluster 21
Cluster 22
B
C
Low-risk
High-risk
AML

Figure 10 - Phenograph analysis of ILCs in MDS.
(A) UMAP plot showing the distribution of total ILCs (left) and of the 22 phenotypical identical clusters of ILCs identified by Phenograph (right). (B) UMAP plot showing the distribution of ILCs in BM of MDS patients (low-risk n=15, orange; high-risk n=15, red) compared to C (n=15, blue) and AML patients (n=15, grey), all at time of diagnosis. (C) Balloon heatmap showing the marker expression of Phenograph clusters (expressed as frequency and Median of Fluorescence Intensity, MFI. (D) Summary statistical graphs showing the frequency (mean+SD), and related phenotypes, of cluster 1, 5, 6, 7, 8, 13, 21 on total ILCs in MDS patients compared to C and AML patients, all at time of diagnosis.
*Two way anova; *p<0.05, **p<0.01, ***p<0.001.*

We next investigated cluster distribution in different patient groups and we observed that C and LR patients were characterized by the expansion of cluster 1 ,5 and 7, mainly composed by CD94/NKG2A^{pos} NCR^{pos} CD56^{dim} NK cells. On the contrary, high-risk patients were characterized by a decreased frequency of cluster 6, composed by CD158b1b2j^{pos} CD56^{dim} NK cells, and by the expansion, similarly to AML patients, of cluster 8, 13 composed by NCR^{neg} ILC1s and unlicensed CD158b1b2j^{neg} CD94/NKG2A^{neg} unCD56^{dim}/CD56^{dim} NK cells, respectively. In addition, in AML patients we observed the enrichment of cluster 21 composed by unCD56^{dim} and ILCps (**Figure 10D**).

7.5 High-risk MDS patients show an altered expression of NCRs and NKG2A in ILCs

Phenograph analysis revealed a decrease of clusters of mature NK cells expressing NKG2A and/or NCRs (clusters 1, 5, 7) in high-risk MDS and AML patients, that is counterbalanced by the increase of the cluster composed by ILC1s NCR^{neg} (cluster 8). We thus evaluated the expression of NCRs and NKG2A on BM ILCs by manual gating strategy.
We indeed confirm that ILC1s were characterized by a decreased expression of NKp30 in high-risk MDS and AML patients (**Figure 11A**). We also confirm that total NK cells from high-risk MDS and AML patients have a reduced expression of both NKp30 and NKp46 (**Figure 11B**).
Since NKG2A is mainly expressed by CD56^{bright} NK cell subset after the education process, while is progressively lost during the transition to CD56^{dim} NK cell subset, we next investigated its expression on CD56^{bright} NK cell subset. (125) We observed that high-risk MDS and AML patients show a reduced frequency of NKG2A^{pos} CD56^{bright} NK cells (**Figure 11C**) suggesting an expansion of unlicensed NK cells.
Moreover, it has been demonstrated that environmental stresses like hypoxia and high concentration of ROSs, as in MDS BM niche, can induce the downregulation of NCRs only on CD56^{dim} NK cells, we wonder if the reduction of NCR expression affects CD56^{bright} NK cells. (41, 155-158) Looking at the expression of NKp30 and NKp46, we observed a reduced

expression on both CD56^{bright} (**Figure 11D**) and CD56^{dim} (not shown) NK cell subsets from high-risk MDS and AML patients.

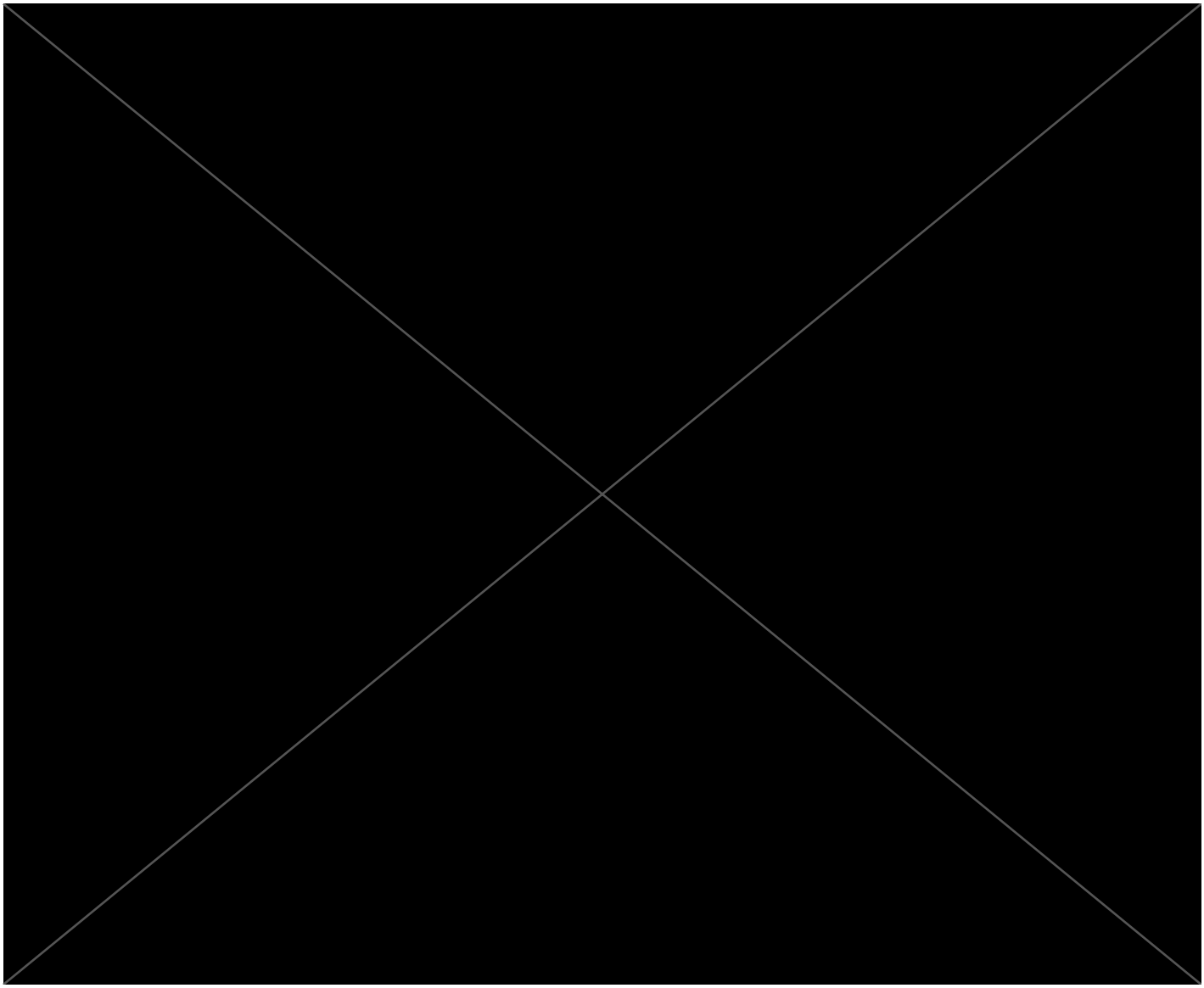

Figure 11 – NCR and NKG2A expression on ILC in MDS.
(A-D) Summary statistical graphs showing the percentage (mean+SD) of (A) NKp30 on ILC1s, (B) NCRs on total NK cells, (C) NKG2A and (D) NCRs on CD56^{bright} NK cells in BM of MDS patients (low blasts n=73, high blasts n=33) compared to HC (n=20), C (n=36) and AML patients (n=52), all at time of diagnosis.
*Kruskall-Wallis test; *p<0.05, **p<0.01, ***p<0.001.*

7.6 High-risk MDS patients show an altered ILC function

The lower expression of NCRs by both NK cells and ILC1s in high-risk and AML patients, suggest a possible impairment in their capability to recognize targets and to exert their effector functions, making them unable to carry out tumor immune surveillance. (159) Moreover, the high percentage of unlicensed NKG2A^{neg} CD56^{bright} NK cells in high-risk

patients suggests a possible inability of these cells to spare self-cells. For these reasons, we assessed the functional ability of BM ILCs performing an *in vitro* degranulation assay by using K562 and 221.G target cells.

The data obtained demonstrated that NK cells from high-risk patients have a reduced content of cytolytic molecules (Granzyme B and/or Perforin) at steady state as well as after the stimulation with K562 and 221.G targets (**Figure 12A**).

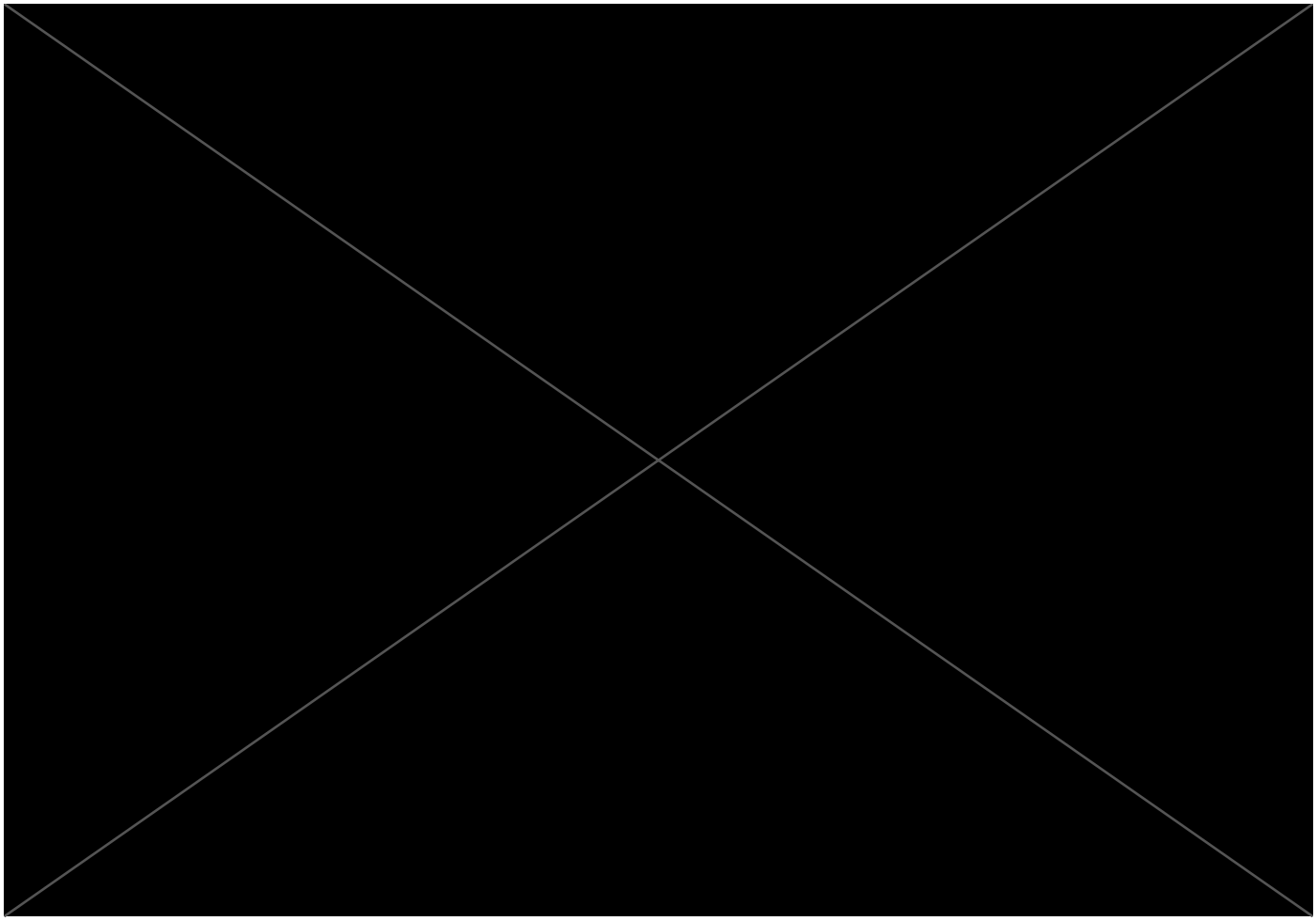

Figure 12 - ILC function in MDS patients.

(A) Summary statistical graph showing the percentage (mean+SD) of NK cells containing cytolytic granules (Granzyme B and/or Perforin) after the incubation for 4 hours alone or in presence of K562 or 221.G cell lines. (B) Summary statistical graph showing the percentage (mean+SD) of IFNγ^{pos} NK cells after the incubation for 4 hours alone or in presence of 221.G cell lines. (C) Summary statistical graphs showing the percentage (mean+SD) of IFNγ^{pos} and TNFα^{pos} ILC1s after the incubation for 4 hours in presence of PMA/Iono. (D) Summary statistical graphs showing the percentage (mean+SD) of Granzyme B^{pos} and Perforin^{pos} ILC1s after the incubation for 4 hours in presence of PMA/Ionomycin (PMA/Iono).

Results are from 2 HC (green), 4 C (blue), 4 low-risk (yellow), 4 high-risk (red) and 4 AML patients (grey), all at time of diagnosis.

*Kruskall-Wallis test; *p<0.05, **p<0.01, ***p<0.001.*

Moreover, we observed that NK cells from high-risk patients produce more IFNγ at steady state and also in presence of HLA-E^{pos} 221.G target cells (**Figure 12B**), probably attributable to the expansion of unlicensed CD56^{bright} NK cells. Unfortunately, due to staining issues, we were not able to distinguish between CD56^{bright} and CD56^{dim} cells and to assess degranulation capability of NK cells trough CD107a detection.
We also observed a decreased frequency of IFNγ^{pos} and TNFα^{pos} ILC1s from high-risk MDS and AML patients after the stimulation with PMA/Ionomycin (**Figure 12C**). Moreover, given the recently described functional impairment of BM and PB CD56^{pos} ILC1-like cells in AML patients (137) we investigated the cytolytic granule content of these cells at steady state and we observed a reduced percentage of Granzyme B^{pos} and Perforin^{pos} cells in high-risk MDS patients (**Figure 12D**).

7.7 High-risk MDS and AML patients show the expansion of ILC precursors

During the analysis of flow cytometry data for the identification of NK cells, we observed in high-risk MDS patients an increased frequency of lineage^{neg} cells that do not express neither CD56 nor CD16 (double negative cells, DN) (**Figure 13A**). The analysis of these DN cells show that they are significantly increased in the BM of high-risk MDS patients compared to

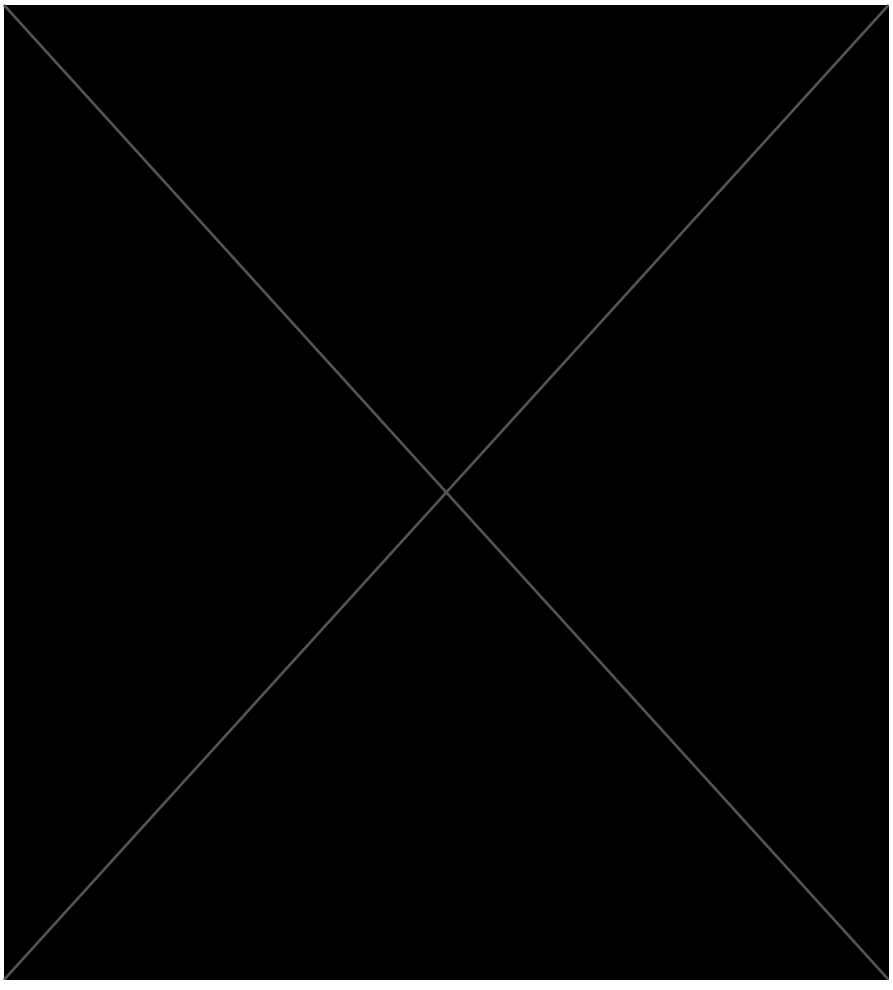

Figure 13 – Detection of DN cells in MDS patients.
(A) Representative dot plot of CD56 versus CD16 expression on lineage negative viable lymphocytes in the PB of a HC (left) and of a high-risk patient at time of diagnosis (right). (B-C) Statistical graphs showing the percentage (median + SD) of CD56negCD16neg double negative (DN) cells in BM (B) and PB (C) of MDS patients (low blasts n=73, high blasts n=33) compared to HC (n=20), C (n=36) and AML patients (n=52), all at time of diagnosis.
*Kruskall-Wallis test; *p<0.05, **p<0.01, ***p<0.001, ****p<0.0001.*

low-risk MDS patients (**Figure 13B**). We also observed a significant expansion of circulating DN cells in high-risk MDS patients (**Figure 13C**).

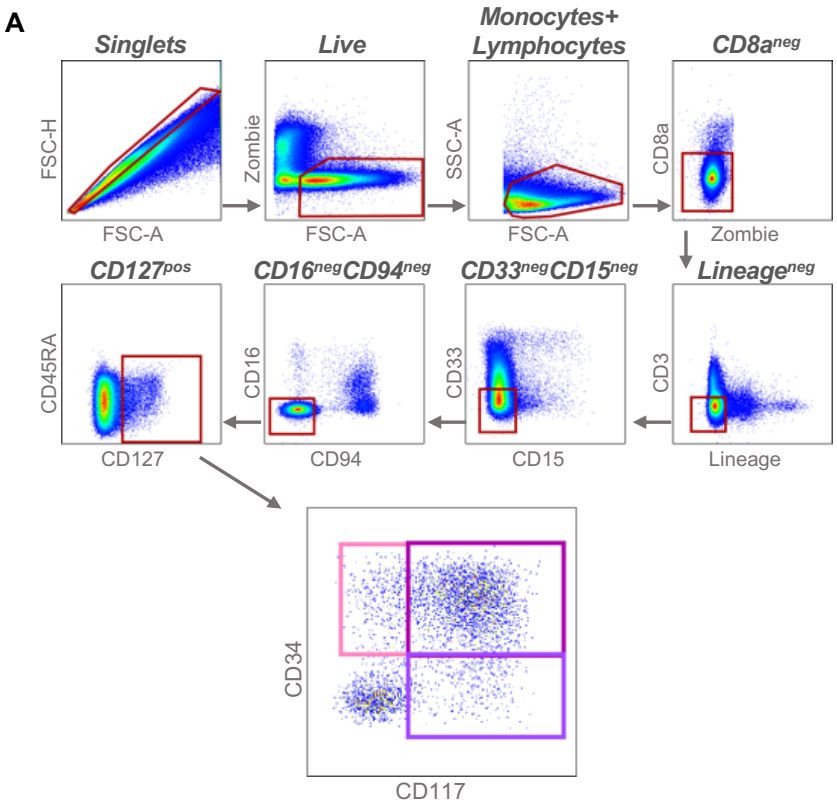

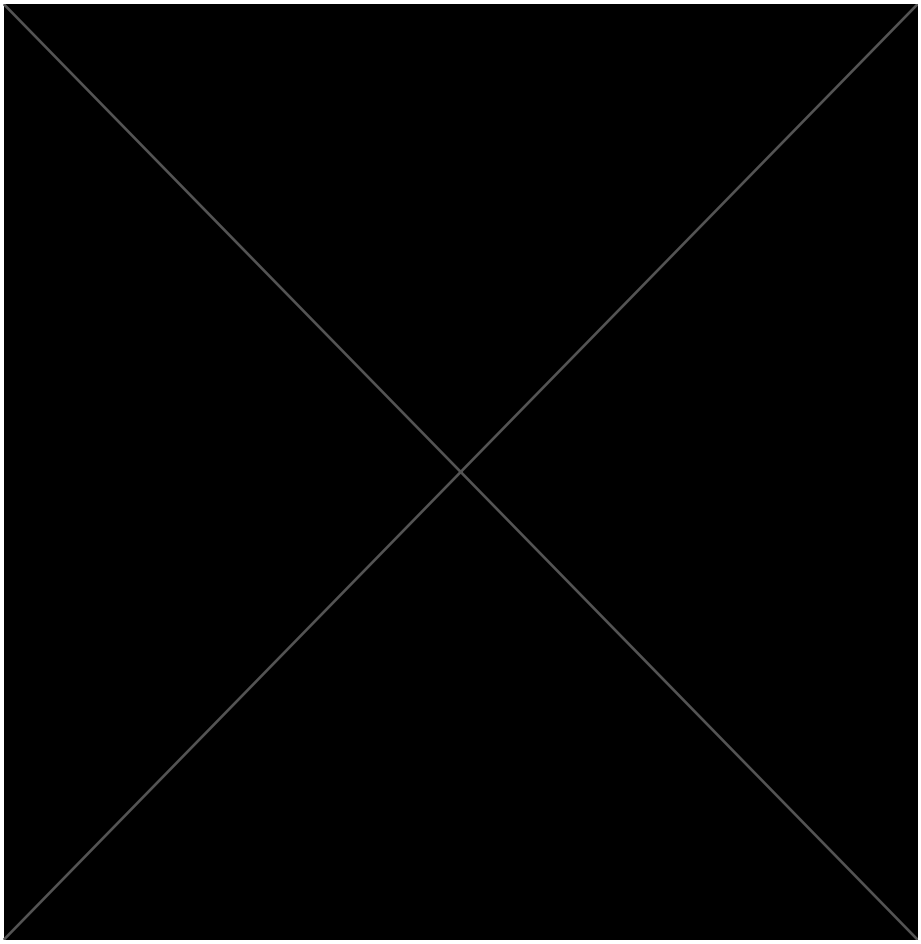

Figure 14 - ILC precursors in MDS patients.
(A) Representative flow cytometry dot plots from a HC showing the gating strategy used to investigate ILC precursor distribution. In the last plots ETP1 (light pink), ETP2 (pink) and iNK/ILCp (violet) are depicted. (B-C) Summary graphs showing the distribution (median + SD) of different ILC maturation stage on total ILC precursors in BM (B) and PB (C) of MDS patients compared to HC, C and AML patients, all at time of diagnosis. (D-E) Statistical graphs showing the percentage (median + SD) of CD34+CD117+ ETP2s on total precursors in BM (D) and CD34+ ETPs on total precursors in PB (E) of MDS patients compared to HC, C and AML patients, all at time of diagnosis.
*Kruskall-Wallis test; *p<0.05, **p<0.01, ***p<0.001, ****p<0.0001.*

Since we observed a decreased frequency of total NK cells with a maturation skewing toward less differentiated NK cell subsets, we wonder if among these DN cells, besides HSCs and MDS/AML clones, there were also ILC precursors. To this aim, we developed a second extensive multi-color flow cytometry panel to investigate ILC precursors and different differentiation steps.

According to literature, ILC precursors were detected as $CD3^{neg}/CD19^{neg}/CD20^{neg}/CD15^{neg}/CD33^{neg}/CD203c^{neg}/Fc\varepsilon RI^{neg}/CD16^{neg}/CD45RA^{pos}/CD127^{pos}$ and different step of differentiation were identified according to differential expression of CD34 and CD117: $CD34^{pos}CD117^{neg}$ ETP1s, $CD34^{pos}CD117^{pos}$ ETP2s and $CD34^{neg}CD117^{pos}$ iNK/ILCp precursors (**Figure 14A**). (54) Indeed, as mentioned in the introduction, iNKs, the last step of differentiation of NK cells identified before the discovery of helper ILCs, show overlapping features with the recently identified ILCps. For this reason, we refer to this last stage of differentiation as iNK/ILCps.

We did not observed differences in total ILC precursor frequency among different group of patients, however, looking at the distribution of different step of differentiation we observed that in BM of high-risk MDS and AML patients there is an expansion of ETP2s at the expense of ETP1 and iNK/ILCp precursors (**Figure 14B**), while in PB of high-risk MDS and AML patients there is an increased fraction of ETP1s and ETP2s at the expense of iNK/ILCps (**C**), in line with the ILC subset distribution described in **7.3**.

Indeed, gating on $CD34^{pos}CD117^{pos}$ ETP2 precursors and total $CD34^{pos}$ ETP1 and ETP2 precursors we confirm their expansion, respectively, in BM (**Figure 14D**) and PB (**Figure 14E**) of high-risk MDS and AML patients.

7.8 Precursors isolated from high-risk patients failed in generating mature NK cells *in-vitro*

The unbalance toward less differentiated ILC precursors and NK cell subsets, together with the reduced frequency of total mature NK cells, suggest a possible impairment of ILC differentiation and NK cell maturation. To test this hypothesis, we sorted $CD3^{neg}/CD14^{neg}/CD19^{neg}/CD16^{neg}$ viable lymphocytes, in order to exclude terminally differentiated cells, from the BM of 4 C patients and 4 high-risk MDS patients and we co-cultured them with OP9 cell line, as feeder layer cells, for 30 days. Firstly, we observed that sorted cells from C and high-risk, which comprises also MDS clones, have a different impact on the stromal cells. Indeed, in wells with cells from C patients, stromal cells maintain their fibroblast-like morphology and tend to reorganize themselves surrounding sorted cells

(**Figure 15A**). On the other hand, in presence of sorted CD3^{neg}/CD14^{neg}/CD19^{neg}/CD16^{neg} cells from high-risk patients, stromal cells lose their fibroblast-like morphology and acquire a morphology similar to that of adipocytes, characterized by the presence of intracellular lipid droplets without any spatial organization of cells (**Figure 15B**).

By studying the phenotype and differentiation of sorted CD3^{neg}/CD14^{neg}/CD19^{neg}/CD16^{neg} cells, we observed that cells purified from C patients generate mature NK cells already before day 10 of co-culture. However, in our experimental conditions, we mainly obtained from sorted cells from C mainly CD56^{bright} NK cells and, to a lesser extent, unCD56^{dim}, but not CD56^{dim} NK cell cells (not shown). This could be probably due to the lack of specific stimuli as, for example, the expression of ligand for the Notch signaling on stromal cells. (160)

On the other hand, cells purified from high-risk patients in the same culture conditions do not differentiate into mature NK cells (**Figure 15C**). Only in one high-risk sample we observed high frequency of NK cells with a lineage^{neg} CD56^{bright} starting from day 21. However, given the high expression of CD8 (not shown), we hypothesized that these cells may not be NK cells.

Figure 15 - ILC in-vitro differentiation.

(*A-B) Image from light microscope showing representative wells of lineage^{neg} sorted cells from a C patient (A) and a high-risk patient (B) at day 13 of coculture with OP9 cells. (C) Statistical graph showing total NK cell percentages generated at 10, 15, 21 and 30 days from sorted lineage^{neg} cells from C patients (blue, n=4) and high-risk patients (red, n=4) cocultured with OP9 cells. (D) Heatmap showing marker expression of total NK cells generated at 10, 15, 21 and 30 days from sorted lineage^{neg} cells from C patients (left, n=4) and high-risk patients (right, n=4)*, both at time of diagnosis, *cocultured with OP9 cells. (E) Summary graph showing the percentage (median + SD) of cytokines, cytolytic granules and CD107a produced by NK cells stimulated after with PMA/Ionomycin for 4 hours. (F-G) Statistical graph showing total helper ILCs (F) and ILC1 (G) percentages generated at 10, 15, 21 and 30 days from sorted lineage^{neg} cells from C patients (blue, n=4) and high-risk patients (red, n=4)*, both at time of diagnosis, *cocultured with OP9 cells. Mann-whitney test vs respective time point, *p<0.05.*

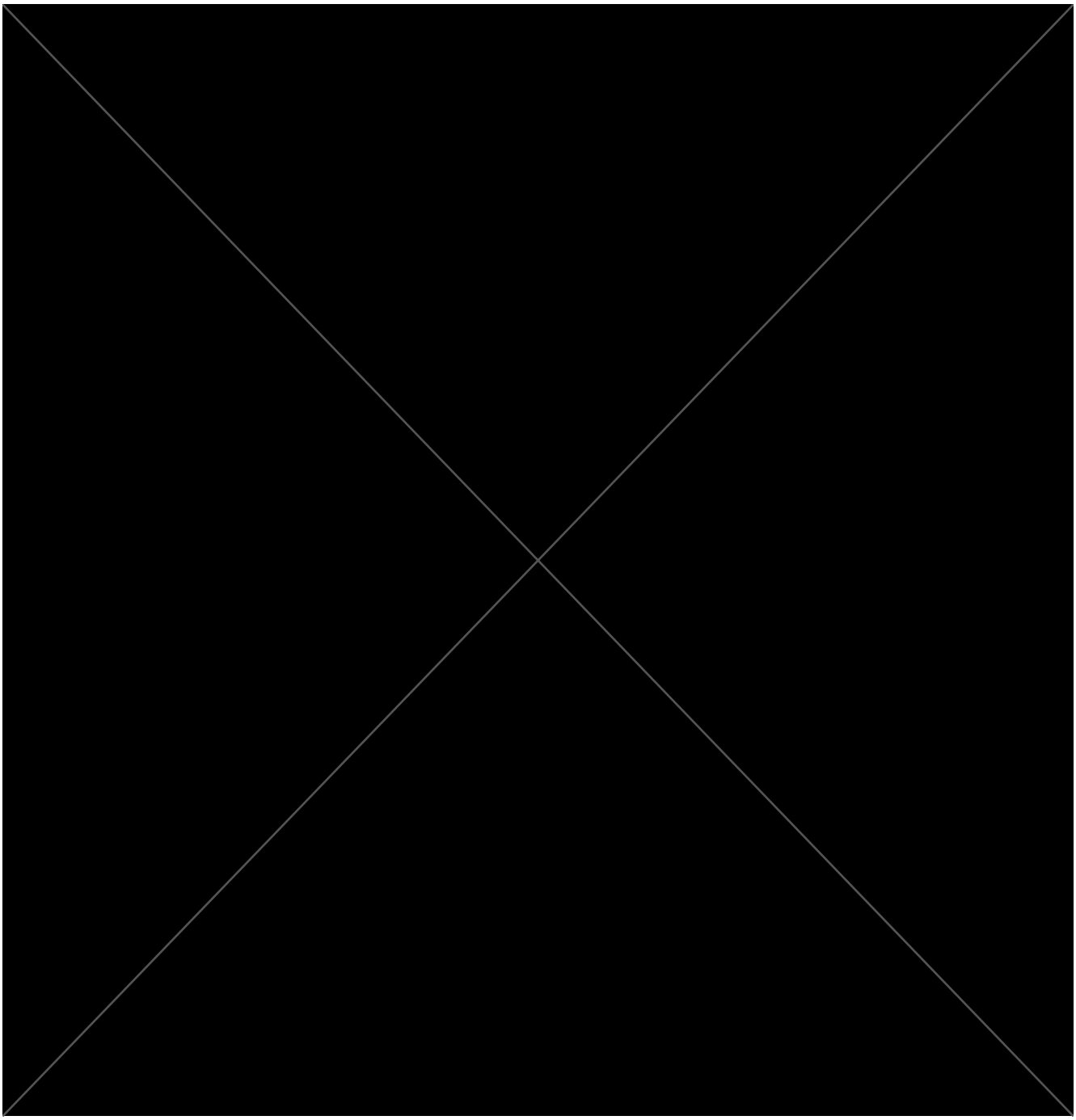

Looking at marker expression of the NK cells obtained from the cocultures, we observed that those obtained from C patients express CD94/NKG2A and CD117 from day 0 and started to express the NCR NKp44 and CD158b1b2j starting from the day 10. The phenotype of these NK cells suggested that, despite the absence of $CD56^{dim}$ NK cell subset, the NK cells that we obtained are acquiring a mature phenotype similar to that of $CD56^{dim}$ NK cells with the downregulation of CD94/NKG2A and NKp44, as well as the up-regulation of CD158b1b2j. (89)

However, this was not true for the few NK cells generated from sorted $CD3^{neg}/CD14^{neg}/CD19^{neg}/CD16^{neg}$ cells from high-risk patients which do not express CD94/NKG2A and NKp44, except at day 21 in which results are drove by the expanded

CD8^{pos}/lineage^{neg}/CD56^{bright} cells (**Figure 15D**). Despite their different phenotype, NK cells *in vitro* generated by sorted cells from both C and high-risk MDS patients, show similar production of IFNγ, TNFα, Granzyme B and Perforin, together with degranulation capability after stimulation with PMA/Ionomycin (**Figure 15E**).

By studying helper ILCs in our co-culture system we observed that sorted cells from high-risk patients contained higher percentage of total ILCs, compared to that sorted from C, these cells were not maintained during the co-culture with stromal cells and indeed their frequency decrease in time (**Figure 15F**). Similarly to the data obtained by studying the ILC subset distribution in the different groups of patients (Figure 9E), our *in vitro* system revealed that cells sorted from high-risk patients generated high frequencies of ILC1s, while cells purified from C generated high frequencies of ILCp (**Figure 15G**).

7.9 Cytokine imbalance in high-risk MDS and AML patients

Together with the assessment of differentiation capability of precursors from high-risk MDS patients, we wonder if these patients, besides having altered levels of pro-inflammatory cytokines as described in literature, could also have an imbalance of levels of cytokines involved in ILC development and NK cell maturation. To this aim, we measured levels of FLT3L, IL10, IL15, IL1α, IL1β, IL2, IL3, IL7, SCF and TGF-β in the BM and PB plasma sample of MDS, AML, C patients and HC.

While no differences were observed in the BM cytokine concentration of different patient groups (not shown), we observed that levels of IL15, IL7, IL2, IL1α and IL1β tend to decrease in PB of high-risk MDS and AML patients (**Figure 16A**). However, we did not find any statistical difference and more samples need to be included in the analysis.

Given the high variability of our results, to understand the role of the measured cytokines in the maturation of ILCs, we correlated them with the percentage of ILC precursors, total NK cells and NK cell subsets. We observed that low levels of IL7, mainly observed in of high-risk MDS and AML patients, correlate with higher percentages of total ILC precursors. (**Figure 16B**). Moreover, even if we did not observe any trend in the concentration of IL10 (not shown), its levels negatively correlate with total NK cell and CD56^{dim} NK cell subset percentages and positively correlate with CD56^{bright} NK cell and CD34^{pos} ETP1 and ETP2 precursor percentages in PB (**Figure 16C**) and BM (not shown).

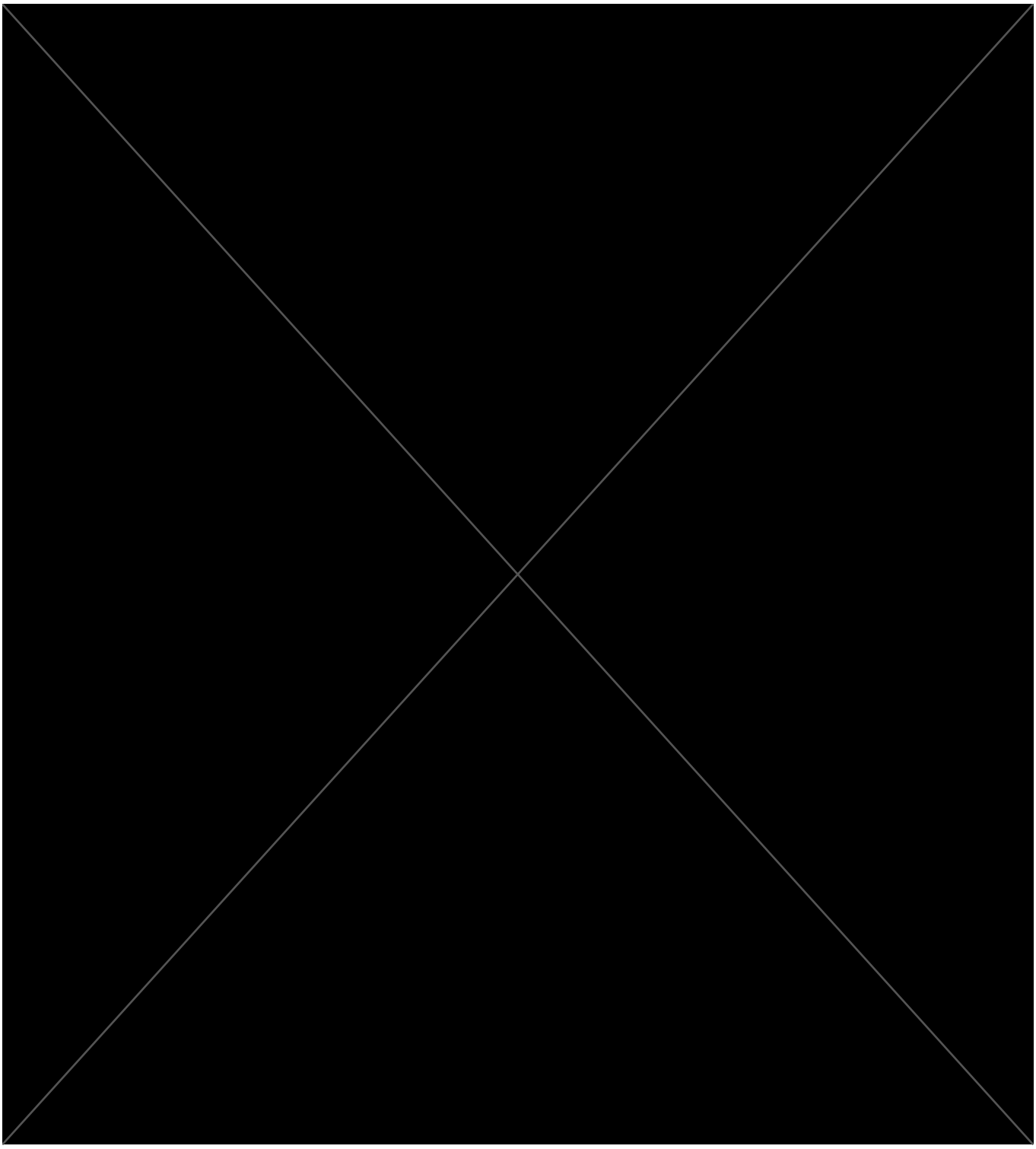

Figure 16 - Cytokine quantification in MDS patients.
(A) Summary graphs showing cytokine concentration in plasma of MDS patients (LR n=16 ,HR n=12) compared to HC (n=8), C (n=10) and AML (n=7) patients, all at time of diagnosis. (B-C) Graphs showing the correlation (black line) and the relative confidence interval at 95% (dashed line) between IL7 plasmatic levels and percentages of circulating $CD34^{+}$ ILC precursors, ETP1 and ETP2, on $lineage^{neg}$ cells (B) and between IL10 plasmatic levels and percentages of total circulating NK cells on lymphocytes, $CD56^{dim}$ and $CD56^{bright}$ on NK cells and circulating $CD34^{+}$ ILC precursors, ETP1 and ETP2, on $lineage^{neg}$ cells.

7.10 HMA treatment partially restore NK cell maturation in high-risk MDS and AML patients

HMA treatment represents the first line treatment in patients with high-risk MDS or that progress towards AML after MDS. However less than half of the patients respond to it and no predictive marker have been identified, so far, to identify patients that really benefit from HMA treatment. Moreover, the response to HMA therapy is limited in time and few is known about its effect on the immune cells of the patients. For these reasons, to investigate the effects of HMAs on ILC compartment, high-risk MDS and AML patients receiving the treatment were grouped together and subdivided in responder, for those having a stable disease or a complete response after treatment, and not responder, for those patients experiencing a disease relapse or progression after the HMA treatment. In these two groups we characterized both helper ILCs and NK cells from BM samples before (pre) the administration of HMA and after (post) the treatment at two specific time points: first evaluation (1^{st} EV), in which the patient respond to the therapy, and second evaluation (2^{nd} EV), usually one year after the beginning of the therapy, at which the patients experience a disease relapse or progression.

Looking at total NK cells in the BM of treated patients, we observed that the NK cell frequency increased at the 1^{st} EV compared to the pre-treatment time point. Moreover, our data demonstrated that patients who respond to the therapy have a higher percentage of total NK cells compared to patients that do not respond to HMA treatment (**Figure 17A**).

Focusing on the NK cell subset distribution, we observed no statistical differences in $CD56^{bright}$ NK cell subset frequencies before and after the HMA treatment (not shown). On the contrary, we observed an increase of $CD56^{dim}$ NK cell frequency at the 1^{st} EV, compared to the time point before the beginning of the treatment, with a tendency to decrease at the 2^{nd} EV. This was also evident in patients who respond to the therapy, compared to pre-treatment (**Figure 17B**). On the other hand, the frequency of $unCD56^{dim}$ NK cell subset decreased at the 1^{st} EV compared to the pre-treatment time point, as well as in patients who respond to the therapy compared to patients that do not respond to HMA treatment (**Figure 17C**).

By analyzing total helper ILC frequency, we observed that they decreased after the therapy, with no differences among the group of responder and not responder patients (**Figure 17D**). In addition, we did not detect any difference in ILC subset distribution after HMA therapy (not shown).

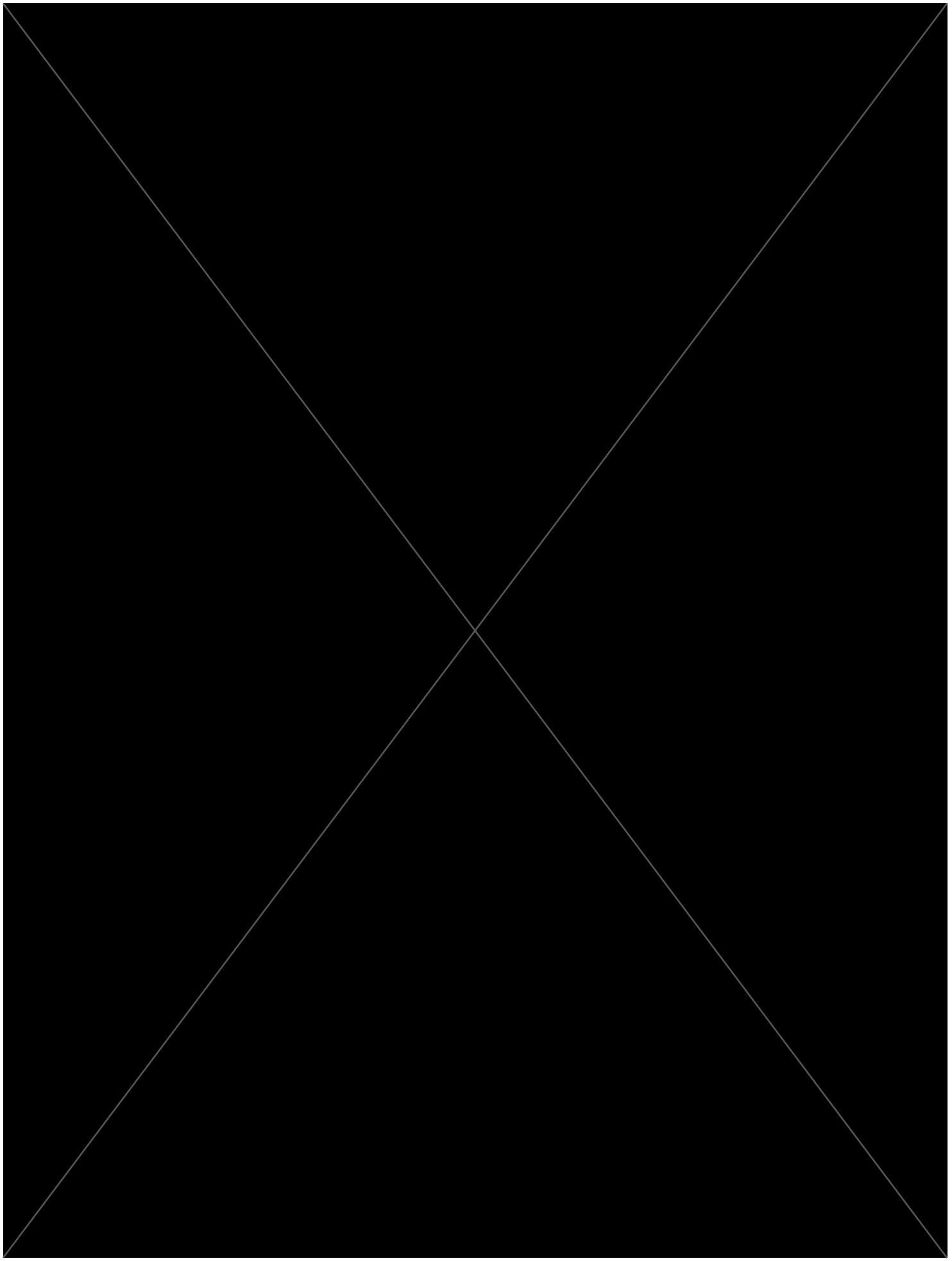

Figure 17 - Effect of HMA treatment on ILC in MDS and AML patients.
*(A-D) Graphs showing the percentage of (A) total NK cells, (B) CD56dim, (C) unCD56dim and (D) total helper ILCs in longitudinal samples (left) and as mean + SD (right) in BM of high-risk and AML patients subdivided according to time of the HMA therapy and therapy response. (E-H) Graphs showing the percentage (mean + SD) of (E) total NK cells, (F) CD56dim, (G) unCD56dim and (H) total helper ILCs in PB of high-risk and AML patients subdivided according to time of the HMA therapy and therapy response. (I-L) Graphs showing the percentage of total NK cell (I) and total helper ILCs (L) generated at 10, 15, 21 and 30 days from sorted lineage^{neg} cells from 4 high-risk patients cocultured with OP9 cells in presence or not of the HMA agent azacytidine (AZA). Statistics were calculated with paired t-test for longitudinal comparisons and with Kruskall-Wallis test to compare different group of patients; *p<0.05.*

Similar results were observed also in the PB of these patients, with a lower percentage of total NK cells in the group of patients that do not responder to HMA compared to patients who respond to the therapy (**Figure 17E**). While CD56^{dim} NK cells tend to increase (**Figure 17F**), unCD56^{dim} NK cell subset tends to decrease (**Figure 17G**) in the group of responder patients compared to pre-therapy. In addition, similar to BM, total helper ILCs tend to decrease in response to HMA treatment (**Figure 17H**).

Given these results, we wonder if the exposure to HMAs of precursors cells could affect their ability to differentiate *in-vitro* into mature NK cells and helper ILCs. For this reason, we cocultured sorted CD3^{neg}/CD14^{neg}/CD19^{neg}/CD16^{neg} cells from high-risk patients with stromal OP9 cell line, in presence of the hypomethylating agent 5-azacytidine (AZA). Our data demonstrated that AZA treatment does not affect the generation of total mature NK cells (**Figure 17I**) On the other hand and in contrast with our *ex-vivo* data, the production of total helper ILCs tend to increase in presence of AZA (**Figure 17L**).

7.11 High-risk MDS patients following haplo-HSCT show an altered ILC immune reconstitution

Since we observed an altered ILC differentiation and NK cell maturation in high-risk MDS patients, we wonder if the HSCT, which represents the only curative approach for AML and MDS patients, could restore the ILC distribution. To this end, we investigated the ILC immune-reconstitution (IR) in a total of 4 MDS patients undergoing haplo-HSCT, comparing the results with lymphoma patients receiving a haplo-HSCT as well. Clinical features of patients are listed in **Table 7**.

N	Sex: d/r	r: age	d: age	Disease; status before transplant	HCMV d/r	HCMV-I/R (Y/N; day post-h-HSCT)	aGVHD (Y/N; day post-h-HSCT; grade)	cGVHD (Y/N; day post-h-HSCT)	Follow-up (weeks; Reason for stopping)
1	F/F	20	51	HL; CR	-/-	N	N	N	53; End of the study
2	M/F	22	52	HL; CR	-/+	Y; 58	Y; 66; II	Y; 183	55; End of the study
3	F/M	53	47	NHL; PR	+/+	Y; 44	N	N	9; Deceased
4	F/F	33	61	HL; CR	+/+	N	N	N	55; End of the study
5	M/F	34	29	HL; CR	-/-	N	Y; 33; II	N	50; End of the study
6	M/M	25	51	NHL; CR	+/+	N	Y; 40; I	N	53; End of the study
7	F/M	47	38	HL; CR	+/+	Y; 33	Y; 61; I	N	47; End of the study
8	M/M	62	35	NHL; PR	+/-	Y; 62	Y; 34; II	Y; 167	50; End of the study
9	F/F	42	49	NHL; PR	+/+	Y; 65	Y; 30; I	N	54; End of the study
10	M/F	40	48	HL; PR	+/+	Y; 34	N	N	43; Deceased
11	M/F	21	52	HL; PR	-/-	N	Y; 41; I	N	9; Deceased
12	M/M	37	47	HL; PD	-/-	N	N	N	15; Deceased
13	F/M	44	27	NHL; PR	+/+	Y; 42	N	N	144; Deceased
14	M/F	47	45	NHL; PD	+/+	Y; 50	Y; 41; II	N	11; Deceased
15	M/M	49	56	MDS; SD	-/-	N	Y; 104; II	Y; 209	53; End of the study
16	M/M	38	53	HL; CR	+/-	Y; 42	Y; 19; II	Y; 224	47; End of the study
17	F/F	28	29	HL; CR	+/+	Y; 21	N	N	12; Consent withdrawal
18	M/M	70	32	MDS; CR	+/+	Y; 39	N	N	6; Consent withdrawal
19	M/M	20	47	HL; PR	-/+	Y; 39	Y; 37; II	N	50; End of the study
20	M/M	25	28	HL; CR	+/-	Y; 40	N	N	40; Other*
21	M/M	70	37	MDS; SD	-/+	Y; 31	Y; 63; I	N	52; End of the study
22	M/F	56	33	HL; CR	-/+	Y; 27	Y; 97; I	N	32; Other*
23	M/F	26	62	HL; CR	+/-	N	Y; 72; I	N	51; End of the study
24	F/F	48	41	MDS; CR	-/-	N	Y; 48; I	N	35; Consent withdrawal
25	F/F	36	42	HL; PR	-/-	N	N	N	43; Other*

Table 7 – Clinical characteristics of patients undergoing haplo-HSCT.
Table showing clinical features of the 25 patients (4 MDS, 21 lymphoma) receiving haplo-HSCT included in the experiments.
Abbreviations: d, donor; r, recipient; F, Female; M, Male; HL, Hodgkin Lymphoma; NHL, Non-Hodgkin Lymphoma; MDS, Myelodysplastic Syndrome; CR, complete response; PR, partial response; SD, stable disease; PD, progressive disease; HCMV, Human Cytomegalovirus; HCMV-I/R, HCMV infection/reactivation; Y, yes; N, no; h-HSCT, haploidentical hematopoietic stem cell transplantation.
** patient stopped coming to the clinic*

Firstly, we assessed helper ILC IR (**Figure 18**). We observed that total ILCs start to immune reconstitute immediately after the transplant in both MDS and lymphoma patients and reach levels comparable to that of donor grafts after only 1 month from the transplant. We also observed that helper ILCs expand in MDS transplanted patients at 2-3 months after the transplant, reaching percentages similar to that of high risk MDS patients before the transplant, as showed in paragraph **7.3** (**Figure 9**). Looking at the helper ILC subset distribution after haplo-HSCT, we observed that in both MDS and lymphoma patients ILC1s have lower frequencies compared to donor grafts. This is mainly due to the expansion of $CD56^{pos}$ ILC1-like cells immediately after the transplant (not shown). Our data also showed

that ILCps median frequency tends to be higher in MDS transplanted patients compared to lymphoma patients at all time points analyzed starting from the first month after the transplant.

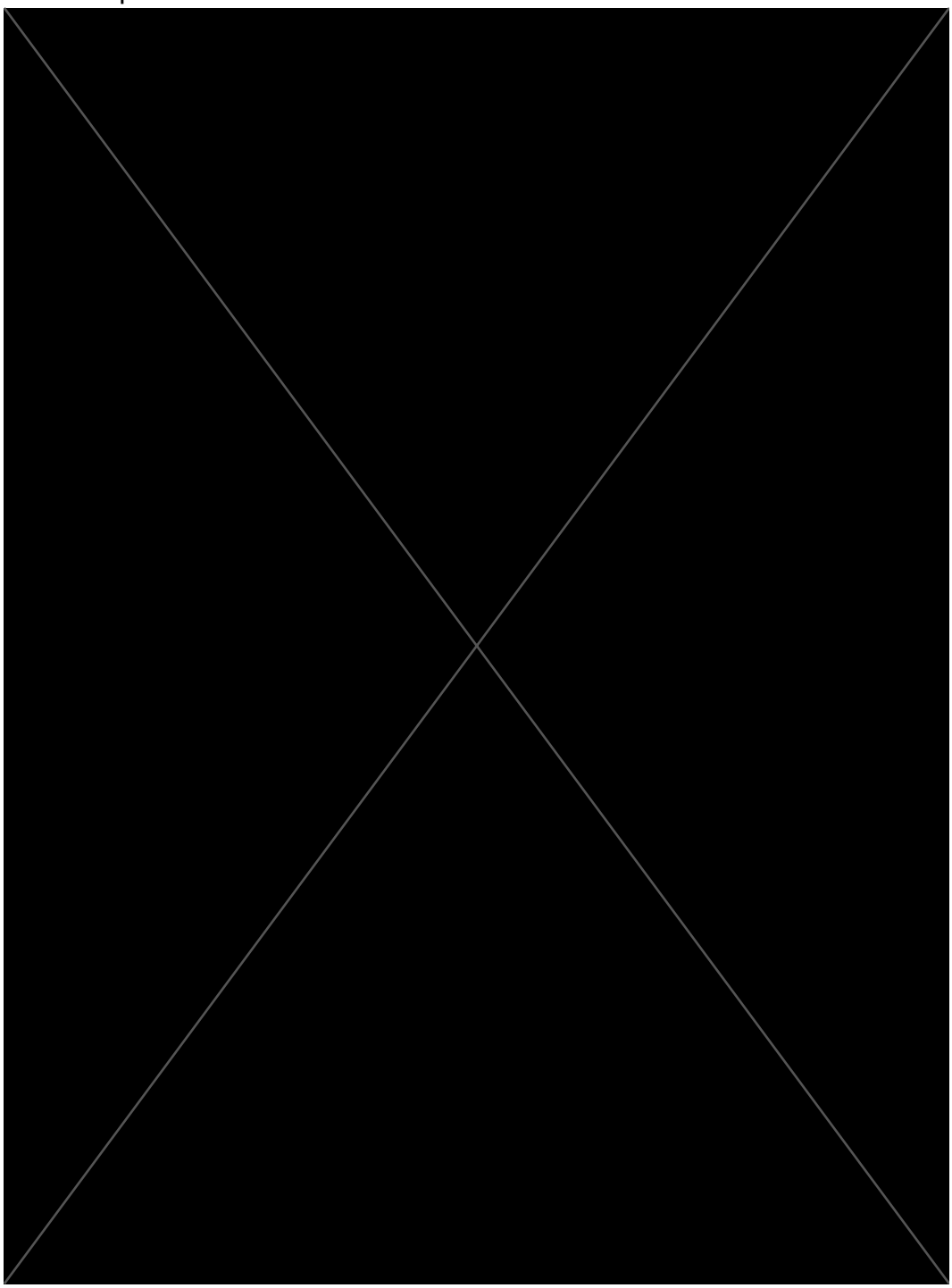

Figure 18 - ILC immune reconstitution after HSCT. *Summary statistical graphs showing helper ILCs and ILC subsets immune reconstitution after haploidentical HSCT in MDS patients (n=4, left) and lymphoma patients (n= 21, right). Dotted line represents the mean frequency in HC. One-way ANOVA vs donor grafts, *p<0.05, **p<0.01, ***p<0.001.*

We then investigated the NK cell IR after halpo-HSCT (**Figure 19**). As we and other previously demonstrated (73, 93), NK cell IR started immediately after the transplant with the expansion of less differentiated $CD56^{bright}$ and $unCD56^{dim}$ NK cell subsets, which are progressively outnumbered by $CD56^{dim}$ NK cells reaching at 7-12 months after the transplant a subset distribution similar to that of donor grafts.

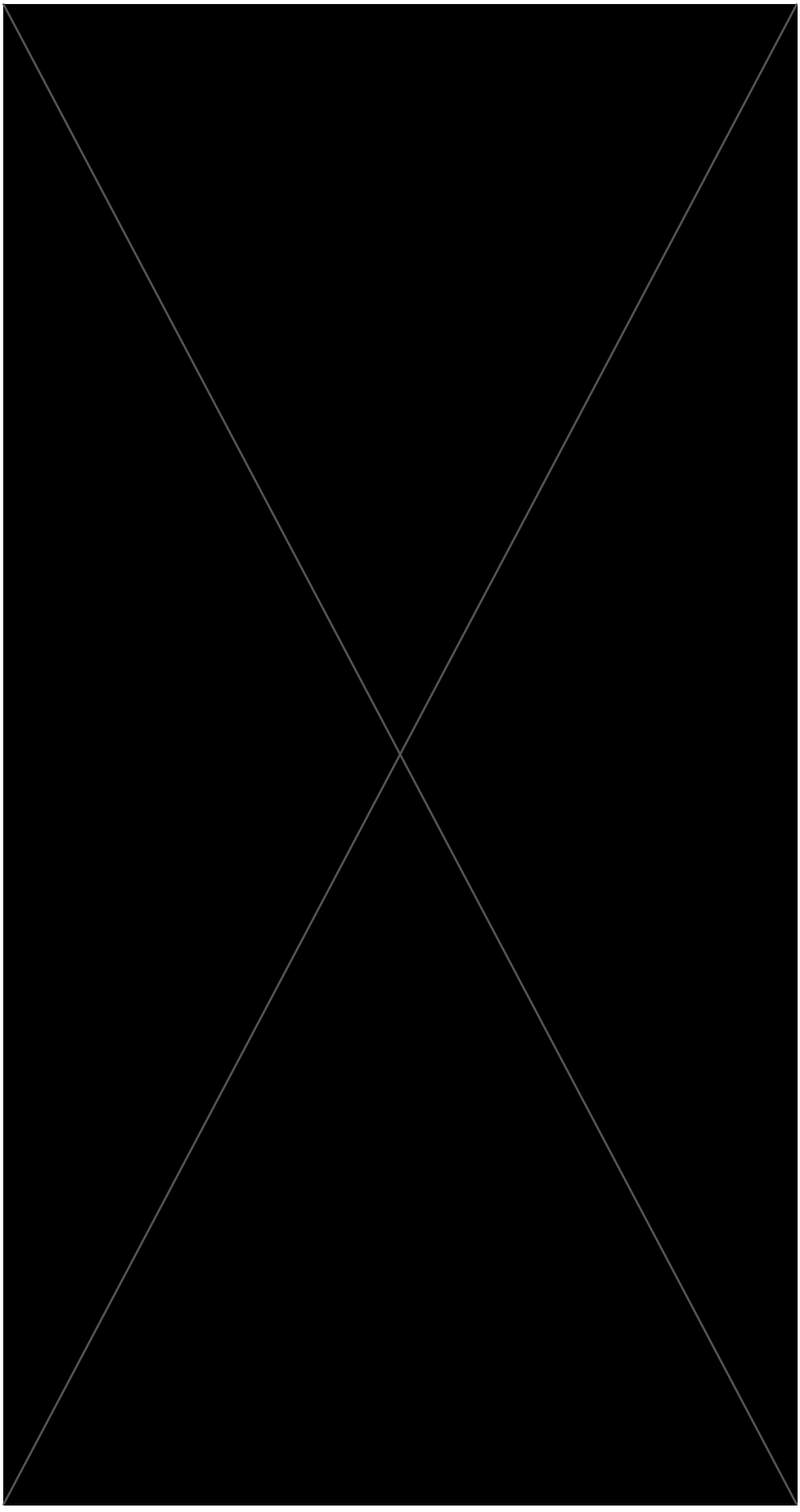

Figure 19 - NK cell immune reconstitution after HSCT.
*Summary statistical graphs showing NK cell and NK cell subsets immune reconstitution after haploidentical HSCT in MDS patients (n=4, left) and lymphoma patients (n= 21, right). Dotted line represents the mean frequency in HC. One-way ANOVA vs donor grafts, *p<0.05, **p<0.01, ***p<0.001.*

The analysis of total NK cell IR in MDS patients demonstrated that the frequency of total NK cells is comparable to that of lymphoma patients. However, the NK cell subset distribution appears to be altered in MDS transplanted patients. In particular, at 10-12 months after the transplant, MDS patients showed higher frequencies of $CD56^{bright}$ NK cells at the expense of $CD56^{dim}$ NK cell subsets, compared to both lymphoma transplanted patients and donor grafts.

8 Conclusions

MDS are a heterogenous group of clonal disorders of hematopoietic stem and progenitor cells, characterized by ineffective hematopoiesis, peripheral cytopenias, and a variable risk of progression to AML (1, 2). Different mechanisms are involved in the pathogenesis of MDS including genetic, epigenetic and bone marrow niche abnormalities. However, the definite pathogenetic mechanism of MDS is still not fully clarified, hindering the clinical decision-making process. Indeed, frontline pharmacological therapies, mainly based on the use of HMAs, are not curative and the current patient risk stratification ineffectively predicts patient prognosis and response to therapies.

Immune dysregulation is emerging as a hallmark in MDS. Low-risk MDS patients are characterized by pro-inflammatory immune response and higher numbers of effector-type cells, while high-risk group is instead marked by predominantly immune-tolerant milieu with significant expansion of immunosuppressive cells. Despite this evidence, the primary orchestrators of the dysregulated MDS microenvironment have not yet been identified.

In this context, ILCs are emerging as important actors in the pathophysiology of different cancers, by generating a suppressive and tolerant environment. Others and we demonstrated that ILC subset distribution and functions in AML contribute to a reduced immune surveillance. However, a comprehensive immune-phenotypic characterization of ILCs aiming at investigating their involvement in MDS pathogenesis and progression is still lacking.

Herein, we provide an extensive characterization of the innate lymphoid compartment in MDS, focusing on its role in the natural history of the disease as well as on the impact of HMA treatment and haplo-HSCT on ILC distribution and phenotype.

Firstly, we subdivided our cohort of patients according to the IPSS-R score into two groups: the low-risk group composed by very low/low/intermediate patients and the high-risk group composed by high/very high patients. (21) However, this classification was ineffective since results from the two groups were characterized by great variability and we were not even able to confirm the few results about NK cells reported in literature by different independent laboratories. (52, 131-133) This could be also due to the sample size imbalance of the two groups (85 low-risks vs 16 high-risks). Moreover, the IPSS-R scoring system is mainly based on aspecific clinical and hematological data, able to successfully predict the risk of disease progression, but ineffective in predicting the response to disease-modifying therapies. (3)

We thus decided to simplify patient risk stratification by subdividing patients only based on blast count, that represents the main clinical parameter in the risk assessment.

By using this classification, in line with literature, we firstly confirm a decrease in total circulating NK cells in high-risk MDS patients. (131) However, in contrast with previous findings, we could not detect any differences in the percentage of total NK cells in BM of these patients. (161)

We also demonstrated an expansion, in both BM and PB of high-risk MDS patients, of the less differentiated $CD56^{bright}$ and $unCD56^{dim}$ NK cell subsets, at the expense of $CD56^{dim}$ NK cells as already described. (131)

This altered NK cell subsets distribution is directly related to the disease and is not due to age-related changes in NK cell maturation. Indeed, in age and sex matched C patients this NK cell subset redistribution has not been observed. Moreover, evidence in literature demonstrated that, as a consequence of the age-associated changes in the number and function of hematopoietic stem cells and of the BM impairment in the production of new NK cells the proportion of peripheral blood $CD56^{bright}$ NK cells is usually reduced in elderly individuals. (162)

Phenotypic analyses of NK cells in high-risk MDS and AML patients, highlighted an impairment of NK cell functions, characterized by a decreased expression of the activating receptors NKp30 and NKp46 and a reduced content of cytolytic molecules. Even the stimulation with K562 or 721.221.G target cells was not able to upregulate the production of Granzyme B and Perforin, thus suggesting a reduced ability of NK cells from high-risk MDS patients to perform cytotoxic responses. This could be attributable to the decrease of $CD56^{dim}$ NK cell fraction and/or to the defective non-MHC-restricted recognition of targets from these NK cells. (163) In this context, the BM microenvironment of MDS patients, characterized by hypoxia and high levels of ROSs, certainly plays a main role in lowering the expression of NKp30 and NKp46 on NK cells.(41, 155-158)

Together these results further implement previous works done in restricted cohorts of MDS patients in which a reduced expression of NKp30 and the lower production of cytolytic molecules in NK cells from MDS patients compared to healthy subjects were observed. (52, 141) We indeed demonstrated that, in our larger cohort of MDS patients, stratified based on blast count as an index of disease severity, the decreased expression of NKp30, together with that of NKp46, and the reduced production of cytolytic molecules was restricted only in the higher risk group.

The reduced number of total NK cells coupled to their hypofunctional phenotype in high-risk MDS patients, suggest an ineffective anti-tumor activity of NK cells in these patients leading to the evasion of immune-surveillance mechanisms by MDS clones. However, to understand

if the total number of NK cells and their expression levels of NKp30 and NKp46 could be included in the score for risk stratification, correlation studies with clinical data are needed.

In line with previous observations, the phenotypic analysis of $CD56^{bright}$ NK cells expanded in high-risk MDS patients also showed that this NK cell subset is characterized by a high fraction of unlicensed $NKG2A^{neg}$ cells (3, 131). Moreover, our data demonstrated that the absence of NKG2A expression is responsible of the ability of $CD56^{bright}$ NK cells from high-risk MDS patients to release high amounts of IFN-γ at steady state as well as in presence of HLA-E overexpressing target cells. These observations highlight once more the inefficient generation of mature and competent NK cells in MDS patients and propose possible role of $NKG2A^{neg}/CD56^{bright}$ NK cells in exacerbating the inflamed status of the BM niche of MDS patients. Furthermore, the absence of the NKG2A inhibitory receptor suggest a NK cell hyporesponsiveness and tolerance to MHC-deficient cells and/or a reduced tolerance toward self-cells that could contribute to the auto-reactive immunologic activity described in MDS patients, triggering apoptosis of myeloid precursor cells and leading to cytopenia. (85, 164)

Further analyses are needed to understand if the decreased licensing of NK cells is attributable to a reduced expression of HLA-I by the hematopoietic or stromal compartment in the BM niche of high-risk MDS patients. (84)

Differently from NK cells, our data also showed a higher frequency of total helper ILCs in high-risk MDS patients, mainly due to the expansion of dysfunctional ILC1s counterbalanced by the decrease of ILC2s and ILCps. We previously reported similar changes also in *de-novo* AML patients, in which we demonstrated an expansion of dysfunctional ILC1s mainly at the expense of ILCps. (138) Moreover, the frequency of circulating helper ILCs in *de-novo* AML patients was positively correlated to the percentage of circulating leukemic blasts. Herein, we indeed observed the expansion of helper ILCs only in the high-risk patient group characterized by high blast counts and not in low-risk ones. On the contrary, we did not observe any expansion of helper ILCs in patients developing AML post-MDS, suggesting that the immune dysregulation in these two subgroups of AML is different. (138)

A possible explanation of the ILC1 increase in high-risk MDS patients can be found in the plasticity phenomenon distinguishing ILCs. Indeed, in induced tumor mouse models, it has been reported that TGF-β regulates the conversion of NK cells into ILC1s, which in turn are not able to control tumor growth or metastasis formation, due to an impairment in the production of IFN-γ. (66, 67) Although we did not detect any differences in the levels of TGF-

β in BM and PB of high-risk MDS patients, it has been recently showed that MSCs isolated from MDS patients can induce a suppressive phenotype in monocytes with the up-regulation of membrane-bound TGF-β, able to suppress NK cell function in a contact-mediated way. (41) Despite in humans the ILC1-NK cell plasticity phenomenon has not be yet described, this mechanism could be also responsible for the conversion of NK cells into dysfunctional ILC1s.

The higher percentage of helper ILCs, coupled with the decrease of total circulating NK cells, could be also attributable to a defect in NK cell differentiation, in which ILC1s constitute an alternative pathway of differentiation of ILC precursors. Indeed, in a recent work it has been demonstrated that the major mechanism leading to the increase in ILC1 production in *de-novo* AML patients, and likely responsible for the loss of circulating mature NK cells, is the skewing of ILCp maturation toward ILC1s at the expense of NK cells, in a mechanism dependent on the activation of the AHR, key transcription factor in ILCs, by AML clones. (165)

Additional investigations are warranted to test whether the block of NK cells differentiation observed in our cohort of MDS patients could be caused by either to the upregulation of monocyte membrane-bound TGF-β or to the release of AHR ligands by MDS clones.

By studying the ILC differentiation process, we also showed in the BM and PB of high-risk MDS and AML patients an imbalance in the distribution of ILC precursors ETP1s, ETP2s and iNK/ILCps. In particular, we detected a higher proportion of ETP2s in the BM, coupled to the accumulation of both ETP1 and ETP2 in the PB of high-risk MDS and AML patients. With these data we demonstrated that the impairment of NK cell differentiation, which is in turn responsible of the lower detection of total circulating NK cells in high-risk MDS patients, could be localized at a precise step of ILC differentiation, corresponding to ETP2. Due to this block, a higher portion of ETP1 and ETP2s is released in the PB of high-risk MDS and AML patients, probably due to a compensatory mechanism.

We next investigated if this block in the differentiation was related to defect endowed by ILC progenitors through the *in vitro* differentiation assay that we set up. We firstly observed that precursors isolated from high-risk MDS patients can shape mesenchymal feeder layer cells, which acquire an adipocyte-like morphology. In the future, we will perform OILred O staining to assess if these cells are real adipocytes. This would demonstrate that MDS progenitors, which likely include MDS clones, are able to push MSCs toward an adipogenic differentiation. As previously observed in *de-novo* AML patients, this could support the survival and proliferation of blasts at the expense of an effective hemopoiesis.(166) In

agreement, our data also demonstrated that BM precursors isolated from high-risk MDS patients are ineffective in generating NK cells *in vitro* compared to those isolated from C patients. Moreover, similar to our data on circulating ILCs, our *in vitro* experiments demonstrated that precursors isolated from high-risk MDS patients gave rise to a higher fraction of ILC1s compared to precursors of C patients.

By studying the phenotype of *in vitro* generated NK cells, again we observed that precursors from high-risk MDS patients give rise to NK cells with a reduced education and licensing (low expression of CD94/NKG2A and CD158b1b2j) and by a low activation (low levels of NKp44) compared to NK cells differentiated from low-risk MDS patient precursors. Despite these phenotypic differences, the unspecific stimulation with PMA/Ionomycin of NK cells obtained from precursors of high-risk MDS patients promotes cytokine and cytolytic molecule production comparable to that obtained from precursors of C patients, as well as degranulation capability.

To investigate the contribution of cytokines in determining a defective ILC-poiesis and an impairment in NK cell effector-functions, we measured cytokine levels in both BM and PB samples. The data obtained demonstrated that several cytokines involved at different levels in ILC differentiation are altered in MDS patients. We indeed observed in high-risk MDS and AML patients a decrement of IL7, IL15, IL2, IL1α and IL1β plasmatic levels and we demonstrated that low levels of IL7 correlated with higher percentages of circulating ETP1 and ETP2 precursors. This finding underlines the contribute of IL7 in the differentiation impairment observed in high-risk MDS and AML patients. Moreover, though no difference in IL10 levels was detected in BM and PB of different groups of patients, we found that it negatively correlated with the percentage of total NK cells and of $CD56^{dim}$ NK cell subset, while it positively correlated with the percentage of $CD56^{bright}$ NK cell subset and of ETP1 and ETP2. These results suggest that the increase of IL10 concentration contributes to the impairment of ILC differentiation and the altered NK cell maturation that we observed in high-risk MDS and AML patients. For these reasons, correlations with clinical data are needed to better understand if the reduction of IL7 and the increase of IL10 might constitute risk factors that could help in identifying patients with a worse prognosis. Moreover, given the high variability of both cytokine measurement and of ILC phenotypic assessment during the natural history of the disease, we need to correlate our biological data with clinical one in order to find correlation which may highlight some prognostic marker which might be included in patient risk stratification. Moreover, both IPSS-R and classification based on blast count do not consider predisposing and potential driving mutations and immune

signatures, which are rather included in the new and recently publisher IPSS-M score. For this reason, we will re-analyze our data according to this new stratification to understand if it better reflects the immunological status of MDS patients.

In this PhD thesis, we also investigated the effects of the two main therapeutic interventions used for the treatment of high-risk MDS and AML patients, by means of HMA therapy and HSCT, on the ILC compartment and the possible role of ILC composition in predicting the response to current therapeutic strategies.

HMA treatment is known to have a role in the induction of cell maturation and, in line with this, it is able to shape KIR repertoire of NK cells of treated patients. (167) However, the effect of HMAs on ILC differentiation has never been investigated. Here, we observed that patients responding to HMA treatment showed an increased percentage of total NK cells and of $CD56^{dim}$ NK cell subset, as well as the reduction of $unCD56^{dim}$ NK cells. In parallel, we also observed a reduction of helper ILCs independently from the response to HMA therapy. However, we were not able to reproduce this shift in ILC differentiation *in vitro* by using high-risk MDS precursors differentiated in presence of azacytidine.

Previous findings underlined the importance of NK cell function in predicting patient response to the therapy, indeed patients showing higher NK cell cytotoxicity following HMA treatment had significantly improved overall survival. (168) With our data, we further support that the characterization of NK cell compartment upon HMA treatment could be exploited for the identification of patients responding to the therapy. In particular, total mature NK cell percentage and NK cell subset distribution, together with NK cell cytotoxicity, could be considered as biomarkers to evaluate patient response to therapy.

Together, these results suggested that HMA can induce a partial restoration of ILC subset distribution and ILC-poiesis, which likely exert their function not on ILC precursors, but rather on BM niche components constituted by HMA clones and MSCs. (169)

However, further studies are needed to characterize the effect of HMA treatment on the BM niche, including cytokine production, of responder patients compared with that of patients that do not respond to HMA treatment. This would lead to the identification of predictive biomarkers that could help in the choice of the best therapeutic intervention, as suitable as possible for the patient. These would be of relevance for the elderly population, which often displays lower response to HMAs and higher toxicity rates. However, it is unlikely finding a single predictive biomarker that fits all MDS patients, considering the complexity of the disease and the role of several genetic, immunologic, and environmental factors in its

pathophysiology. Hence, a more comprehensive and combinatorial approach, which uses several biomarkers to better predict the patient response to the HMAs, is necessary. (3)

In addition to HMAs, the only curative strategy to treat MDS patients is haplo-HSCT, a recent implemented transplantation protocol that expand patient eligibility also to elderly people. Our preliminary data demonstrated that NK cells in high-risk MDS patients treated with haplo-HSCT show alteration in the IR of $CD56^{bright}$ and $CD56^{dim}$ subsets. Indeed, one year following the transplantation, these patients had a higher proportion of $CD56^{bright}$ NK cells compared to the graft, at the expense of $CD56^{dim}$ NK cell subset. This underlined again the role of BM niche dysfunctions in MDS patients, which do not properly support NK cell maturation from ILC precursors deriving from the healthy graft.

Enlarging our cohort, we will be able to deep our analysis in order to evaluate if the altered BM niche of the transplanted patients is able to perturbate ILC-poiesis by inducing in mature ILCs the same phenotype and functional observed in untreated patients.

To conclude, together our data demonstrate, as shown in the graphical abstract below (**Figure 20**), that MDS patients, and especially those with high blast counts, have a deficient ILC-poiesis characterized by the accumulation of ETP2s, a preferential differentiation toward dysfunctional ILC1s, accompanied by the reduction of total NK cells, with a skewing toward less differentiated NK cell subsets that are functionally impaired.

This pathological ILC differentiation is related to properties endowed by MDS clones and/or ILC progenitors, which are able to modify the morphology and functional properties of MSCs in the BM niche causing among other an unbalance in cytokines levels in the BM microenvironment. Moreover, we highlighted the importance of ILC compartment in treatment response. Indeed, we demonstrated that patients who respond to HMA therapy are marked by a restoration of ILC differentiation and maturation, attributable to a re, compared to those not responding to the treatment. On the other hand, we also showed a defective NK cell maturation in MDS patients undergone haplo-HSCT, underline again the importance of the BM niche.

Further studies will be devoted in the identification of the molecular causes of ILC progenitor differentiation defects, but also to understand if other microenvironmental alterations, including HLA-I expression on HSCs, monocyte membrane-bound TGF-β, hypoxia status and/or ROS production, are involved in the creation of a BM niche that does not support a correct ILC development. In this purpose, we will analyze, in collaboration with the Leukemia and Myelodysplasia Unit at Humanitas, the RNA sequencing data of blasts from the same

patients included in our analysis. This will help us in highlighting the role of MDS clones in shaping the BM niche and in altering the ILC developmental process.

These results are of utmost importance, since they underline the importance of ILCs in disease progression and in treatment response, paving the way for *ad hoc* immunotherapeutic intervention aimed at improving functional NK cell generation to induce tumor immune-surveillance. Indeed, we believe that the creation of a new prognostic/diagnostic scoring system comprehensive of immunologic data is needed and it could further help to better stratify MDS patients, rapidly identify patients who really benefit from HMA therapies as well as to develop novel effective immunotherapies.

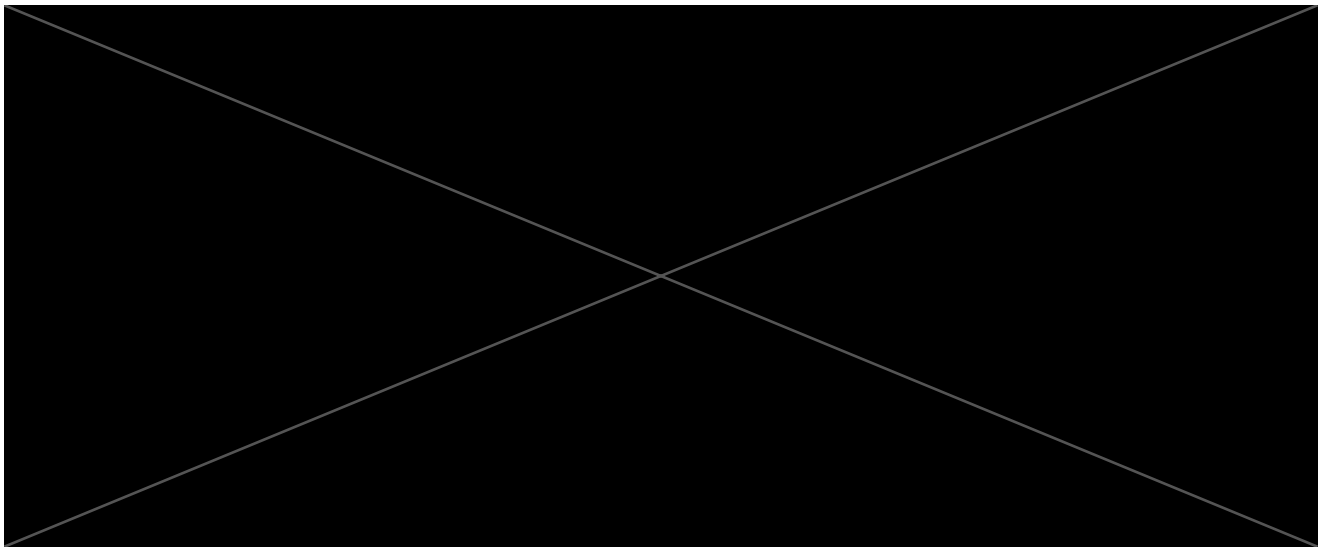

Figure 20 - Graphical abstract
MDS: Myelodysplastic syndrome; ILC: Innate lymphoid cells; NK: Natural killer; BM: Bone marrow; HMA: Hypomethylating agents; HSCT: Hematopoietic stem cell transplantation; IR: Immune reconstitution.

9 Acknowledgments

I would first like to thank all the patients enrolled in this study and their families.

I express my very profound gratitude to my tutor Professor Domenico Mavilio and to my supervisor Doctor Clara Di Vito for guiding and supporting me during this project, in particular for data interpretation and the correction of this thesis.

I am also grateful to all the present and past members of the Clinical and Experimental Immunology Laboratory, especially Doctor Elisa Zaghi, Doctor Alessandro Frigo and Doctor Nicolò Coianiz who mostly helped me in sample processing and in performing experiments.

In conclusion, this work would not have been possible without the support of the fellowships provided by University of Milan and by Associazione Italiana per la Ricerca sul Cancro (AIRC).

10 References

1. Tefferi A, Vardiman JW. Myelodysplastic syndromes. N Engl J Med. 2009;361(19):1872-85.
2. Ades L, Itzykson R, Fenaux P. Myelodysplastic syndromes. Lancet. 2014;383(9936):2239-52.
3. Winter S, Shoaie S, Kordasti S, Platzbecker U. Integrating the "Immunome" in the Stratification of Myelodysplastic Syndromes and Future Clinical Trial Design. J Clin Oncol. 2020;38(15):1723-35.
4. Cazzola M. Myelodysplastic Syndromes. N Engl J Med. 2020;383(14):1358-74.
5. Arber DA, Orazi A, Hasserjian R, Thiele J, Borowitz MJ, Le Beau MM, et al. The 2016 revision to the World Health Organization classification of myeloid neoplasms and acute leukemia. Blood. 2016;127(20):2391-405.
6. Hosono N. Genetic abnormalities and pathophysiology of MDS. Int J Clin Oncol. 2019;24(8):885-92.
7. Pellagatti A, Boultwood J. The molecular pathogenesis of the myelodysplastic syndromes. Eur J Haematol. 2015;95(1):3-15.
8. Papaemmanuil E, Cazzola M, Boultwood J, Malcovati L, Vyas P, Bowen D, et al. Somatic SF3B1 mutation in myelodysplasia with ring sideroblasts. N Engl J Med. 2011;365(15):1384-95.
9. Yoshida K, Sanada M, Shiraishi Y, Nowak D, Nagata Y, Yamamoto R, et al. Frequent pathway mutations of splicing machinery in myelodysplasia. Nature. 2011;478(7367):64-9.
10. Graubert TA, Shen D, Ding L, Okeyo-Owuor T, Lunn CL, Shao J, et al. Recurrent mutations in the U2AF1 splicing factor in myelodysplastic syndromes. Nat Genet. 2011;44(1):53-7.
11. Haferlach T, Nagata Y, Grossmann V, Okuno Y, Bacher U, Nagae G, et al. Landscape of genetic lesions in 944 patients with myelodysplastic syndromes. Leukemia. 2014;28(2):241-7.
12. Papaemmanuil E, Gerstung M, Malcovati L, Tauro S, Gundem G, Van Loo P, et al. Clinical and biological implications of driver mutations in myelodysplastic syndromes. Blood. 2013;122(22):3616-27; quiz 99.
13. Nimer SD. Clinical management of myelodysplastic syndromes with interstitial deletion of chromosome 5q. J Clin Oncol. 2006;24(16):2576-82.

14. Schanz J, Tuchler H, Sole F, Mallo M, Luno E, Cervera J, et al. New comprehensive cytogenetic scoring system for primary myelodysplastic syndromes (MDS) and oligoblastic acute myeloid leukemia after MDS derived from an international database merge. J Clin Oncol. 2012;30(8):820-9.
15. Sloand EM, Pfannes L, Chen G, Shah S, Solomou EE, Barrett J, et al. CD34 cells from patients with trisomy 8 myelodysplastic syndrome (MDS) express early apoptotic markers but avoid programmed cell death by up-regulation of antiapoptotic proteins. Blood. 2007;109(6):2399-405.
16. Malcovati L, Stevenson K, Papaemmanuil E, Neuberg D, Bejar R, Boultwood J, et al. SF3B1-mutant MDS as a distinct disease subtype: a proposal from the International Working Group for the Prognosis of MDS. Blood. 2020;136(2):157-70.
17. Cazzola M, Della Porta MG, Malcovati L. The genetic basis of myelodysplasia and its clinical relevance. Blood. 2013;122(25):4021-34.
18. Moran-Crusio K, Reavie L, Shih A, Abdel-Wahab O, Ndiaye-Lobry D, Lobry C, et al. Tet2 loss leads to increased hematopoietic stem cell self-renewal and myeloid transformation. Cancer Cell. 2011;20(1):11-24.
19. Lindsley RC, Mar BG, Mazzola E, Grauman PV, Shareef S, Allen SL, et al. Acute myeloid leukemia ontogeny is defined by distinct somatic mutations. Blood. 2015;125(9):1367-76.
20. Menssen AJ, Walter MJ. Genetics of progression from MDS to secondary leukemia. Blood. 2020;136(1):50-60.
21. Greenberg PL, Tuechler H, Schanz J, Sanz G, Garcia-Manero G, Sole F, et al. Revised international prognostic scoring system for myelodysplastic syndromes. Blood. 2012;120(12):2454-65.
22. Cargo CA, Rowbotham N, Evans PA, Barrans SL, Bowen DT, Crouch S, et al. Targeted sequencing identifies patients with preclinical MDS at high risk of disease progression. Blood. 2015;126(21):2362-5.
23. Nazha A, Al-Issa K, Hamilton BK, Radivoyevitch T, Gerds AT, Mukherjee S, et al. Adding molecular data to prognostic models can improve predictive power in treated patients with myelodysplastic syndromes. Leukemia. 2017;31(12):2848-50.
24. Bersanelli M, Travaglino E, Meggendorfer M, Matteuzzi T, Sala C, Mosca E, et al. Classification and Personalized Prognostic Assessment on the Basis of Clinical and Genomic Features in Myelodysplastic Syndromes. J Clin Oncol. 2021;39(11):1223-33.

25. Bernard E, Tuechler H, Greenberg PL, Hasserjian RP, Ossa JEA, Nannya Y, et al. Molecular International Prognostic Scoring System for Myelodysplastic Syndromes. NEJM Evidence. 2022;1(7):EVIDoa2200008.
26. Sanz J, Labopin M, Sanz MA, Aljurf M, Sousa AB, Craddock C, et al. Hematopoietic stem cell transplantation for adults with relapsed acute promyelocytic leukemia in second complete remission. Bone Marrow Transplant. 2021;56(6):1272-80.
27. Copelan EA. Hematopoietic stem-cell transplantation. N Engl J Med. 2006;354(17):1813-26.
28. Bacigalupo A, Ballen K, Rizzo D, Giralt S, Lazarus H, Ho V, et al. Defining the intensity of conditioning regimens: working definitions. Biol Blood Marrow Transplant. 2009;15(12):1628-33.
29. Cutler CS, Lee SJ, Greenberg P, Deeg HJ, Perez WS, Anasetti C, et al. A decision analysis of allogeneic bone marrow transplantation for the myelodysplastic syndromes: delayed transplantation for low-risk myelodysplasia is associated with improved outcome. Blood. 2004;104(2):579-85.
30. Saygin C, Carraway HE. Current and emerging strategies for management of myelodysplastic syndromes. Blood Rev. 2021;48:100791.
31. Kennedy AL, Shimamura A. Genetic predisposition to MDS: clinical features and clonal evolution. Blood. 2019;133(10):1071-85.
32. Fenaux P, Mufti GJ, Hellstrom-Lindberg E, Santini V, Finelli C, Giagounidis A, et al. Efficacy of azacitidine compared with that of conventional care regimens in the treatment of higher-risk myelodysplastic syndromes: a randomised, open-label, phase III study. Lancet Oncol. 2009;10(3):223-32.
33. Carraway HE. Treatment options for patients with myelodysplastic syndromes after hypomethylating agent failure. Hematology Am Soc Hematol Educ Program. 2016;2016(1):470-7.
34. Bernard E, Nannya Y, Hasserjian RP, Devlin SM, Tuechler H, Medina-Martinez JS, et al. Implications of TP53 allelic state for genome stability, clinical presentation and outcomes in myelodysplastic syndromes. Nat Med. 2020;26(10):1549-56.
35. Chen X, Li N, Weng J, Du X. Senescent Mesenchymal Stem Cells in Myelodysplastic Syndrome: Functional Alterations, Molecular Mechanisms, and Therapeutic Strategies. Front Cell Dev Biol. 2020;8:617466.
36. Cogle CR, Saki N, Khodadi E, Li J, Shahjahani M, Azizidoost S. Bone marrow niche in the myelodysplastic syndromes. Leuk Res. 2015;39(10):1020-7.

37. Lynch OF, Calvi LM. Immune Dysfunction, Cytokine Disruption, and Stromal Changes in Myelodysplastic Syndrome: A Review. Cells. 2022;11(3).
38. Gao F, Chiu SM, Motan DA, Zhang Z, Chen L, Ji HL, et al. Mesenchymal stem cells and immunomodulation: current status and future prospects. Cell Death Dis. 2016;7:e2062.
39. Zhou S, Greenberger JS, Epperly MW, Goff JP, Adler C, Leboff MS, et al. Age-related intrinsic changes in human bone-marrow-derived mesenchymal stem cells and their differentiation to osteoblasts. Aging Cell. 2008;7(3):335-43.
40. Medyouf H, Mossner M, Jann JC, Nolte F, Raffel S, Herrmann C, et al. Myelodysplastic cells in patients reprogram mesenchymal stromal cells to establish a transplantable stem cell niche disease unit. Cell Stem Cell. 2014;14(6):824-37.
41. Sarhan D, Wang J, Sunil Arvindam U, Hallstrom C, Verneris MR, Grzywacz B, et al. Mesenchymal stromal cells shape the MDS microenvironment by inducing suppressive monocytes that dampen NK cell function. JCI Insight. 2020;5(5).
42. Poon Z, Dighe N, Venkatesan SS, Cheung AMS, Fan X, Bari S, et al. Bone marrow MSCs in MDS: contribution towards dysfunctional hematopoiesis and potential targets for disease response to hypomethylating therapy. Leukemia. 2019;33(6):1487-500.
43. Franceschi C, Garagnani P, Vitale G, Capri M, Salvioli S. Inflammaging and 'Garb-aging'. Trends Endocrinol Metab. 2017;28(3):199-212.
44. Pardanani A, Finke C, Lasho TL, Al-Kali A, Begna KH, Hanson CA, et al. IPSS-independent prognostic value of plasma CXCL10, IL-7 and IL-6 levels in myelodysplastic syndromes. Leukemia. 2012;26(4):693-9.
45. Raaijmakers MH. Myelodysplastic syndromes: revisiting the role of the bone marrow microenvironment in disease pathogenesis. Int J Hematol. 2012;95(1):17-25.
46. Epling-Burnette PK, List AF. Advancements in the molecular pathogenesis of myelodysplastic syndrome. Curr Opin Hematol. 2009;16(2):70-6.
47. Kordasti SY, Afzali B, Lim Z, Ingram W, Hayden J, Barber L, et al. IL-17-producing CD4(+) T cells, pro-inflammatory cytokines and apoptosis are increased in low risk myelodysplastic syndrome. Br J Haematol. 2009;145(1):64-72.
48. Kerkhoff N, Bontkes HJ, Westers TM, de Gruijl TD, Kordasti S, van de Loosdrecht AA. Dendritic cells in myelodysplastic syndromes: from pathogenesis to immunotherapy. Immunotherapy. 2013;5(6):621-37.
49. Epling-Burnette PK, Painter JS, Rollison DE, Ku E, Vendron D, Widen R, et al. Prevalence and clinical association of clonal T-cell expansions in Myelodysplastic Syndrome. Leukemia. 2007;21(4):659-67.

50. Saft L, Bjorklund E, Berg E, Hellstrom-Lindberg E, Porwit A. Bone marrow dendritic cells are reduced in patients with high-risk myelodysplastic syndromes. Leuk Res. 2013;37(3):266-73.
51. Lopes MR, Traina F, Campos Pde M, Pereira JK, Machado-Neto JA, Machado Hda C, et al. IL10 inversely correlates with the percentage of CD8(+) cells in MDS patients. Leuk Res. 2013;37(5):541-6.
52. Epling-Burnette PK, Bai F, Painter JS, Rollison DE, Salih HR, Krusch M, et al. Reduced natural killer (NK) function associated with high-risk myelodysplastic syndrome (MDS) and reduced expression of activating NK receptors. Blood. 2007;109(11):4816-24.
53. Aggarwal S, van de Loosdrecht AA, Alhan C, Ossenkoppele GJ, Westers TM, Bontkes HJ. Role of immune responses in the pathogenesis of low-risk MDS and high-risk MDS: implications for immunotherapy. Br J Haematol. 2011;153(5):568-81.
54. Calvi M, Di Vito C, Frigo A, Trabanelli S, Jandus C, Mavilio D. Development of Human ILCs and Impact of Unconventional Cytotoxic Subsets in the Pathophysiology of Inflammatory Diseases and Cancer. Front Immunol. 2022;13:914266.
55. Artis D, Spits H. The biology of innate lymphoid cells. Nature. 2015;517(7534):293-301.
56. Spits H, Artis D, Colonna M, Diefenbach A, Di Santo JP, Eberl G, et al. Innate lymphoid cells--a proposal for uniform nomenclature. Nat Rev Immunol. 2013;13(2):145-9.
57. Vivier E, van de Pavert SA, Cooper MD, Belz GT. The evolution of innate lymphoid cells. Nat Immunol. 2016;17(7):790-4.
58. Vivier E, Artis D, Colonna M, Diefenbach A, Di Santo JP, Eberl G, et al. Innate Lymphoid Cells: 10 Years On. Cell. 2018;174(5):1054-66.
59. Shih HY, Sciume G, Poholek AC, Vahedi G, Hirahara K, Villarino AV, et al. Transcriptional and epigenetic networks of helper T and innate lymphoid cells. Immunol Rev. 2014;261(1):23-49.
60. Panda SK, Colonna M. Innate Lymphoid Cells in Mucosal Immunity. Front Immunol. 2019;10:861.
61. Mjosberg J, Spits H. Human innate lymphoid cells. J Allergy Clin Immunol. 2016;138(5):1265-76.
62. Ebbo M, Crinier A, Vely F, Vivier E. Innate lymphoid cells: major players in inflammatory diseases. Nat Rev Immunol. 2017;17(11):665-78.
63. Mebius RE. Organogenesis of lymphoid tissues. Nat Rev Immunol. 2003;3(4):292-303.

64. Ercolano G, Wyss T, Salome B, Romero P, Trabanelli S, Jandus C. Distinct and shared gene expression for human innate versus adaptive helper lymphoid cells. J Leukoc Biol. 2020;108(2):723-37.
65. Bal SM, Golebski K, Spits H. Plasticity of innate lymphoid cell subsets. Nat Rev Immunol. 2020;20(9):552-65.
66. Gao Y, Souza-Fonseca-Guimaraes F, Bald T, Ng SS, Young A, Ngiow SF, et al. Tumor immunoevasion by the conversion of effector NK cells into type 1 innate lymphoid cells. Nat Immunol. 2017;18(9):1004-15.
67. Cortez VS, Ulland TK, Cervantes-Barragan L, Bando JK, Robinette ML, Wang Q, et al. SMAD4 impedes the conversion of NK cells into ILC1-like cells by curtailing non-canonical TGF-beta signaling. Nat Immunol. 2017;18(9):995-1003.
68. Murphy JM, Ngai L, Mortha A, Crome SQ. Tissue-Dependent Adaptations and Functions of Innate Lymphoid Cells. Front Immunol. 2022;13:836999.
69. Trabanelli S, Gomez-Cadena A, Salome B, Michaud K, Mavilio D, Landis BN, et al. Human innate lymphoid cells (ILCs): Toward a uniform immune-phenotyping. Cytometry B Clin Cytom. 2018;94(3):392-9.
70. Sonnenberg GF, Mjosberg J, Spits H, Artis D. SnapShot: innate lymphoid cells. Immunity. 2013;39(3):622- e1.
71. Fan YY, Yang BY, Wu CY. Phenotypically and functionally distinct subsets of natural killer cells in human PBMCs. Cell Biol Int. 2008;32(2):188-97.
72. Caligiuri MA. Human natural killer cells. Blood. 2008;112(3):461-9.
73. Cooper MA, Fehniger TA, Caligiuri MA. The biology of human natural killer-cell subsets. Trends Immunol. 2001;22(11):633-40.
74. Juelke K, Romagnani C. Differentiation of human innate lymphoid cells (ILCs). Curr Opin Immunol. 2016;38:75-85.
75. Daussy C, Faure F, Mayol K, Viel S, Gasteiger G, Charrier E, et al. T-bet and Eomes instruct the development of two distinct natural killer cell lineages in the liver and in the bone marrow. J Exp Med. 2014;211(3):563-77.
76. Fuchs A, Vermi W, Lee JS, Lonardi S, Gilfillan S, Newberry RD, et al. Intraepithelial type 1 innate lymphoid cells are a unique subset of IL-12- and IL-15-responsive IFN-gamma-producing cells. Immunity. 2013;38(4):769-81.
77. Gordon SM, Chaix J, Rupp LJ, Wu J, Madera S, Sun JC, et al. The transcription factors T-bet and Eomes control key checkpoints of natural killer cell maturation. Immunity. 2012;36(1):55-67.

78. Post M, Cuapio A, Osl M, Lehmann D, Resch U, Davies DM, et al. The Transcription Factor ZNF683/HOBIT Regulates Human NK-Cell Development. Front Immunol. 2017;8:535.
79. Friedrich C, Taggenbrock R, Doucet-Ladeveze R, Golda G, Moenius R, Arampatzi P, et al. Effector differentiation downstream of lineage commitment in ILC1s is driven by Hobit across tissues. Nat Immunol. 2021;22(10):1256-67.
80. Vivier E, Raulet DH, Moretta A, Caligiuri MA, Zitvogel L, Lanier LL, et al. Innate or adaptive immunity? The example of natural killer cells. Science. 2011;331(6013):44-9.
81. Takeda K, Cretney E, Hayakawa Y, Ota T, Akiba H, Ogasawara K, et al. TRAIL identifies immature natural killer cells in newborn mice and adult mouse liver. Blood. 2005;105(5):2082-9.
82. Klose CSN, Artis D. Innate lymphoid cells control signaling circuits to regulate tissue-specific immunity. Cell Res. 2020;30(6):475-91.
83. Beaulieu AM. Memory responses by natural killer cells. J Leukoc Biol. 2018;104(6):1087-96.
84. Boudreau JE, Liu XR, Zhao Z, Zhang A, Shultz LD, Greiner DL, et al. Cell-Extrinsic MHC Class I Molecule Engagement Augments Human NK Cell Education Programmed by Cell-Intrinsic MHC Class I. Immunity. 2016;45(2):280-91.
85. Shifrin N, Raulet DH, Ardolino M. NK cell self tolerance, responsiveness and missing self recognition. Semin Immunol. 2014;26(2):138-44.
86. Parham P. MHC class I molecules and KIRs in human history, health and survival. Nat Rev Immunol. 2005;5(3):201-14.
87. Braud VM, Allan DS, O'Callaghan CA, Soderstrom K, D'Andrea A, Ogg GS, et al. HLA-E binds to natural killer cell receptors CD94/NKG2A, B and C. Nature. 1998;391(6669):795-9.
88. Wada H, Matsumoto N, Maenaka K, Suzuki K, Yamamoto K. The inhibitory NK cell receptor CD94/NKG2A and the activating receptor CD94/NKG2C bind the top of HLA-E through mostly shared but partly distinct sets of HLA-E residues. Eur J Immunol. 2004;34(1):81-90.
89. Freud AG, Caligiuri MA. Human natural killer cell development. Immunol Rev. 2006;214:56-72.
90. Poli A, Michel T, Theresine M, Andres E, Hentges F, Zimmer J. CD56bright natural killer (NK) cells: an important NK cell subset. Immunology. 2009;126(4):458-65.

91. Nagler A, Lanier LL, Cwirla S, Phillips JH. Comparative studies of human FcRIII-positive and negative natural killer cells. J Immunol. 1989;143(10):3183-91.
92. Romagnani C, Juelke K, Falco M, Morandi B, D'Agostino A, Costa R, et al. CD56brightCD16- killer Ig-like receptor- NK cells display longer telomeres and acquire features of CD56dim NK cells upon activation. J Immunol. 2007;178(8):4947-55.
93. Jacobs R, Stoll M, Stratmann G, Leo R, Link H, Schmidt RE. CD16- CD56+ natural killer cells after bone marrow transplantation. Blood. 1992;79(12):3239-44.
94. Kim BS, Artis D. Group 2 innate lymphoid cells in health and disease. Cold Spring Harb Perspect Biol. 2015;7(5).
95. Neill DR, Wong SH, Bellosi A, Flynn RJ, Daly M, Langford TKA, et al. Nuocytes represent a new innate effector leukocyte that mediates type-2 immunity. Nature. 2010;464(7293):1367-70.
96. Moro K, Kabata H, Tanabe M, Koga S, Takeno N, Mochizuki M, et al. Interferon and IL-27 antagonize the function of group 2 innate lymphoid cells and type 2 innate immune responses. Nat Immunol. 2016;17(1):76-86.
97. Monticelli LA, Osborne LC, Noti M, Tran SV, Zaiss DM, Artis D. IL-33 promotes an innate immune pathway of intestinal tissue protection dependent on amphiregulin-EGFR interactions. Proc Natl Acad Sci U S A. 2015;112(34):10762-7.
98. Fonseca W, Lukacs NW, Elesela S, Malinczak CA. Role of ILC2 in Viral-Induced Lung Pathogenesis. Front Immunol. 2021;12:675169.
99. Meininger I, Carrasco A, Rao A, Soini T, Kokkinou E, Mjosberg J. Tissue-Specific Features of Innate Lymphoid Cells. Trends Immunol. 2020;41(10):902-17.
100. Califano D, Cho JJ, Uddin MN, Lorentsen KJ, Yang Q, Bhandoola A, et al. Transcription Factor Bcl11b Controls Identity and Function of Mature Type 2 Innate Lymphoid Cells. Immunity. 2015;43(2):354-68.
101. Hochdorfer T, Winkler C, Pardali K, Mjosberg J. Expression of c-Kit discriminates between two functionally distinct subsets of human type 2 innate lymphoid cells. Eur J Immunol. 2019;49(6):884-93.
102. Oyesola OO, Duque C, Huang LC, Larson EM, Fruh SP, Webb LM, et al. The Prostaglandin D2 Receptor CRTH2 Promotes IL-33-Induced ILC2 Accumulation in the Lung. J Immunol. 2020;204(4):1001-11.
103. Stier MT, Zhang J, Goleniewska K, Cephus JY, Rusznak M, Wu L, et al. IL-33 promotes the egress of group 2 innate lymphoid cells from the bone marrow. J Exp Med. 2018;215(1):263-81.

104. Nagasawa M, Heesters BA, Kradolfer CMA, Krabbendam L, Martinez-Gonzalez I, de Bruijn MJW, et al. Correction: KLRG1 and NKp46 discriminate subpopulations of human CD117(+)CRTH2(-) ILCs biased toward ILC2 or ILC3. J Exp Med. 2019;216(9):2221-2.
105. Huang Y, Guo L, Qiu J, Chen X, Hu-Li J, Siebenlist U, et al. IL-25-responsive, lineage-negative KLRG1(hi) cells are multipotential 'inflammatory' type 2 innate lymphoid cells. Nat Immunol. 2015;16(2):161-9.
106. Montaldo E, Juelke K, Romagnani C. Group 3 innate lymphoid cells (ILC3s): Origin, differentiation, and plasticity in humans and mice. Eur J Immunol. 2015;45(8):2171-82.
107. An Z, Flores-Borja F, Irshad S, Deng J, Ng T. Pleiotropic Role and Bidirectional Immunomodulation of Innate Lymphoid Cells in Cancer. Front Immunol. 2019;10:3111.
108. Ishizuka IE, Chea S, Gudjonson H, Constantinides MG, Dinner AR, Bendelac A, et al. Single-cell analysis defines the divergence between the innate lymphoid cell lineage and lymphoid tissue-inducer cell lineage. Nat Immunol. 2016;17(3):269-76.
109. van de Pavert SA. Lymphoid Tissue inducer (LTi) cell ontogeny and functioning in embryo and adult. Biomed J. 2021;44(2):123-32.
110. Klose CS, Artis D. Innate lymphoid cells as regulators of immunity, inflammation and tissue homeostasis. Nat Immunol. 2016;17(7):765-74.
111. Bar-Ephraim YE, Cornelissen F, Papazian N, Konijn T, Hoogenboezem RM, Sanders MA, et al. Cross-Tissue Transcriptomic Analysis of Human Secondary Lymphoid Organ-Residing ILC3s Reveals a Quiescent State in the Absence of Inflammation. Cell Rep. 2017;21(3):823-33.
112. Lim AI, Li Y, Lopez-Lastra S, Stadhouders R, Paul F, Casrouge A, et al. Systemic Human ILC Precursors Provide a Substrate for Tissue ILC Differentiation. Cell. 2017;168(6):1086-100 e10.
113. Mebius RE, Rennert P, Weissman IL. Developing lymph nodes collect CD4+CD3-LTbeta+ cells that can differentiate to APC, NK cells, and follicular cells but not T or B cells. Immunity. 1997;7(4):493-504.
114. Spits H, Di Santo JP. The expanding family of innate lymphoid cells: regulators and effectors of immunity and tissue remodeling. Nat Immunol. 2011;12(1):21-7.
115. Scoville SD, Freud AG, Caligiuri MA. Cellular pathways in the development of human and murine innate lymphoid cells. Curr Opin Immunol. 2019;56:100-6.
116. Freud AG, Yokohama A, Becknell B, Lee MT, Mao HC, Ferketich AK, et al. Evidence for discrete stages of human natural killer cell differentiation in vivo. J Exp Med. 2006;203(4):1033-43.

117. Scoville SD, Mundy-Bosse BL, Zhang MH, Chen L, Zhang X, Keller KA, et al. A Progenitor Cell Expressing Transcription Factor RORgammat Generates All Human Innate Lymphoid Cell Subsets. Immunity. 2016;44(5):1140-50.
118. Bar-Ephraim YE, Koning JJ, Burniol Ruiz E, Konijn T, Mourits VP, Lakeman KA, et al. CD62L Is a Functional and Phenotypic Marker for Circulating Innate Lymphoid Cell Precursors. J Immunol. 2019;202(1):171-82.
119. Mazzurana L, Czarnewski P, Jonsson V, Wigge L, Ringner M, Williams TC, et al. Tissue-specific transcriptional imprinting and heterogeneity in human innate lymphoid cells revealed by full-length single-cell RNA-sequencing. Cell Res. 2021;31(5):554-68.
120. Chen L, Youssef Y, Robinson C, Ernst GF, Carson MY, Young KA, et al. CD56 Expression Marks Human Group 2 Innate Lymphoid Cell Divergence from a Shared NK Cell and Group 3 Innate Lymphoid Cell Developmental Pathway. Immunity. 2018;49(3):464-76 e4.
121. Brooks AG, Posch PE, Scorzelli CJ, Borrego F, Coligan JE. NKG2A complexed with CD94 defines a novel inhibitory natural killer cell receptor. J Exp Med. 1997;185(4):795-800.
122. Townsend MJ, Weinmann AS, Matsuda JL, Salomon R, Farnham PJ, Biron CA, et al. T-bet regulates the terminal maturation and homeostasis of NK and Valpha14i NKT cells. Immunity. 2004;20(4):477-94.
123. Colucci F, Caligiuri MA, Di Santo JP. What does it take to make a natural killer? Nat Rev Immunol. 2003;3(5):413-25.
124. Mace EM, Gunesch JT, Dixon A, Orange JS. Human NK cell development requires CD56-mediated motility and formation of the developmental synapse. Nat Commun. 2016;7:12171.
125. Roberto A, Di Vito C, Zaghi E, Mazza EMC, Capucetti A, Calvi M, et al. The early expansion of anergic NKG2A(pos)/CD56(dim)/CD16(neg) natural killer represents a therapeutic target in haploidentical hematopoietic stem cell transplantation. Haematologica. 2018;103(8):1390-402.
126. Stabile H, Nisti P, Morrone S, Pagliara D, Bertaina A, Locatelli F, et al. Multifunctional human CD56 low CD16 low natural killer cells are the prominent subset in bone marrow of both healthy pediatric donors and leukemic patients. Haematologica. 2015;100(4):489-98.

127. Vulpis E, Stabile H, Soriani A, Fionda C, Petrucci MT, Mariggio E, et al. Key Role of the CD56(low)CD16(low) Natural Killer Cell Subset in the Recognition and Killing of Multiple Myeloma Cells. Cancers (Basel). 2018;10(12).
128. Stabile H, Nisti P, Peruzzi G, Fionda C, Pagliara D, Brescia PL, et al. Reconstitution of multifunctional CD56(low)CD16(low) natural killer cell subset in children with acute leukemia given alpha/beta T cell-depleted HLA-haploidentical haematopoietic stem cell transplantation. Oncoimmunology. 2017;6(9):e1342024.
129. Porzsolt F, Heimpel H. Natural killer cell activity in preleukaemia. Lancet. 1982;1(8269):449.
130. Porzsolt F, Heimpel H. Impaired T-cell and NK-cell function in patients with preleukemia. Blut. 1982;45(4):243-8.
131. Hejazi M, Manser AR, Frobel J, Kundgen A, Zhao X, Schonberg K, et al. Impaired cytotoxicity associated with defective natural killer cell differentiation in myelodysplastic syndromes. Haematologica. 2015;100(5):643-52.
132. Carlsten M, Baumann BC, Simonsson M, Jadersten M, Forsblom AM, Hammarstedt C, et al. Reduced DNAM-1 expression on bone marrow NK cells associated with impaired killing of CD34+ blasts in myelodysplastic syndrome. Leukemia. 2010;24(9):1607-16.
133. Kiladjian JJ, Bourgeois E, Lobe I, Braun T, Visentin G, Bourhis JH, et al. Cytolytic function and survival of natural killer cells are severely altered in myelodysplastic syndromes. Leukemia. 2006;20(3):463-70.
134. Ruggeri L, Capanni M, Urbani E, Perruccio K, Shlomchik WD, Tosti A, et al. Effectiveness of donor natural killer cell alloreactivity in mismatched hematopoietic transplants. Science. 2002;295(5562):2097-100.
135. Bruzzese A, Leardini D, Masetti R, Strocchio L, Girardi K, Algeri M, et al. GATA2 Related Conditions and Predisposition to Pediatric Myelodysplastic Syndromes. Cancers (Basel). 2020;12(10).
136. Gleason MK, Ross JA, Warlick ED, Lund TC, Verneris MR, Wiernik A, et al. CD16xCD33 bispecific killer cell engager (BiKE) activates NK cells against primary MDS and MDSC CD33+ targets. Blood. 2014;123(19):3016-26.
137. Salome B, Gomez-Cadena A, Loyon R, Suffiotti M, Salvestrini V, Wyss T, et al. CD56 as a marker of an ILC1-like population with NK cell properties that is functionally impaired in AML. Blood Adv. 2019;3(22):3674-87.

138. Trabanelli S, Curti A, Lecciso M, Salome B, Riether C, Ochsenbein A, et al. CD127+ innate lymphoid cells are dysregulated in treatment naive acute myeloid leukemia patients at diagnosis. Haematologica. 2015;100(7):e257-60.
139. Wu L, Lin Q, Ma Z, Chowdhury FA, Mazumder MHH, Du W. Mesenchymal PGD2 activates an ILC2-Treg axis to promote proliferation of normal and malignant HSPCs. Leukemia. 2020;34(11):3028-41.
140. Trabanelli S, Chevalier MF, Martinez-Usatorre A, Gomez-Cadena A, Salome B, Lecciso M, et al. Tumour-derived PGD2 and NKp30-B7H6 engagement drives an immunosuppressive ILC2-MDSC axis. Nat Commun. 2017;8(1):593.
141. Zhang W, Xie X, Mi H, Sun J, Ding S, Li L, et al. Abnormal populations and functions of natural killer cells in patients with myelodysplastic syndromes. Oncol Lett. 2018;15(4):5497-504.
142. Raiola AM, Dominietto A, Ghiso A, Di Grazia C, Lamparelli T, Gualandi F, et al. Unmanipulated haploidentical bone marrow transplantation and posttransplantation cyclophosphamide for hematologic malignancies after myeloablative conditioning. Biol Blood Marrow Transplant. 2013;19(1):117-22.
143. Luznik L, O'Donnell PV, Symons HJ, Chen AR, Leffell MS, Zahurak M, et al. HLA-haploidentical bone marrow transplantation for hematologic malignancies using nonmyeloablative conditioning and high-dose, posttransplantation cyclophosphamide. Biol Blood Marrow Transplant. 2008;14(6):641-50.
144. Lee N, Llano M, Carretero M, Ishitani A, Navarro F, Lopez-Botet M, et al. HLA-E is a major ligand for the natural killer inhibitory receptor CD94/NKG2A. Proc Natl Acad Sci U S A. 1998;95(9):5199-204.
145. Cossarizza A, Chang HD, Radbruch A, Akdis M, Andra I, Annunziato F, et al. Guidelines for the use of flow cytometry and cell sorting in immunological studies. Eur J Immunol. 2017;47(10):1584-797.
146. Cossarizza A, Chang HD, Radbruch A, Acs A, Adam D, Adam-Klages S, et al. Guidelines for the use of flow cytometry and cell sorting in immunological studies (second edition). Eur J Immunol. 2019;49(10):1457-973.
147. Cossarizza A, Chang HD, Radbruch A, Abrignani S, Addo R, Akdis M, et al. Guidelines for the use of flow cytometry and cell sorting in immunological studies (third edition). Eur J Immunol. 2021;51(12):2708-3145.

148. Saeys Y, Van Gassen S, Lambrecht BN. Computational flow cytometry: helping to make sense of high-dimensional immunology data. Nat Rev Immunol. 2016;16(7):449-62.
149. Mair F, Hartmann FJ, Mrdjen D, Tosevski V, Krieg C, Becher B. The end of gating? An introduction to automated analysis of high dimensional cytometry data. Eur J Immunol. 2016;46(1):34-43.
150. Brummelman J, Mazza EMC, Alvisi G, Colombo FS, Grilli A, Mikulak J, et al. High-dimensional single cell analysis identifies stem-like cytotoxic CD8(+) T cells infiltrating human tumors. J Exp Med. 2018;215(10):2520-35.
151. Chen H, Lau MC, Wong MT, Newell EW, Poidinger M, Chen J. Cytofkit: A Bioconductor Package for an Integrated Mass Cytometry Data Analysis Pipeline. PLoS Comput Biol. 2016;12(9):e1005112.
152. Levine JH, Simonds EF, Bendall SC, Davis KL, Amir el AD, Tadmor MD, et al. Data-Driven Phenotypic Dissection of AML Reveals Progenitor-like Cells that Correlate with Prognosis. Cell. 2015;162(1):184-97.
153. DiGiuseppe JA, Cardinali JL, Rezuke WN, Pe'er D. PhenoGraph and viSNE facilitate the identification of abnormal T-cell populations in routine clinical flow cytometric data. Cytometry B Clin Cytom. 2018;94(5):588-601.
154. Becht E, McInnes L, Healy J, Dutertre CA, Kwok IWH, Ng LG, et al. Dimensionality reduction for visualizing single-cell data using UMAP. Nat Biotechnol. 2018.
155. Huang JC, Basu SK, Zhao X, Chien S, Fang M, Oehler VG, et al. Mesenchymal stromal cells derived from acute myeloid leukemia bone marrow exhibit aberrant cytogenetics and cytokine elaboration. Blood Cancer J. 2015;5:e302.
156. Hua Y, Wang C, Jiang H, Wang Y, Liu C, Li L, et al. Iron overload may promote alteration of NK cells and hematopoietic stem/progenitor cells by JNK and P38 pathway in myelodysplastic syndromes. Int J Hematol. 2017;106(2):248-57.
157. Balsamo M, Manzini C, Pietra G, Raggi F, Blengio F, Mingari MC, et al. Hypoxia downregulates the expression of activating receptors involved in NK-cell-mediated target cell killing without affecting ADCC. Eur J Immunol. 2013;43(10):2756-64.
158. Romero AI, Thoren FB, Brune M, Hellstrand K. NKp46 and NKG2D receptor expression in NK cells with CD56dim and CD56bright phenotype: regulation by histamine and reactive oxygen species. Br J Haematol. 2006;132(1):91-8.
159. Barrow AD, Martin CJ, Colonna M. The Natural Cytotoxicity Receptors in Health and Disease. Front Immunol. 2019;10:909.

160. Beck RC, Padival M, Yeh D, Ralston J, Cooke KR, Lowe JB. The Notch ligands Jagged2, Delta1, and Delta4 induce differentiation and expansion of functional human NK cells from CD34+ cord blood hematopoietic progenitor cells. Biol Blood Marrow Transplant. 2009;15(9):1026-37.
161. Aref S, Khaled N, Al Gilany AH, Ayed M, Abouzeid T, Attia D. Impact of Bone Marrow Natural Killer Cells (NK); Soluble TNF-alpha and IL-32 Levels in Myelodysplastic Syndrome Patients. Asian Pac J Cancer Prev. 2020;21(10):2949-53.
162. Solana R, Campos C, Pera A, Tarazona R. Shaping of NK cell subsets by aging. Curr Opin Immunol. 2014;29:56-61.
163. Tremblay-McLean A, Coenraads S, Kiani Z, Dupuy FP, Bernard NF. Expression of ligands for activating natural killer cell receptors on cell lines commonly used to assess natural killer cell function. BMC Immunol. 2019;20(1):8.
164. Braun T, Fenaux P. Myelodysplastic Syndromes (MDS) and autoimmune disorders (AD): cause or consequence? Best Pract Res Clin Haematol. 2013;26(4):327-36.
165. Lordo MR, Wu KG, Altynova E, Shilo N, Kronen P, Nalin AP, et al. Acute Myeloid Leukemia Alters Group 1 Innate Lymphoid Cell Differentiation from a Common Precursor. J Immunol. 2021;207(6):1672-82.
166. Zhang L, Zhao Q, Cang H, Wang Z, Hu X, Pan R, et al. Acute Myeloid Leukemia Cells Educate Mesenchymal Stromal Cells toward an Adipogenic Differentiation Propensity with Leukemia Promotion Capabilities. Adv Sci (Weinh). 2022;9(16):2105811.
167. Santourlidis S, Trompeter HI, Weinhold S, Eisermann B, Meyer KL, Wernet P, et al. Crucial role of DNA methylation in determination of clonally distributed killer cell Ig-like receptor expression patterns in NK cells. J Immunol. 2002;169(8):4253-61.
168. Sohlberg E, Pfefferle A, Andersson S, Baumann BC, Hellstrom-Lindberg E, Malmberg KJ. Imprint of 5-azacytidine on the natural killer cell repertoire during systemic treatment for high-risk myelodysplastic syndrome. Oncotarget. 2015;6(33):34178-90.
169. Wenk C, Garz AK, Grath S, Huberle C, Witham D, Weickert M, et al. Direct modulation of the bone marrow mesenchymal stromal cell compartment by azacitidine enhances healthy hematopoiesis. Blood Adv. 2018;2(23):3447-61.

11 List of tables and figures

12 Appendix

1) Alessandra Roberto, Clara Di Vito, Elisa Zaghi, Emilia Maria Cristina Mazza, Arianna Capucetti, Michela Calvi, Paolo Tentorio, Veronica Zanon, Barbara Sarina, Jacopo Mariotti, Stefania Bramanti, Elena Tenedini, Enrico Tagliafico, Silvio Bicciato, Armando Santoro, Mario Roederer, Emanuela Marcenaro, Luca Castagna, Enrico Lugli, and Domenico Mavilio. **The early expansion of anergic NKG2Apos/CD56dim/CD16neg natural killer cells represents a therapeutic target in haploidentical haematopoietic stem cell transplantation.** Haematologica, 2018.

2) Elisa Zaghi, Michela Calvi, Emanuela Marcenaro, Domenico Mavilio, Clara Di Vito. **Targeting NKG2A to elucidate natural killer cell ontogenesis and to develop novel immune-therapeutic strategies in cancer therapy.** Journal of Leukocyte Biology, 2019.

3) Elisa Zaghi, Michela Calvi, Clara Di Vito and Domenico Mavilio. **Innate Immune Responses in the Outcome of Haploidentical Hematopoietic Stem Cell Transplantation to Cure Hematologic Malignancies.** Frontiers in Immunology, 2019.

4) Silvia Pesce, Sara Trabanelli, Clara Di Vito, Marco Greppi, Valentina Obino, Fabio Guolo, Paola Minetto, Matteo Bozzo, Michela Calvi, Elisa Zaghi, Simona Candiani, Roberto Massimo Lemoli, Camilla Jandus, Domenico Mavilio, Emanuela Marcenaro. **Cancer Immunotherapy by Blocking Immune Checkpoints on Innate Lymphocytes.** Cancers, 2020.

5) Luca Castagna, Viviana Valli, Inna Timofeeva, Rossana Capizzuto, Stefania Bramanti, Jacopo Mariotti, Chiara De Philippis, Barbara Sarina, Daniele Mannina, Laura Giordano, Federica De Paoli, Jasper J P van Beek, Elisa Zaghi, Michela Calvi, Clara Di Vito, Domenico Mavilio, Roberto Crocchiolo, Enrico Lugli. **Feasibility and Efficacy of CD45RA+ Depleted Donor Lymphocytes Infusion After Haploidentical Transplantation With Post-Transplantation Cyclophosphamide in Patients With Hematological Malignancies.** Transplantation and Cellular Therapy, 2021.

6) Jasper J P Van Beek, Simone Puccio, Alessandra Roberto, Federica De Paoli, Giulia Graziano, Elisa Salviato, Giorgia Alvisi, Veronica Zanon, Alice Scarpa, Elisa Zaghi, Michela

Calvi, Clara Di Vito, Rossana Mineri, Barbara Sarina, Chiara De Philippis, Armando Santoro, Jacopo Mariotti, Stefania Bramanti, Francesco Ferrari, Luca Castagna, Domenico Mavilio, Enrico Lugli. **Single-cell profiling reveals the dynamics of cytomegalovirus-specific T cells in haploidentical hematopoietic stem cell transplantation.** Haematologica, 2021

7) Elisa Zaghi, Michela Calvi, Simone Puccio, Gianmarco Spata, Sara Terzoli, Clelia Peano, Alessandra Roberto, Federica De Paoli, Jasper Jp van Beek, Jacopo Mariotti, Chiara De Philippis, Barbara Sarina, Rossana Mineri, Stefania Bramanti, Armando Santoro, Vu Thuy Khanh Le-Trilling, Mirko Trilling, Emanuela Marcenaro, Luca Castagna, Clara Di Vito. **Single-cell profiling identifies impaired adaptive NK cells expanded after HCMV reactivation in haploidentical HSCT.** JCI Insight, 2021

8) Giuseppe Lia, Clara Di Vito, Stefania Bruno, Marta Tapparo, Lucia Brunello, Armando Santoro, Jacopo Mariotti, Stefania Bramanti, Elisa Zaghi, Michela Calvi, Lorenzo Comba, Martina Fascì, Luisa Giaccone, Giovanni Camussi, Eileen M Boyle, Luca Castagna, Andrea Evangelista, Domenico Mavilio, Benedetto Bruno. **Extracellular Vesicles as Biomarkers of Acute Graft-vs.-Host Disease After Haploidentical Stem Cell Transplantation and Post-Transplant Cyclophosphamide.** Frontiers in Immunology, 2022

9) Michela Calvi, Clara Di Vito, Alessandro Frigo, Sara Trabanelli, Camilla Jandus, **Domenico Mavilio. Development of human ILCs and impact of unconventional cytotoxic subsets in the pathophysiology of inflammatory diseases and cancer.** Frontiers in Immunology, 2022

13 Dissemination of results

Preliminary results of this project were presented as posters in meeting/congresses listed below:

1. **4th Workshop BioMeTra. Segrate, Italy, 23th September 2019.**
Michela Calvi, Clara Di Vito, Elisa Zaghi, Marianna Rossi, Marta Ubezio, Lucio Morabito, Matteo Giovanni Della Porta and Domenico Mavilio.
Title: Phenotypic characterization of innate lymphoid cells in myelodysplastic syndromes: towards the comprehension of their role in disease etiology and prognosis.

2. **Humanitas research day. Rozzano, Italy, 28th November 2019.**
Michela Calvi, Clara Di Vito, Elisa Zaghi, Marianna Rossi, Marta Ubezio, Lucio Morabito, Matteo Giovanni Della Porta and Domenico Mavilio.
Title: Phenotypic characterization of innate lymphoid cells in myelodysplastic syndromes: towards the comprehension of their role in disease etiology and prognosis.

3. **SIICA 2022, XIII National congress. Naples, Italy, May 23th-26th 2022.**
Michela Calvi, Clara Di Vito, Alessandro Frigo, Nicolò Coianiz, Marta Ubezio, Alessia Campagna, Antonio Russo, Matteo Giovanni Della Porta and Domenico Mavilio.
Title: Phenotypic characterization of innate lymphoid cells in myelodysplastic syndromes: towards the comprehension of their role in disease etiology and prognosis.

4. **Milan meets immunology. Milan, Italy, 8th June 2022.**
Michela Calvi, Clara Di Vito, Alessandro Frigo, Nicolò Coianiz, Marta Ubezio, Alessia Campagna, Antonio Russo, Matteo Giovanni Della Porta and Domenico Mavilio.
Title: Phenotypic characterization of innate lymphoid cells in myelodysplastic syndromes: towards the comprehension of their role in disease etiology and prognosis.

5. **4th International Conference on Innate Lymphoid Cells (ILC4). Big Island, Hawaii, USA, 20th-23th September 2022 (posponed from 2020).**
Michela Calvi, Clara Di Vito, Alessandro Frigo, Antonio Russo, Matteo Giovanni Della Porta and Domenico Mavilio.
Title: Altered ILC developmental pathways in myelodysplastic syndrome patients.

Moreover, being a recipient of the AIRC fellowship from April 2022, I presented the aim of the association to the third-year students at a high school (Liceo scientifico delle scienze applicate, G. Galilei, Crema, Cremona). In that occasion, I explained to the students my PhD project and the results that I obtained, so far.

In the future months, I'm going to hold an internal seminar at Humanitas to disseminate the results of this project to all the researchers working in this institute.